Using single cell RNA sequencing to assess immunological responses in quails injected with porcine circovirus-like particles

By

Lekita Govindasamy (Singh)

Thesis presented for the degree of

DOCTOR OF PHILOSOPHY

In the Department of Molecular and Cell Biology,

Faculty of Science, University of Cape Town

January 2025

Supervisor: A/Prof Inga Hitzeroth

Co-supervisors: Prof Ed Rybicki and Dr Dorit Hockman

Declaration

The work described in this thesis was conducted in the Biopharming Research Unit (Department of Molecular and Cell Biology, University of Cape Town) under the supervision of A/Prof Inga Hitzeroth, Prof Ed Rybicki and Dr Dorit Hockman.

I, Lekita Govindasamy, hereby declare that the work on which this thesis is based is my original work (except where acknowledgements indicate otherwise) and that neither the whole work nor any part of it has been or is being submitted for another degree in this or any other university. I authorise the university to reproduce for the purpose of research either the whole or any portion of the contents in any manner whatsoever.

Lekita Govindasamy (Singh)

Contents

Acknowledgements

A journey that began with two of my proudest supporters cheering me on and ended with one becoming an angel. I dedicate this PhD to my parents.

- "True education is not for a mere living, but for a fuller and meaningful life."-**Sri Sathya Sai Baba**. This PhD has enhanced the meaning of my life in every possible way. I owe this glory to God.

- My amazing family. I have been blessed to have the love and support of four incredible parents, grandparents and siblings. I am grateful for their unwavering support and encouragement throughout this journey. To my parents, thank you for always believing in me and for providing me with the strength, guidance, and love that I needed to push through the challenges. Your sacrifices and endless support have been a constant source of motivation.

- My darling beloved, who became my husband during this adventure, Kaveshen Govindasamy. Thank you for your constant support, patience, and love that has been invaluable throughout this journey. Your belief in me, even during the most challenging times, meant the world to me.

- Prof Inga Hitzeroth for project supervision, support and exceptional guidance. Your expertise, insightful feedback, and constant support were instrumental in shaping this PhD. I truly appreciate the time and effort you dedicated to helping me. Your mentorship has been invaluable, and I am deeply grateful to have had you as a supervisor.

- Dr Dorit Hockman for project supervision, outstanding guidance and expertise. Your invaluable insights, constructive feedback, and encouragement has been instrumental in helping me navigate this project. Your mentorship has profoundly shaped my academic growth, and I am truly grateful for the opportunity to work under your supervision.

- Prof Ed Rybicki for project supervision and guidance. Thank you for your help and encouragement and motivating me to approach this project with creativity and determination. Your mentorship has enriched my academic experience, and I am grateful for the opportunity to work with you.

- Liselo Labs and David Jarvis I am extremely grateful for the incredible opportunity, resources, support and advice that you provided. A big thank you to the Liselo team for helping make this possible. My gratitude must also be expressed to Dr Mike Jarvis for his eagerness to assist with crucial aspects of the project and dedication to devoting a significant amount of his time to ensuring its success.

- The extraordinary team at the Biopharming Research Unit and Department of Molecular and Cell Biology. To all my lab mates, who became amazing friends, thank you for sharing the many late nights together, the endless hours of laughter and encouragement to keep moving forward.

- Dr Sandiswa Mbewana and Dr Alta van Zyl, thank you for the support, advice and motivation. You always helped me with such care and enthusiasm. Thank you!

- The staff at the Research Animal Facility, thank you for performing the animal experiments with such care and dedication. I am grateful to the team.

- Mohammed Jaffer at the Electron Microscope Unit, thank you for all the advice, patience and assistance with the TEM. I am grateful to you for the amazing images we were able to capture.

- Dr Vuyani Moses, thank you for your invaluable assistance and willingness to help with parts of the coding. I am grateful to you for sharing your brilliance with such enthusiasm.

- The ICTS High Performance Computing team, thank you for your assistance and guidance. The bioinformatic computations were performed using facilities provided by the University of Cape Town's ICTS High Performance Computing team.

- The South African Department of Trade, Industry and Competition and the Poliomyelitis Research Foundation for project funding. Thank you for making this opportunity a possibility.

Abstract

Using single cell RNA sequencing to assess immunological responses in quails injected with porcine circovirus-like particles

By
Lekita Govindasamy (Singh)

Biopharming Research Unit
Department of Molecular and Cell Biology, Faculty of Science,
University of Cape Town, South Africa

Animal models play a pivotal role in studying molecular characteristics of host responses to infection. Based on physical characteristics, Japanese quails may be suitable for use as animal models and hold many advantages compared to their model counterparts, the chicken. However, little is known about the immunological responses of Japanese quails during viral exposure. It is imperative to understand how these animals handle adverse conditions when exposed to foreign invaders, such as viruses. Detailed information regarding their innate and adaptive immune responses can be obtained by studying the transcriptome of peripheral blood mononuclear cells (PBMCs). Such information is poorly researched in these birds and can provide helpful information for future studies.

This study aimed at using porcine circovirus type 2 (PCV-2) to assess the evolution of the immune response of quails using single cell RNA sequencing (scRNA-seq) and computational methods. PCV-2 has a single stranded circular DNA genome that encodes the single capsid protein (CP) as well as a replication-associated protein. The impacts of infection with PCV-2 have had devastating effects on the swine industry, causing major stress to the socio-economic state of many countries, and therapies are needed.

This study successfully expressed PCV-2 capsid protein in *E.coli,* with the formation of virus-like particles (VLPs). The purified VLPs were assessed by transmission electron microscopy and groups of quails were immunised either with the VLPs or with buffer. A specific antibody response was elicited and detected in both the blood and egg samples of quails immunised with PCV-2 VLPs. For analysis of the transcriptome from the immunized quails, the 10X

Genomics Chromium platform was used to isolate the PBMC samples into individual droplets, extract the mRNA from each cell, and synthesize barcoded cDNA that was then sequenced. Sequenced reads were analysed bioinformatically using software packages in R and Python. Datasets analysed were, the pooled and integrated dataset obtained from the two quail experimental groups, as well as the demultiplexed dataset that separated the pooled samples into the individual PBMC replicates. Analyses revealed 14 clusters for the pooled PBMC dataset, and 11 clusters for the demultiplexed dataset. Six cell types belonging to the innate and adaptive immune system were identified in both datasets, with macrophages being the most dominant cell type and T cells being the second largest cell type in both the PCV-2 datasets. Differential gene expression revealed genes that were uniquely upregulated in specific cell types and subtypes, while many differentially expressed genes (DEGs) were shared between cell types. The similarity in immune response between the control and PCV-2 quail groups in this study demonstrated that quails could tolerate exposure to PCV-2 capsid protein with no major harm. Based on upregulated and downregulated DEGs as well as identified molecular functions and biological processes, an innate immune response was induced with early stages of the adaptive immune response and a regulated pro-inflammatory response. Increased levels of cell differentiation and metabolism was activated during the response. These outcomes highlight the immunological response of Japanese quails to PCV-2.

Abbreviations

A	
AIV	Avian influenza virus
ALV-J	Avian leukosis virus subgroup J
APCs	Antigen presenting cells
ATP	Adenosine triphosphate
B	
BAM	Binary alignment and map
BCIP	5-bromo-4-chloro-3-indolyl phosphate
BCR	B cell receptor
bp	Base pair
BP	Biological Process
BSA	Bovine serum albumin
C	
CC	Cellular Component
cDNA	Complementary deoxyribonucleic acid
CEL-seq	Cell Expression by Linear amplification and Sequencing
CP	Capsid protein
CSV	Comma Separated Value
ctrl	Control
D	
DC	Dendritic cells
DEG	Differential gene expression
dH_2O	Distilled water
DNA	Deoxyribonucleic acid
Drop-seq	Droplet Sequencing
dT	Deoxythymidine
E	
E.coli	*Escherichia coli*
EDTA	Ethylenediaminetetraacetic acid
F	
FACS	Fluorescence-activated cell sorting
G	
GEM	Gel beads-in-emulsion
GO	Gene Ontology
H	
HCl	Hydrochloric acid
His	Histidine

I

IBV	Infectious bronchitis virus
IFNs	Interferons
IgG	Immunoglobulin G
IgY	Immunoglobulin Y
IL	Interleukin
IPTG	Isopropyl β-D-thiogalactopyranoside

K

KCl	Potassium chloride
KH_2PO_4	Monopotassium phosphate
KNN	K-nearest neighbor

L

lac	Lactose
LB	Luria bertani
LCM	Laser capture microdissection

M

M	Molecular weight marker
MARS-seq	Massively parallel RNA single cell sequencing
MF	Molecular Function
MHC	Major histocompatibility complex
mRNA	Messenger ribonucleic acid

N

Na_2HPO_4	Disodium hydrogen phosphate
NaCl	Sodium chloride
NBT	Nitro blue tetrazolium
NDV	Newcastle disease virus
NK	Natural killer cells
NLS	Nuclear localization signal

O

OD	Optical density
ORFs	Open reading frames

P

PAGE	Polyacrylamide gel electrophoresis
PBMCs	Peripheral blood mononuclear cells
PBS	Phosphate buffer saline
PC	Principal component
PCA	Principal component analysis
PCR	Polymerase chain reaction
PCV	Porcine circovirus
PCVAD	Porcine circovirus associated diseases
PHA	Phytohaemagglutinin

PRR	Pattern recognition receptors
PRRSV	Porcine reproductive and respiratory syndrome virus

Q

QC	Quality control

R

Rep	Replication-associated protein
RNA	Ribonucleic acid
rRNA	Ribosomal ribonucleic acid
RT	Reverse transcription
rTEV	Recombinant tobacco etch virus

S

scRNA-seq	Single cell RNA-sequencing
SDS	Sodium dodecyl sulfate
SMART-seq	Switching Mechanism At the 5' end of RNA Template
SNV	Single-nucleotide variant

T

TCR	T cell receptor complex
TEM	Transmission electron microscopy
Th1	T helper 1
Th2	T helper 2
TNF	Tumour necrosis factor
Tregs	T regulatory cells
tRNA	Transport ribonucleic acid
TSP	Total soluble protein

U

UMAP	Uniform manifold approximation and projection
UMI	Unique molecular identifier

V

VLP	Virus-like particle

Symbols

α	Alpha	µg	Microgram(s)
β	Beta	µl	Microliter(s)
%	Percentage	µM	Micromolar
°C	Degrees celsius	ml	Millilitre(s)
g	Gram(s)	mg	Milligram(s)
k	Kilo	nm	Nanometre(s)
kDa	Kilodalton(s)	γ/δ	Gamma/Delta

Supplementary Data

Link to Supplementary Data

Supplementary Data 1 - Elbow plots for pooled and integrated dataset and for demultiplexed dataset

Supplementary Data 2 - 100 most highly conserved genes per cluster for pooled and integrated dataset

Supplementary Data 3 - UMAP plots showing the expression of some PBMC genes of interest

Supplementary Data 4 - Dispersion plots and heatmaps of significant DEGs per cell type

Supplementary Data 5 - DEG lists per cell type

Supplementary Data 6 - Full list of GO terms per cell type

Supplementary Data 7 - GO driver terms for DEGs of each cell type of upregulated and downregulated genes

Supplementary Data 8 - UpSet plot interaction list and full list of GO terms per cell type

Supplementary Data 9 - GO driver terms for unique DEGs per cell type from UpSet plot

Code availability

Link to scripts

Script 1- CellRanger pipeline

Script 2- Demultiplexing using Samtools

Script 3- Demultiplexing using Samtools

Script 4- Demultiplexing using Samtools

Script 5- Demultiplexing using Samtools

Script 6- Demultiplexing using Freebayes

Script 7- Demultiplexing to concatenate files

Script 8- Demultiplexing using bcftools

Script 9- Demultiplexing using scSplit

Script 10- Demultiplexing using scSplit

Script 11- Quality control using Seurat pipeline

Script 12- Data normalization, scaling and integration pipeline

Script 13- Clustering analysis

Script 14- Cluster marker identification

Script 15- Quality control, data normalization, scaling, clustering and cluster marker identification for demultiplexed samples

Script 16- DESeq-2 pipeline

1. Chapter 1: Literature Review

1.1 Introduction

Using molecular techniques to understand host responses to infection or disease can allow for great medical interventions in treatment plans and potential drug discoveries. Animal models are helpful in studying complex biological systems. Understanding the complexities of the immune system of potential animal models is useful when studying relationships such as host-virus interactions. This in turn may allow for the development of efficacious vaccines, therapeutics, preventative strategies and understanding of disease biology. Immune imbalances or dysregulation, caused by viral infection, remain a major problem and understanding these imbalances and host susceptibility is important (Seo et al., 2014). The response is characterised by a complex system of cellular interactions, gene expression and regulatory pathways. The response to many viral infections can be extreme, resulting in a "cytokine storm" or "immune paralysis" which may then lead to severe disease (Agrati et al., 2023). Identifying biomarkers, responding cell populations and regulatory pathways can determine the severity of disease as well as potential intervention strategies (Agrati et al., 2023). A humoral or cell-mediated immune response is generally able to control and clear an infection without causing much harm to the host. Analysing the transcriptome of a sample can provide detail into the state of an immune response, which can be enhanced using cutting-edge technology, like single cell RNA sequencing (scRNA-seq). Such technology provides detailed, high-resolution transcriptional information from individual cells (Zhang et al., 2020).

Animal models play a pivotal role in studying molecular characteristics of host responses to infection. They provide valuable information related to disease severity and progression, pathogenesis, and particularly host immune responses to infection and vaccination. They also play an essential role in therapeutic and vaccine development and establishing medical interventions (Rong and Liu, 2023). Japanese quails (*Coturnix japonica*) have been commonly used in the poultry industry for meat and eggs. Early studies have shown their value as a model system for scientific research (Baumgartner, 1994). Quails may be attractive in the laboratory, compared to their model counterparts, the chicken. Quails become sexually mature at least 18 to 21 weeks earlier than chickens, they require less

space, labour and cost to maintain compared to the same number of chickens (Kirrella et al., 2023). They also lay large numbers of eggs during most of the year (Salter et al., 1999). Due to these many beneficial characteristics, quails have several potential advantages as scientific animal models (Huss et al., 2008). Their immunological responses to model antigens will provide detail into understanding innate and adaptive immune responses which may provide information of host response to infection and also supply therapeutics in the form of antibodies.

The single-stranded circular DNA porcine circoviruses are part of the *Circoviridae* family, genus *Circovirus*. These viruses infect pigs worldwide with certain species causing great harm. Porcine circovirus type 2 (PCV-2) is one of four species of porcine circoviruses to be identified, and the first type shown to be pathogenic to pigs. This virus causes porcine circovirus-associated diseases (PCVAD)which differentiates it from PCV-1, PCV-3 and PCV-4 (M. Cao et al., 2024). Due to extensive pig farming and the international trade of live swine, PCVADs are a global problem in the swine industry (Dei Giudici et al., 2023). Recent studies have found PCV-2 in many animal species which, indicates the potential to act as fomites (Zhai et al., 2019). Porcine circoviruses have also been isolated in environmental samples such as water and air (Zhai et al., 2019). These viruses can survive in diverse environments which widens their ability to infect.

This study focused on producing full-length capsid protein (CP) of PCV-2 in an *Escherichia coli* (*E.coli*) expression system, with the object of forming virus-like particles (VLPs). The VLPs were injected into Japanese quails to stimulate an immune response as well as raise PCV-2 specific antibodies. To study the immune response, peripheral blood mononuclear cells (PBMCs) were isolated from each group of quails and transcriptomic analyses performed using scRNA-seq (Satija et al., 2015). A detailed, high-resolution transcriptomic library was obtained from PBMCs, isolated from the PCV-2 injected or control quail groups, which provided information about the cell types and subtypes, gene expression levels and regulatory pathways involved in the quail immune response against PCV-2.

1.2 Porcine circovirus

1.2.1 Classification and taxonomy of porcine circoviruses

Porcine circoviruses belong to the *Circoviridae* family and *Circovirus* genus. PCV-2 is a non-enveloped, circular, single-stranded DNA virus with a small genome of approximately 1800 nucleotides. Circoviruses infect mammals, avian species and fish, amongst others. Presently, four species within the genus have been identified in pigs, including PCV-1, PCV-2, PCV-3 and PCV-4. PCV-1 is non-pathogenic to pigs, unlike the other three species (Cao et al., 2024a). This species of the virus was first detected as a contaminant of a porcine kidney cell line (PK-15). Due to the common presence of PCV-1 in pigs, they produce antibodies against PCV-1 and remain mostly unaffected (Ouyang et al., 2019).

PCV-2 is one of the most dreadful viruses affecting the swine industry and is ubiquitous in most pig farms (Sagrera et al., 2024). This immunosuppressive DNA virus has had a severe global impact, with great economic loss, on the swine industry. PCV-3 and PCV-4 were the last to be identified in pigs (Opriessnig et al., 2020). PCV-3, while genetically distinct from PCV-2, may also lead to disease in pigs. However, the development and progression of disease caused by PCV-3 is less severe than by PCV-2 (Opriessnig et al., 2020). Porcine circoviruses have the highest mutation rate for single-stranded DNA viruses (Li et al., 2018). Genotyping results have found that PCV-2 can be divided into at least nine distinct genotypes, PCV-2a to PCV-2i (Maity et al., 2023). PCV-2 has an evolutionary rate of approximately 1.2×10^{-3} substitutions per site per year. As shown in Figure 1.1, PCV-2 is present in most countries, with PCV-2a, PCV-2b and PCV-2d more widely spread throughout the world.

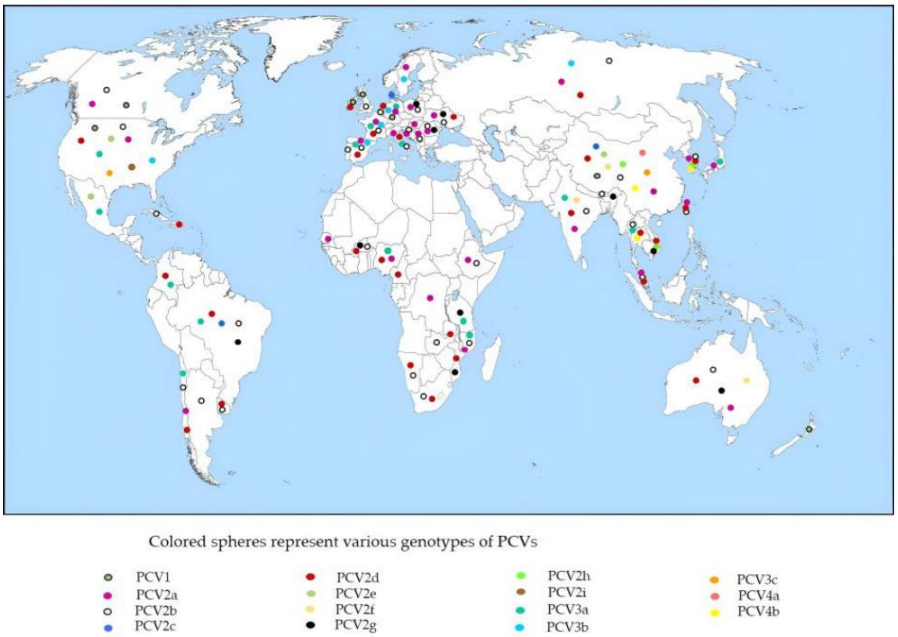

Figure 1.1: The global distribution of various porcine circovirus species (image from Maity et al., 2023, open access article)

Pigs on all continents have shown the presence of PCV-2 (Maity et al., 2023; Opriessnig et al., 2020). Recently, PCV-4 has been detected in Europe (Holgado-Martín et al., 2023) as well as in the Americas (Kroeger et al., 2024). An Italian study, consisting of more than 300 pigs, found that PCV-2 was detected in more than half the sampled cohort (Dei Giudici et al., 2023). Another dataset showing the greater prevalence of PCV-2 compared to PCV-3 was in a study conducted by Cao et al., 2024a, that tested over 1300 samples from 15 different provinces within China.

1.2.2 PCV-2 phylogeny and genome structure

Porcine circovirus virions have a diameter of approximately 17 nm (Gunter et al., 2019). The PCV-2 genome consists of three main open reading frames (ORFs) (Figure 1.2). Viral replication is regulated by the Rep protein encoded for by ORF1. Capsid protein (CP) is encoded by ORF2, while ORF3 is involved with cell apoptosis. Two intergenic regions exist with a stem loop structure at the origin of replication. The CP is the only structural protein and is responsible for viral attachment and antigenicity (Rai et al., 2020). From a genome sequence study, it was determined that GC content of the PCV-2 genome is 48.36% (Cao et al., 2024b). The ORF1 encompasses 945 nucleotides that encodes the replication-associated

protein (Rep), made up of 314 amino acids. The ORF2 encompasses 702 nucleotides and encodes the capsid protein that is made up of 234 amino acids (Cao et al., 2024b). The capsid is localised within the nucleus of the host and contains a nuclear localization signal (NLS) which is rich in arginine residues at the N-terminus. This protein contains epitopes that bind neutralizing monoclonal antibodies and neutralizing serum samples, making it suitable as a vaccine candidate. The N-terminus, located within the capsid, interacts with the viral DNA. The C-terminus is located on the surface of the capsid.

The capsid transcript begins at nucleotide 1238 with an untranslated leader sequence linked to an exon of ORF1 (Mankertz et al., 2004). The ORF1 encodes two DNA replication-associated proteins (Rep from the full length ORF1 and Rep' from the alternatively spliced ORF1). Replication of the virus is initiated by both Rep and Rep' and relies on host cell machinery (Mankertz et al., 2004).

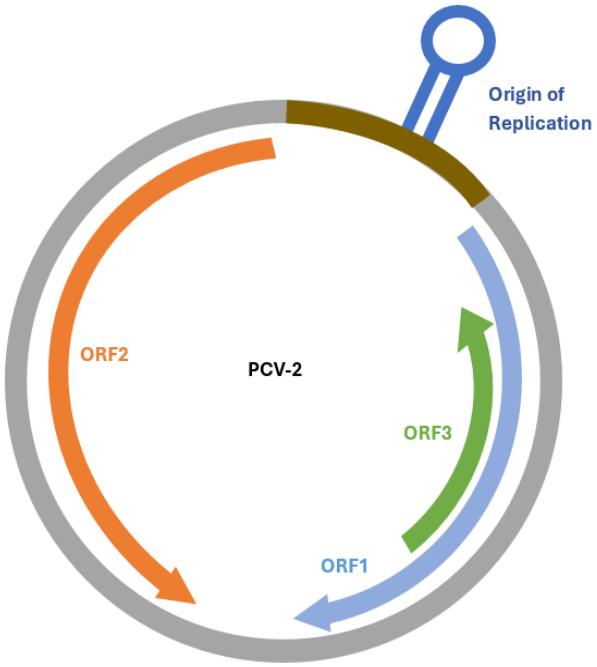

Figure 1.2: Genome organisation of PCV-2. Three open reading frames (ORF) depicted with the stem loop structure positioned between ORF1 and ORF2. The site for replication initiation is shown as the origin of replication (figure adapted from Maity et al., 2023, open access article).

1.2.3 PCV-2 related diseases

PCV-2 causes many clinical signs in pigs, which are collectively referred to as porcine circovirus-associated diseases (PCVADs), while some pigs may remain asymptomatic. Diseases caused by exposure to the virus include PCV-2-systemic disease, PCV-2-reproductive disease and porcine dermatitis and nephropathy syndrome (Cao et al., 2024b). Piglets between the ages of 8 and 16 weeks can be affected by post-weaning multisystem wasting syndrome. Clinical signs experienced by these young animals include enlarged lymph nodes, diarrhoea, weakness and emaciation, shortness of breath, skin paleness and jaundice (Maity et al., 2023). Histopathological results confirm lymphocytic-histiocytic infiltration in the kidneys, lungs and liver, reduction of mature lymphocytes in the spleen, wasting of pancreatic acinar cells and changes in the lymph nodes. Disease and death rates in affected pigs range between 4 to 30% (Maity et al., 2023).

Infection with PCV-2 weakens the host's immune system, resulting in pigs that are more vulnerable to secondary infections. While PCV-2 may act as the main pathogen of PCVAD, co-infections contribute to severe clinical disease and possible death. Co-existence of multiple PCV-2 genotypes is possible and may also result in more severe disease (Zhai et al., 2011). A study conducted in China by, Zhai et al., 2011, found that more than 30% of diseased pigs indicated a PCV-2 genotype co-existence. Another study found that co-infections between porcine reproductive and respiratory syndrome virus (PRRSV) and PCV-2 increases an animal's susceptibility to other infections (Sagrera et al., 2024). This may have a detrimental effect to the animal by increasing its risk to more lethal diseases. Co-infection of PRRSV and PCV-2 have been reported in up to 50% of cases, increasing the likelihood of severe disease (Sagrera et al., 2024).

1.2.4 Treatment strategies

Before the use of vaccines, measures to control the virus centred around the use of antibiotics for secondary bacterial infections, improved sanitation, animal isolation and improved housing practices. Other control measures included administration of vitamins and regular vaccinations against common pathogens. However, current practices involve the use of PCV-2 specific vaccines (Guo et al., 2022). Vaccination allows for efficient control and reduction in the prevalence of the virus, considering its ubiquitous nature in pig farms, but does not prevent infection (Sagrera et al., 2024). The commercialized vaccines currently used are subunit vaccines and inactivated whole virus vaccines that utilize the capsid protein as the immunogen (Gunter et al., 2019). These vaccines can reduce the clinical effects of PCV-2 infection and improve growth in pigs affected by post-weaning multisystem wasting syndrome. However, due to large vaccination schemes, a reduction in herd immunity was noted, leading to groups of animals without any natural viral exposure (Sagrera et al., 2024). For this reason, it is important to closely look at vaccine strategies and determine the optimal age for young animals to be vaccinated as well as re-evaluate control measures implemented against PCV-2. At present, piglets are vaccinated at 3 to 4 weeks old (weaning age) (Sagrera et al., 2024).

Subunit vaccines or virus-like particles (VLPs) are nano-sized, self-assembling protein complexes that mimic viral capsids. These particles lack a viral genome, which makes them non-infectious and non-replicative, thus improving their safety. Virus-like particles improve drug efficacy by increasing target delivery and are stable for drug encapsulation. Such particles also allow for easy modification and are immunogenic. They are well tolerated by the host, consequently reducing toxic effects or adverse immune responses (Taghizadeh et al., 2024). VLPs are advantageous over traditional attenuated or inactivated whole virus vaccines. They follow a safer production method, high protein yield, may be made safely at low costs, can be expressed in many types of expression systems, and elicit a robust immune response (Gao et al., 2022). Subunit vaccines use the capsid protein as the immunogenic component of the virus. The neutralizing epitopes on the capsid protein elicits a protective immune response within the host (Gunter et al., 2019). The resemblance to a natural virus in respect to shape, size and surface proteins is what misleads the host's immune system

into reacting while not causing any actual harm to the host. Both innate and adaptive immune responses may be elicited by VLPs, which favour their use for vaccine development and immunotherapy (Taghizadeh et al., 2024). Expression of the VLP can occur in many expression systems, such as bacteria, plants, yeast, insects or mammalian cell lines. A single virus type is generally used for VLP creation. However, more than one virus type may be used for chimaeric VLP creation. Chimaeric VLPs have multiple therapeutic benefits as they combine structural proteins from different viral types, creating a surface with many antigens (Taghizadeh et al., 2024). Many studies have created PCV-2 VLPs using various expression systems such as plants, insects, yeast or bacteria (Gunter et al., 2019; Kim and Hahn, 2021; Li et al., 2023; Park et al., 2021; Rai et al., 2020). *E.coli* are commonly used as bacterial expression systems. Using *E.coli* has many benefits as it replicates at an incredibly rapid rate, it results in high expression yields and scaling-up of production is simple and cost effective (Yang et al., 2021).

Pigs injected intramuscularly with PCV-2 VLPs, can mount a specific antibody response. The neutralizing antibodies are produced because of the antigenic properties that the VLP has based on the capsid protein. This form of a subunit vaccine has gained favour due to its perceived low cost, ease in preparation and overall safety (Kim et al., 2024). Commercial subunit vaccines used for PCV-2 currently include Ingelvac CircoFLEX (Boehringer Ingelheim Animal Health), Porcilis PCV (MSD Animal Health), Circumvent PCV (Merck) and Cirbloc M Hyo (Ceva) (Guo et al., 2022; Kim et al., 2024). These vaccines are all expressed in a baculovirus expression system, except for Cirbloc M Hyo which is an inactivated vaccine.

When testing the Porcilis PCV®, an efficacy study found that one dose of the vaccine elicited cell-mediated immunity and reduced PCV-2 viraemia when challenged against various PCV-2 isolates (Fort et al., 2009). Another study found that vaccinations with CircoflexTM and Porcilis PCV® resulted in a reduced viral load and shedding, reduced PCV-2 antigens in the lymph nodes, greater levels of neutralizing antibodies and an improved cellular mediated immune response (Seo et al., 2014).

1.2.5 PCV-2 transmission

Transmission of PCV-2 is often due to direct contact by exposure to infected excrement, urine and saliva. The most likely form of transmission is by direct nose-to-nose contact. However, vertical transmission, mother to offspring, is also possible with PCV-2 (Maity et al., 2023). While it is not yet known if infection is possible by means of airborne PCV-2, it is known that the virus can be airborne. A study conducted by Verreault et al., 2010 detected up to 10^7 genomes per cubic meter of PCV-2 in air samples. The samples were taken in swine confinement areas and proved that the virus can be found in an airborne state. Some insects, such as the housefly, may carry the virus, thus acting as a vector for the spread of PCV (Blunt et al., 2011).

Porcine circovirus type 2 has been isolated from free-ranging and domesticated pigs as well as wild boars. Dei Giudici et al., 2023 found that a larger proportion of free-ranging pigs were infected with PCV-2 as compared to domestic pigs, at 87.3% and 36.27%, respectively. The difference in infection rate might be indicative of different immunological responses to PCV-2 vaccines or due to good farm practice and control measures. A high infection rate of 73.53% found in wild boars might indicate that free-range pigs are responsible for viral spreading (Dei Giudici et al., 2023)

1.2.6 Host cell interactions

PCV-2 interacts with its host by cell attachment and entry. The PCV-2 attachment receptors on host cells are heparan sulphate and chondroitin sulphate B, which are found in the plasma membrane of host cells (Misinzo et al., 2006). Viral replication takes place mainly in epithelial and endothelial cells, while some replicate in host macrophages (Segalés et al., 2013). Viral components have been found in some blood cells, immune cells and lymphoid tissues of various organs (Fehér et al., 2023). Immune cells affected include macrophages, dendritic cells (DC) and monocytes. Infection of these cells allow for further infiltration into various tissues within the host thus causing multiple cells to become infected. Entry into monocytes and DC occur via clathrin-mediated endocytosis and into epithelial cells via actin- and Rho GTPase-dependent pathways (Fehér et al., 2023).

The incubation period within the host until disease development, is between 18 and 25 days (Segalés et al., 2013). By disrupting cellular processes, the virus can reduce the host's innate immune response, thereby allowing co-infection of other pathogens. In PCVAD, PCV-2 has also been shown to effect levels of depletion in natural killer (NK) cells, B cells and T cells (Fehér et al., 2023). The weakened immune system, together with the presence of interferons (IFNs), promote initiation of viral replication in early infection. A study conducted by Du et al., 2018, showed that infection with PCV-2 reduces the T helper 1 (Th1) response of hosts by supressing IL-20p40 expression. This in turn reduces the production of pro-inflammatory cytokines. PCV-2 is successful in establishing infection due to its ability to weaken the host's immune response. To gain more information about host immune responses to PCV-2 as well as improve treatment options, studying its presence in animal models is highly advantageous. Animal models are essential in studying viral infections as they can shed light on the biological processes involved in the infection, pathogenesis, immune responses and subsequent development of effective treatments and vaccines.

1.3 Japanese quails and their immunity

1.3.1 Taxonomy/Morphology

Japanese quail (*Coturnix japonica*) is an avian species originating from East Asia. These birds belong to the order Galliformes and the family Phasianidae. They are naturally found in grasslands, croplands and areas alongside fresh water sources. Although originally found in East Asia, including Eastern Russia, these birds later migrated to the Middle East, America and Europe (Huss et al., 2008). They are commonly used for meat and egg production, but were originally bred for the enjoyment of their vocalizations (Ball and Balthazart, 2010). Their high egg-laying capacity, nutrient rich meat and egg composition, and fast growth rates make them an attractive source for farming and business. These small birds are generally brown in colour with small black patches scattered on their feathers. The wild birds weigh between 90 and 100 grams, while the domesticated birds weigh between 130 to 140 grams. The males generally weigh less than their females counterparts and are smaller in size (Baer et al., 2015). Japanese quails have a short lifespan of between 2 to 3 years in the wild (Huss et al., 2008). While little is known about the taste and smell senses of Japanese quails, it is known that they have colour vision and lower field myopia. The myopia enables them to

focus on the ground while monitoring the sky for predators at the same time. They can detect sound in an auditory range between 1 and 4 kHz (Mills et al., 1997). Japanese quail are anatomically and physiologically very similar to chickens and share a similar genome (Baer et al., 2015).

1.3.2 Use as a scientific animal

The use of Japanese quails in research, as an animal model, was first done in 1959 (Huss et al., 2008). Quails have been used as a model in research fields such as immunology, virology, endocrinology, angiogenesis, behavioural studies, developmental biology and aging, amongst others (Baer et al., 2015). Their small size, low cost of housing and breeding, low consumption levels, rapid maturation, resistance to infection and high egg production levels are some of the benefits of using quails as an animal model. Within the laboratory, they are easy to breed, they are hardy in research treatments, and transgenic lines and a sequenced genome is available (Baer et al., 2015).

They may be housed individually or in groups in either pens or cages but are social animals and thrive living in groups rather than in isolation. The area in which they are kept should be well ventilated, maintained at ambient temperature and receive suitable light. Reproduction and egg laying is controlled by photoperiodic states. Exposing a female quail to 12 to 16 hours of light per day ensures egg laying, while less than 12 hours of light per day will prevent the bird from laying eggs (Ball and Balthazart, 2010).

Quails become sexually mature at around 6 to 7 weeks old, instead of 24 to 28 weeks for chickens. They are cheaper to house and breed than chickens and produce eggs more frequently than chickens (Salter et al., 1999). Quails can lay between 10 to 12 eggs every fortnight (Baer et al., 2015). These characteristics make quails appealing for research than the commonly used chicken. Following genome sequencing, it was found that the quail genome is similar to the chicken genome (Baer et al., 2015). The two genome assemblies are comparable in annotation, genes and chromosomal groupings. Genes related to immunity are similar to that of chickens, except for some differences to the major

histocompatibility complex (MHC). Quails seem to lack the MHC-Y genes (Morris et al., 2020).

Another attractive feature of using quails as an animal model is the ease of antibody production and retrieval. In female quails, immunoglobulin Y (IgY) accumulates in egg yolks during oogenesis. This results in higher IgY concentrations found in the yolk than in blood (Scholtz et al., 2010). The high levels found in egg yolks provides passive immunity to the developing offspring. Retrieval and isolation of IgYs from eggs is also easier, cheaper and less invasive than conducting a blood withdrawal. Additionally, fewer booster injections are needed to maintain high antibody titres, as birds maintain high titres for long periods of time (Esmailnejad et al., 2019). Causing less stress and harm to the bird is more desirable, making quails a good option for antibody production compared to mammals. Antibody production in mammals is a stressful event as antibody retrieval is only possible via blood collection and often sacrifice (Somasundaram et al., 2020). The concentration of IgY from a single chicken egg yolk is equal to that which can be found in 30 ml of blood (Rajeswari et al., 2018). Therefore, the concentration of antibodies produced by a chicken is comparable to that produced by large animals such as sheep or goats. The IgG antibody produced by mammals are very similar to the IgY antibodies produced by birds, making them a suitable candidate for antibody production (Rajeswari et al., 2018).

1.3.3 The quail immune system

An immune response, either innate or adaptive, is vital in all animals for protection against infectious diseases, foreign invaders, toxins, allergens or damaged cells. This occurs first with the innate immune response and is followed by the adaptive immune response. The first line of defence is antigen-independent and becomes active upon immediate detection of a threat. The second line of defence, the adaptive immune response, is antigen-dependant and becomes active after the initial processes (Chaplin, 2010).

As with many other species, the immune system of avians contain leukocytes (white blood cells) that are responsible for both the innate and adaptive responses, as can be seen in Figure 1.3. The innate immune system begins with the physical barriers that protect animals

from outside invaders. These barriers include the skin, mucus membrane, gastrointestinal tract and feathers (Qu et al., 2022a). Additionally, molecules including some proteins and enzymes as well as phagocytes (heterophils, DCs and macrophages) and NK cells all form part of the innate immune system (Birhan, 2019). Physiologic characteristics such as increased temperature, low pH and inflammation also form part of the innate immune response (Marshall et al., 2018). Cells of the innate immune system develop before cells of the adaptive immune system. This immune response is not specific to pathogens and generally performs in the same manner against all pathogens. Defensins, which belong to the innate immune response, are small peptides that have antimicrobial characteristics (Marshall et al., 2018). They act by disrupting the membranes of infecting microbes, inhibit the cell wall synthesis or neutralize secreted toxins. This initial response involves the swift assembly of immune cells and inflammation, via production of cytokines and chemokines, at the site of infection. Cytokines and chemokines are proteins that enable cell-to-cell communication and mobilisation of other cells required for defence. Cytokines that are initially released are tumour necrosis factor (TNF), interleukin 1 (IL-1) and interleukin 6 (IL-6). Accumulation of these proteins result in localised inflammation and subsequent fever. The phagocytic cells, also involved in this response, engulf and kill some microorganisms, remove cell debris and infected cells, and activate the adaptive immune response (Marshall et al., 2018).

Adaptive immunity incorporates cell mediated immunity (activation of B cells and T cells) and humoral immunity (antibody production by B cells) (Marshall et al., 2018). This immune response is highly specific and reacts towards a particular invader, while also creating memory, unlike the innate immune response. The adaptive response can eliminate a pathogen and create lasting protection through memory. With avians, lymphocytes (B cells and T cells) are produced in the bursa of Fabricius and the thymus. B cells differentiate into plasma cells that produce antibodies. Antibodies bind to pathogens and trigger a signal to other immune cells for further action (Marshall et al., 2018). Antibodies produced in the thymus of quails are regarded as a humoral mediator in an adaptive immune response. A major class of antibody in quails is immunoglobulin Y (IgY). IgY is similar to IgG found in mammals. These antibodies also have two heavy (H) and two light (L) chains, with four constant domains in the heavy chain. These domains (Cv1–Cv4) give them a greater

molecular weight compared to the mammalian IgG (Esmailnejad et al., 2019). The IgY lacks a hinge region which limits its flexibility (Somasundaram et al., 2020). Antigen-specific IgY antibodies can effectively treat bacterial, fungal and viral pathogens (Rajeswari et al., 2018). With the high levels of IgY that can be extracted from egg yolks, high epitope specificity and lack of cross reactivity with the mammalian immune system, these antibodies are widely used as therapeutics (Rajeswari et al., 2018). The proteins can withstand harsh conditions by remaining stable at temperatures between 30 to 70 °C and active at a pH of 3 to 11 (Somasundaram et al., 2020). Young birds rely on antibodies received from their mother and the innate immunity as protection mechanisms against pathogens (Sandell et al., 2009).

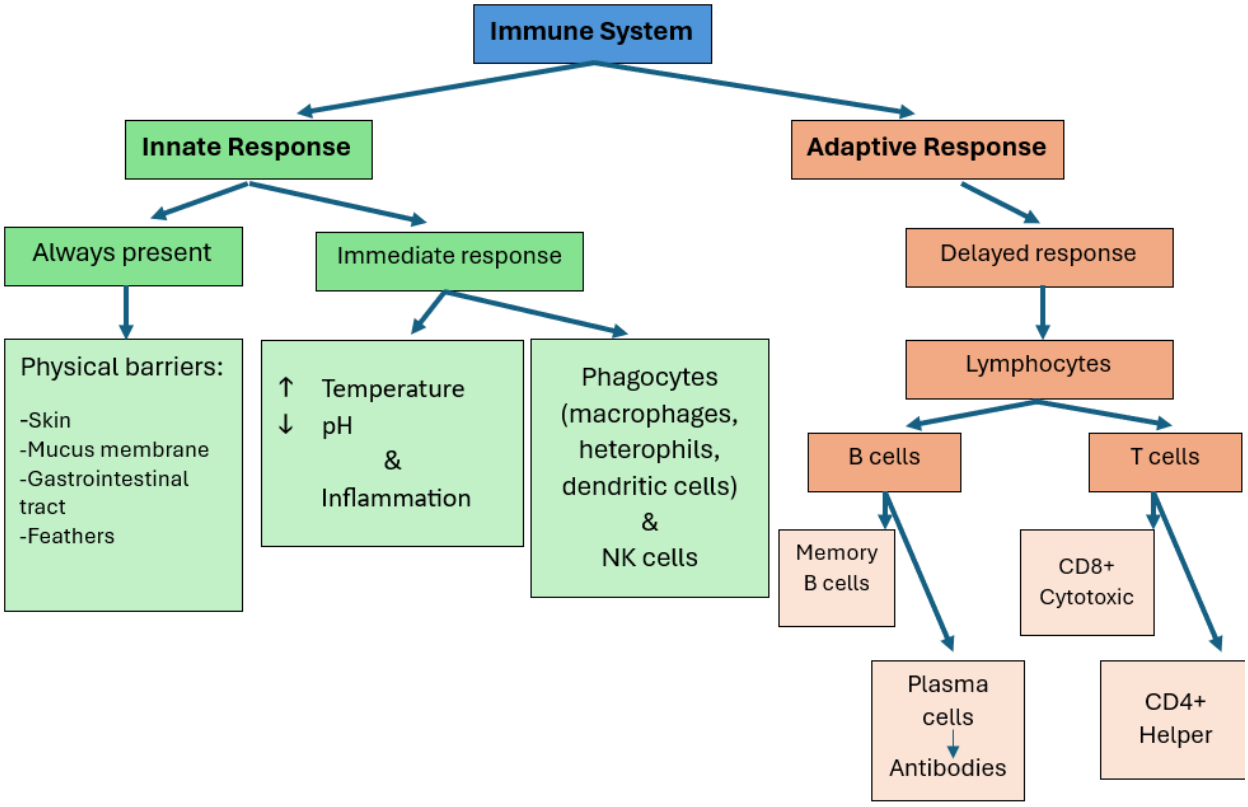

Figure 1.3: Overview of the avian immune system. The immune system encompasses the innate and adaptive responses. The innate immune response can be immediate acting or always present and includes physical and physiological characteristics. The adaptive immune response has a delayed response and includes B cells and T cells.

T cells are involved in the antigen-specific component of the adaptive immune response (Qu et al., 2022a). These cells develop in the thymus and have T cell receptors (TCR), which allow for antigen recognition. In avians, T cells are divided into α/β T-cells (CD4+ T cell/ helper T cell) and γ/δ T-cells (CD8+ T cell/ cytotoxic T cell). While many similarities between avians and mammals exist, differences in their immune system involves Toll-like receptors, chemokines and antibodies, with birds lacking eosinophils and lymph nodes (Birhan, 2019). Birds have three immunoglobulin classes (IgA, IgM, IgY) and three TCR types. They also have thrombocytes which function as phagocytes, a major histocompatibility complex (MHC) expressing two Class I and Class II, three T helper cells (Th1, Th2, Th17) and regulatory T cells. Thrombocytes are nucleated and form a large part of the white blood cell group in chickens.

One of the immune response tests, often used in bird related experiments, include the phytohaemagglutinin (PHA) skin test, which looks at the cell mediated immune function. This test measures the T cell inflammatory response in birds by injecting PHA into the wing of the bird to stimulate T cells to release cytokines that lead to inflammation. Changes in the thickness of the wing web is noted and measured before and after the injection to determine immune response (Lavoie et al., 2007). From such a test, and others, a study conducted by, Lavoie et al., 2007, found that age has an effect on quail immunity. They found that quails within a reproductive age range had stronger immunity than younger or older quails. A reduction in T cell related inflammation and antibody production was noted in aged birds. Adult birds showed an increased level of anti-viral titre when infected with H9N2 influenza than younger birds (Lavoie et al., 2007). From their studies though, it was difficult to determine the cell types that were most affected.

1.3.4 VLPs and their interaction with avian immune systems

VLPs are structural proteins that mimic an actual virus. These proteins are antigenic but are not pathogenic as they lack the viral genome. They are, therefore, a non-infectious and harmless form of treatment against viral infections. Typically, the epitopes presented on the VLP triggers a response that activates the antigen-presenting cells (APCs). These cells are immune cells that initiate the adaptive immune system by presenting an antigen for recognition by T cells (Taghizadeh et al., 2024). The VLP binds to pattern recognition receptors (PRR) on the surface of APCs. The epitopes are presented on the surface of APCs by MHC class I and II molecules, along with co-stimulatory molecules for presentation to cytotoxic and helper T cells. Cytotoxic T cells produced in the thymus can destroy invading pathogens, cancerous cells or damaged cells. Helper T cells, also produced in the thymus, activate cytotoxic cells and B cells. B cells then differentiate and produce antibodies (Marshall et al., 2018). Helper T cells are divided into three subtypes, namely Th1, Th2 and Th17 helper cells. The Th1 helper cells activate the cytotoxic cells and macrophages which both help eliminate the pathogen from the body. The Th2 cells release molecules that then activate the B cells, which create antibodies (Qu et al., 2022a).

The VLP vaccine form is used to address many avian diseases (Shen et al., 2013; Taghizadeh et al., 2024; Xu et al., 2020). Newcastle disease virus (NDV) affects many avian species and often results in neurological, gastrointestinal and respiratory problems, leading to high levels of severe disease and possible death. Affected animals are usually treated with live attenuated vaccines. These vaccines, however, have been deemed inadequate due to the high viral mutation rate, undesirable side effects, drug resistance and limited efficacy. According to, Taghizadeh et al., 2024, the use of VLPs may be a suitable alternative for addressing NDV by targeted delivery. Such targeted delivery concentrates a compound in specific cells to boost drug efficacy and reduce side effects. Using VLPs to treat NDV can reduce viral replication, promote a positive immune response and overcome drug resistance. A recent study, using a chimaeric VLP against NDV and H9N2 subtype avian influenza virus (AIV), found adequate protection in chickens against both viruses. The chickens received two vaccines of the chimaeric protein, at 40 μg each. Appropriate antibodies and differentiation of T cells was seen in the chickens that received the chimaeric

VLPs, placing this vaccine as a favourable candidate for controlling NDV and AIV (Xu et al., 2020). Another study, using a single dose (20 µg) of chimaeric NDV and AIV VLP vaccine, enabled immunized chickens to produce virus specific antibodies and displayed complete protection against the viruses following challenge tests (Shen et al., 2013). A different study created a chimaeric VLP vaccine, against NDV and infectious bronchitis virus (IBV) for chickens. The immunised group of chickens achieved successful stimulation of their humoral and cellular immune responses by producing IBV and NDV specific antibodies as well as IL-4 and IFN-γ T cell cytokines. The challenge study showed complete protection against both NDV and IBV (Wu et al., 2019).

Findings from various studies, using VLPs to target virulent pathogens affecting birds, highlight the immunogenic nature of VLPs and their ability to provide high levels of protection, while in some cases providing complete protection. These vaccine candidates are safe and efficient and can be cost effective for veterinary use (El-Husseiny et al., 2021).

1.3.5 Knowledge gap in avian immunology and VLPs

Identification of the cell types affected during immunization, to improve cell target precision, remains a challenge (Taghizadeh et al., 2024). Targeting specific cells or biomarkers is important for efficient drug delivery. Additionally, thorough understanding of immune responses that are triggered by VLPs is vital for host safety, immune evasion and therapeutic efficacy. Differences in innate immunity exist between different avian species. Diptesh et al., 2020, found this to be true between chickens and Japanese quails. They established that there are some unknown mechanisms associated with the quail innate immune response and further studies need to be conducted to determine species-specific variations at the cellular level. Few studies have looked at the immune response of quails against pathogens (Esmailnejad et al., 2019).The quail genome has been sequenced and annotated to some extent. However, it has not been well annotated and many gaps remain in understanding specific pathways and gene regulation (Esmailnejad et al., 2019). Therefore, more information is needed on the genes and specific cell types involved in the quail's immune responses, a better resolution of existing genomes and sequencing of new

avian genomes are required. This information will also improve the development of therapeutics and vaccines.

1.4 Single-cell RNA sequencing

1.4.1 Overview of RNA-seq techniques

Messenger RNA (mRNA) is the genetic code that provides instructions to synthesising proteins. This genetic molecule is derived from DNA sequences for a specific gene and its presence within a cell, indicates that the gene is being expressed. Ribosomal RNA (rRNA) forms part of the ribosome where protein synthesis occurs, and transport RNA (tRNA) moves specific amino acids to the ribosome during protein synthesis. While all cells within a multicellular organism contain the same DNA, the RNA transcriptome within a cell varies according to a cell type. The transcriptome provides information into the current cellular processes, of a biological sample (such as a tissue sample) , at the time of sampling (Caudai et al., 2021). Analysis of gene expression can indicate the different cell types that are present, the stage of cell development and the cellular functions that are occurring within a specific tissue. A powerful technique that may be used to gain such insights is RNA sequencing (Li and Wang, 2021). This can be done using bulk RNA sequencing (bulk RNA-seq), where an average gene expression profile for a sample can be obtained, or using single cell RNA sequencing (scRNA-seq) where expression levels are obtained for individual cells within the sample, providing high-resolution, in-depth information (Hwang et al., 2018).

Bulk RNA-seq offers broad scientific scope, enabling the study of differential gene expression, disease diagnosis, biomarker discovery and treatment options. This technique gives the average expression levels for a population of cells (Hwang et al., 2018). With different cells having different transcriptomes, bulk RNA-seq gives an overall expression profile of the various transcriptomes into one “pooled” sample (Wang et al., 2021). Rare cells, small cell subpopulations and rare genes can be easily missed using bulk RNA-seq resulting in incomplete information.

scRNA-seq is a new and powerful technique that offers a precise, detailed analysis of individual cellular transcriptomes. Quantification of the transcriptome, identification of

genes and cell types, and differential gene expression is possible by this high-throughput sequencing technique. Using scRNA-seq, thousands of cells may be sequenced from a single sample and analysed bioinformatically. For scRNA-seq, the process begins with appropriate single cell isolation and capture to ensure individual cells of high quality are utilized. Individual cells should be captured and compartmentalised to allow individual analysis separate from neighbouring cells. Many techniques exist to isolate single cells, which have been improved using microfluidic devices. Other options include using limiting dilutions and pipettes, capillary pipetting under a microscope, fluorescence -activated cell sorting (FACS) and laser capture microdissection (LCM). These methods, however, may be time-consuming, produce low throughput results, require large starting volumes of sample and are tedious to conduct (Hwang et al., 2018). Microfluidic technology is an automated approach that separates cells into aqueous droplets that are submerged in an oil phase. This approach requires low sample volumes, provides high through-put, precise droplet control, reduced risk of contamination, reduced cell bias, rapid processing and minimal hands-on effort (Hwang et al., 2018). A leading system utilizing this approach is the 10X Genomics Chromium platform (Figure 1.4). This platform captures individual cells in nano-sized droplets. Thousands of cells and barcoded gel beads are simultaneously isolated by a droplet-based encapsulation method creating gel beads-in-emulsion (GEMs). The gel beads are coated in oligonucleotides that encompass sequencing adapters, a unique 16 nucleotide (nt) 10X barcode, a 12 nt unique molecular identifier (UMI) and a 30 nt poly(dT) sequence. Thereafter mRNA is isolated from the encapsulated cell by attachment of the polyadenylated region of the mRNA to the oligo deoxythymidine (dT) beads. Reverse transcription is performed to synthesise barcoded cDNA, which is then amplified and prepared as an indexed DNA library for sequencing (Swaminath and Russell, 2024). As per Figure 1.5, sequenced data is then analysed bioinformatically by mapping reads to a reference genome, creating a cell by gene matrix (where each read is assigned to its cell of origin using the 10X barcode), performing pre-processing and quality control steps to remove low-quality data, normalisation, dimensionality reduction, clustering, differential gene expression and visualization (Wilk et al., 2020).

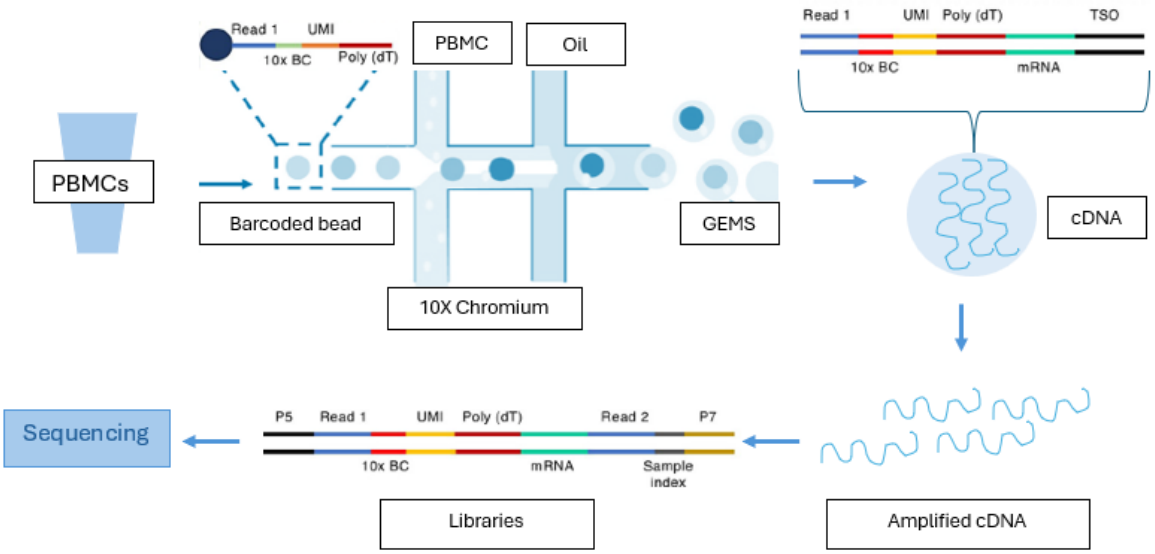

Figure 1.4: scRNA-seq workflow using the 10X Genomics Chromium platform. A single-cell suspension (eg. PBMCs) is loaded into the microfluidic device. The cells, oil and barcoded beads are then partitioned into nanoliter Gel Beads-in-emulsion (GEMs). The cells are then lysed, mRNA captured onto the barcoded beads and reverse transcription takes place to synthesise cDNA tagged with the barcode. Pooled cDNA is then amplified, fragmented, tail ends repaired, and sequencing adapters (P5 and P7) and sample index added. Libraries are then sequenced (adapted from Swaminath and Russell, 2024).

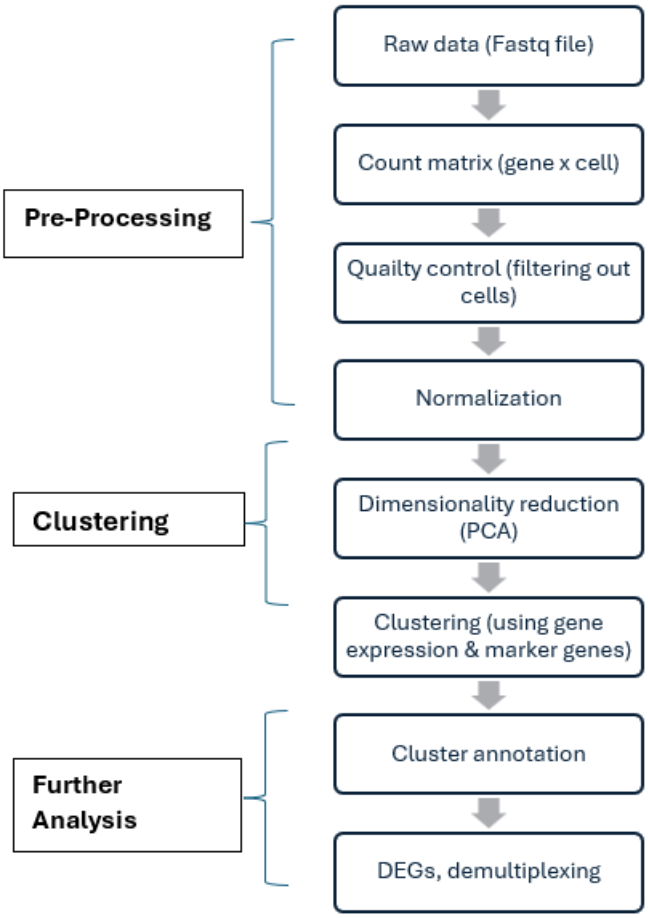

Figure 1.5: Graphical representation of analytical processes followed using bioinformatic tools for single-cell RNA sequencing datasets. Raw data, received in a Fastq format, first undergoes pre-processing, which includes mapping of sequences to a reference genome, conducting quality control to remove low quality reads, and normalization. Data is then dimensionally reduced using principal component analysis (PCA) and clustering using gene expression profiles and marker genes. Clusters are annotated as specific cell types and analysed further to include aspects such as differential gene expression (DEG), demultiplexing, amongst others.

1.4.2 Advantages of scRNA-seq

Detection and discovery of heterogeneous cell populations, rare cells and small sub-populations are possible using scRNA-seq. Small sample volumes are required for scRNA-seq, which allows for the preservation of precious samples and ability to study samples were only small volumes may be obtained. Both coding and non-coding regions within a transcript can be analysed, which may lead to identification of new gene isoforms, non-coding RNAs and alternative splicing events (Chen et al., 2023). Higher resolution of gene expression profiles and cell diversity are possible with scRNA-seq. Both the local environment and dynamic interactions within a single cell can be studied (Chen et al., 2023). Many systems

are automated which reduces error rate, time and the need for cell sorting equipment. Large numbers of cells can be analysed simultaneously with some technologies while also allowing multiple samples to be analysed at the same time (See et al., 2018). scRNA-seq allows an unbiased and comprehensive understanding of complex environments that may easily be depicted in a visual manner (Zhang et al., 2020).

1.4.3 Using scRNA-seq for immunology

The complexity of the immune system arises due to the many different types of cells, tissues and organs that it encompasses that work to defend the host against foreign threats. The heterogeneity of the immune system, therefore, makes it a complex system to understand and study. With the use of microscopy and flow cytometry, one can classify cell types based on specific surface markers. However, not all cell types can be determined using these techniques alone, as many markers may be expressed by various cell lineages or may be differentially expressed under different conditions (See et al., 2018). To better understand the transcriptome of the immune system, it is important to know the variability in gene expression of specific cell types, to ensure no sample contamination and to know the transitional stage that a cell may be in in the case of differentiation during progenitor cell development. scRNA-seq is an appropriate technique in studying immunology. It can be used to identify cell heterogeneity, cell development and differentiation as well as gene regulatory pathways that relate to immune function. Understanding an immune response, during infection or disease, allows for the identification of biomarkers and signalling pathways related to prognosis and diagnosis and subsequent treatment interventions (Zhang et al., 2020). scRNA-seq is often used to visualize immunological responses during disease progression, by analysing the transcriptome of PBMCs in an unbiased and detailed manner (Wang et al., 2021; Wilk et al., 2020; Zhang et al., 2020). PBMCs are isolated from whole blood. Analysing blood samples is a minimally invasive method to assess immune function and health. Due to the complexity and heterogeneity of PBMCs and their large transcriptome, studying individual cells and their RNA patterns can be challenging. Many studies have shown that scRNA-seq is an appropriate tool for examining the heterogeneity of immune cells, their interaction with each other and other cell types (Maxwell et al., 2024; Qu et al., 2022a; Wang et al., 2021).

1.5 scRNA-seq in avian immunology

1.5.1 Overview of recent studies using scRNA-seq in avian immunology

Few studies have been performed in avian species looking at the immune system using scRNA-seq. In a study using peripheral blood from healthy chickens for scRNA-seq analysis, Maxwell et al., 2024, identified major leukocytes, such as B cells, various T cells, monocytes and heterophils. An improved annotation of the chicken genome was possible, using scRNA-seq, compared to other classical immunological methods that require species-specific reagents, that are difficult to obtain for chickens (Maxwell et al., 2024). Qu et al., 2022, was the first to look at the immune response in chickens to a viral infection, using scRNA-seq. Marker genes for T cells involved in avian leukosis virus subgroup J (ALV-J) infection were discovered in this study. They also found that chicken CD4+ T cells can differentiate into Th1-like and Th2-like cells and that the cytotoxic Th1-like cells, as well as CD8+ cells, are responsible for the protection against ALV-J infection (Qu et al., 2022a). Adding to the limited knowledge regarding chicken immunity, Warren et al., 2023, used scRNA-seq to determine immune response during the cytolytic phase of Marek's disease in chickens. The most abundant splenic leukocytes, found in birds that were infected with Marek's disease virus, was T cells. Large amounts of granzymes were present, which were responsible for killing infected cells and protecting against viral infected cells. Granulocytes and macrophages were present indicating an innate response and early viral infection (Warren et al., 2023). From the literature, it does not appear that any scRNA-seq studies, specifically looking at immunological responses, have been performed on Japanese quail samples.

1.5.2 Potential applications of scRNA-seq in understanding avian immune responses

Gaining a clear understanding of the adaptive immune response, by specifically looking at how B cells and T cells react, is vital for vaccine development (Dai et al., 2021a). Such clarity, however, is still lacking in avian immune responses. It is still unclear how these species handle pathogens at the cellular and molecular level. Current methods of using immunofluorescence labelling and flow cytometry for phenotyping of avian immune cells are limited by species-specific reagents and protocols (Dai et al., 2021a). However, using scRNA-seq, it is possible to overcome these limitations and build a stronger understanding of avian immune responses at the cellular level which, will help largely in vaccine

development. Such information can also detail how animals respond to infection throughout development. With many avian species used for farming, meat and egg production, interest in maintaining avian populations, by ensuring longevity through proper health care is important to the agricultural and food industries.

To develop reagents for species-specific immunological markers, a well annotated genome is required that can guide what markers must be developed based on gene expression (Maxwell et al., 2024). Using scRNA-seq, suitable markers, cellular functions and novel cell types can be determined. This can greatly assist in reagent development.

1.6 Research scope

The scope of this research project was to express porcine circovirus-2 (PCV-2) virus-like particles (VLPs) in *Escherichia coli* and purify a large enough amount for antibody production in quails and subsequent immunological analysis. The study will then delve into the immune response biology of PCV-2 by evaluating the evolution of the innate and adaptive immune response of Japanese quail, using scRNA-seq and computational methods for data analysis. More specifically, the aim is to use bioinformatic tools to analyse the cell type-specific gene expression profiles of PBMCs from quails injected with PCV-2 VLPs - a good model antigen - versus naive birds.

1.7 Research aims and objectives

1.7.1 Research aims

1.7.1.1 To produce full-length PCV-2 VLPs using an *E. coli* expression system

1.7.1.2 To raise PCV-2 specific antibodies in Japanese quails

1.7.1.3 To create and investigate a detailed, high-resolution transcriptomic library, as well as identify immunological responses, from samples of immune cells pooled from multiple individual quails

1.7.1.4 To analyse cell types and subtypes, gene expression levels and molecular and biological pathways involved in the immune response to PCV-2

1.7.2 Research objectives

1.7.2.1 To produce and purify PCV-2 VLPs using a codon optimised PCV-2 CP gene in an *E.coli* expression system. VLPs will be confirmed using immunoblots and electron microscopy

1.7.2.2 Vaccinate quails with *E.coli* produced PCV-2 VLPs to raise antibodies in sera and eggs

1.7.2.3 To obtain PBMCs from naive and inoculated quail sera and study the innate and adaptive immune response using scRNA-seq (10X Genomics Chromium) to analyse cell type-specific gene expression profiles, as well as gene functions and pathways

1.7.2.4 Analyse and identify heterogeneity of cell populations, including macrophages, heterophils, NK cells, thrombocytes, B cells and T cells, by utilizing scRNA-seq and bioinformatic tools

2. Chapter 2: PCV-2 VLP expression and purification

2.1 Introduction

PCV-2 is the causative agent of porcine circovirus-associated diseases (PCVAD). The large financial impact of this disease is suffered globally in the swine industry due to subclinical, systemic and reproductive disease that may lead to eventual death and spread between pigs (Fan et al., 2023). Commercial vaccines have been developed and distributed for many years. However, this has not proven successful in eradicating the virus (Li et al., 2017). Due to the direct route of transmission as well as prevalence in the environment, the virus can easily spread between different pig droves and even different farms (Fan et al., 2023).

This virus is possibly the smallest animal viruses discovered to date, with a maximum particle diameter of approximately 17 nm and (Guo et al., 2022). The CP (approximately 27 kDa) is the most antigenic component of the virus. Targeting this protein may allow for the development of new vaccines or production of anti-PCV-2 relevant antibodies in hosts injected with CP-like structures (Trundova and Celer, 2007). Many commercially available PCV-2 vaccines can decrease clinical signs in affected pigs but, are not able to eliminate PCV-2 from blood and tissues (Jiao et al., 2023).

VLPs are highly effective in inducing an adaptive immune response and producing antigen-specific antibodies when injected into a host. Such particles may be expressed in various expression systems such as, plants, insects, yeast or bacteria. *Escherichia coli* (*E.coli*) is one of the most widely used bacterial expression systems for VLPs (Yang et al., 2021). Expression of recombinant proteins in *E.coli* is facilitated by the presence of the lactose operon. Inducing this element is easily done with the non-hydrolysable lactose equivalent; isopropyl β-D-thiogalactopyranoside (IPTG). Expressing recombinant PCV-2 VLPs in *E.coli* involved codon optimisation and preservation of the N-terminus of the protein, which has arginine codons that are important for protein folding and must be preserved (Trundova and Celer, 2007).

This chapter focuses on producing PCV-2 VLPs using an *E.coli* expression system. The purpose of synthesising VLPs is to stimulate an immune response as well as raise antibodies

in Japanese Quails. The *E.coli* codon-optimised PCV-2 CP gene cloned into a bacterial expression vector was used to express the protein. Expressed and purified protein was visualised and quantitated on SDS PAGE gels and identity of PCV-2 CP was confirmed using anti-PCV-2 antibodies on western blots. Finally, electron microscopy was done to validate the confirmation of the VLPs. These VLPs will then be injected into quails for scRNA-seq investigation further on.

2.2 Materials and Methods

2.2.1 Expression and partial purification of recombinant PCV-2 VLPs in *E. coli*

The optimised *E.coli* codon, containing the PCV-2 CP gene, was received from a past student in our group in the Department of Molecular and Cell Biology, UCT (Gunter, 2017). Optimisation of the codon included the use of the whole PCV-2 CP gene (702 bp) derived from a Lithuanian isolate (Genebank accession no. KJ128269), which was subcloned into a pProEX-HTc plasmid (Invitrogen^{TM}, California, USA) using *E. coli* DH5α competent cells as the expression vector.

These cells, as well as the optimised *E. coli* PCV-2 VLP expression protocol, was created and optimised by Gunter, 2017. An empty pProEX-HTc vector in *E. coli* DH5α was used as the negative control. For large-scale VLP expression, the *E.coli* cultures were inoculated and grown in fresh 10 ml Luria Bertani (LB) broth (0.5% yeast extract, 1% sodium chloride (NaCl) and 1% tryptone) supplemented with 100 µg.mL^{-1} ampicillin (diluted 1:100) and incubation at 37 °C, overnight with agitation. The cultures were then further diluted 1:100 in fresh 50 ml LB broth supplemented with 100 µg.mL^{-1} ampicillin and incubated as stated above. The following day, cultures were diluted once more (1:100) and incubated at 37 °C with agitation until an OD_{600} of 0.5 – 1.0 was reached. Thereafter, bacterial cultures were induced with the non-hydrolysable lactose equivalent, isopropyl β-D-thiogalactopyranoside (IPTG) to a final concentration of 0.6 mM, then incubated at 37 °C for 1 hour with agitation. Induced cultures were then centrifuged at 10 000 × g at 4 °C for 10 minutes (Beckman Coulter, Avanti J-25I). A wet pellet was collected and weighed and finally stored at -80 °C until further use.

The two-part partial purification steps of the recombinant protein included the use of BugBuster (Merck, Germany) followed by ultrafiltration using the Amicon Ultra Centrifugal 50k Filters (Millipore). The BugBuster inclusion body cell extraction preparation protocol was followed as per manufacturer's instructions (Merck, Germany). Due to frozen samples releasing more protein, the wet pellet was stored at -80 °C for at least one day before processing. Using BugBuster, the thawed wet cell pellet was resuspended in the BugBuster reagent and 25 units.mL^{-1} Benzonase (Sigma-Aldrich, Missouri, USA) was added to the mixture. The suspension was incubated, at room temperature, for 20 minutes with agitation and solid components then separated by centrifuging at 16 000 x g, at 4 °C for 20 minutes. The pellet was resuspended in BugBuster once more along with 200 µg.mL^{-1} lysozyme (Sigma-Aldrich) and incubated at room temperature for 5 minutes. Six volumes of 1:10 dilute BugBuster was added to the suspension and centrifuged at 16 000 x g, at 4 °C for 15 minutes. Thereafter, the pellet was washed 3 times with 1:10 dilute BugBuster and 10 times with 1 x PBS, pH 7.4 (137 mM NaCl, 2.7 mM KCl, 10mM Na_2HPO_4, 1.8 mM KH_2PO_4). The resulting pellet was then diluted in 2ml of 1 x PBS (pH 7.4) for further purification using a second round of BugBuster followed by ultrafiltration.

For the second round of purification, the resuspended pellet was spun down at 10822 x g, at room temperature for 8 minutes (Eppendorf Centrifuge 5424). Five hundred microliters of BugBuster and 10 ul of Lysozyme was added to the pellet, gently resuspended for 5 minutes and 1 ml of 1:10 dilute BugBuster added. The suspension was spun once again, washed twice with 1:10 dilute BugBuster and 5 times with 1 x PBS, pH 7.4. The pellet was then resuspended in 1x PBS, pH 7.4 for immediate ultra filtration.

The resuspended pellet was loaded into the Amicon Ultra Centrifugal 50k Filters (Millipore) and centrifuged at 5000 x g, at 4 °C for 5 minutes (Beckman Coulter, Avanti J-25I). The pellet was then captured from within the filter interface (retentate) and resuspended in 1 x PBS (pH 7.4) and washed one more time. The filtrate was discarded as it contained undesired, contaminating proteins. The pellet was finally diluted in Endotoxin-free 1 x PBS (pH 7.4) and stored -20 °C until further use.

2.2.2 SDS-PAGE and western blotting

For protein detection, samples of partially purified recombinant protein were combined with 1 x sample application buffer (2% SDS, 100 mM Tris-HCl, pH 7.5, 2 mM EDTA, 52% glycerol, 4.3% β-mercaptoethanol, 0.25% bromophenol blue) and heated at 95 °C for 5 minutes. Denatured samples were resolved on 12.5% SDS PAGE gels at 120V. Gels were then either stained with Coomasie blue stain (48% methanol, 0.1% brilliant blue G-250, 15% glacial acetic acid) at 37 °C for 1 hour and destained (10% glacial acetic acid, 30 methanol) at room temperature, overnight; or analysed by western blot. For western blot, gels were transblotted onto nitrocellulose membranes, pre-soaked with transfer buffer (5.82 g Tris base, 2.93 g glycine, 200 ml methanol and water to 1 L), using a TransBlot Semi-Dry Transfer Cell (Bio-Rad) and running at 15 V for 1.5 hours. Membranes were then transferred to freshly made blocking buffer (5% long life fat-free milk, 1 x PBS (pH 7.4), 1% Tween-20, water) and incubated at room temperature for 30 minutes with gentle agitation. Blocking buffer was removed and membrane submerged in primary antibody (mouse anti-PCV-2 polyclonal serum) diluted in blocking buffer (1:1000). This was probed at 4 °C, overnight with agitation. The next day, the membrane was washed 4 x 15 minutes in blocking buffer with agitation. It was then incubated in a goat anti-mouse alkaline phosphatise-conjugated secondary antibody (Sigma-Aldrich®) diluted in blocking buffer (1:5000) at 37 °C for 1 hour with agitation. Membranes were washed again 4 x 15 minutes in blocking buffer, lacking milk with agitation. Membranes were developed by exposing to NBT/BCIP substrate (Roche) for 15 to 30 minutes. Staining reaction was stopped by rinsing the blot in clean water.

2.2.3 SDS-PAGE gel densitometry

For protein quantification, gel densitometry was used with Bovine serum albumin (BSA, Sigma-Aldrich) as the reference protein standard. A standard curve was created with two-fold dilutions of BSA in 1 x PBS (pH 7.4). The concentrations used ranged from 1 $mg.ml^{-1}$ to 0.125 $mg.ml^{-1}$ BSA. Denatured BSA dilutions and PCV-2 VLP samples were loaded onto a 12.5 % SDS-PAGE gel, run at 120V and then Coomassie-stained. The stained bands were quantified using the SynGene, GeneTools version 4.03.05.0 software.

2.2.4 Transmission electron microscopy analysis

Virus-like particle assembly was verified by viewing the PCV-2 VLP samples under a transmission electron microscope and comparing to the negative control. Carbon-coated copper grids (Agar Scientific, UK) were glow discharged at 25 mA for 30 seconds using a EMS100 Glow Discharge Unit (Electron Microscopy Sciences, USA) to render the carbon surface hydrophilic. Grids were then floated on the PCV-2 VLP or negative control samples at room temperature for 5 minutes. Excess sample was then washed off the grids four times in sterile water, excess water tapped off using filter paper and then negatively stained with 2% uranyl acetate (SPI Supplies, USA) for 30 seconds. Air-dried grids were then viewed using the FEI Tecnai F20 transmission electron microscope (Thermo Fisher (formerly FEI), Eindhoven, Netherlands) operating at 200kV (Lab6 emitter) and fitted with a Tridiem energy filter and Gatan CCD camera (Gatan, UK).

2.3 Results

2.3.1 Expression and partial purification of recombinant PCV-2 VLPs in *E. coli*

E.coli, containing either the pProEX-HTc-PCV-2 or pProEX-HTc empty vector constructs, were induced with IPTG for protein expression. A 500 ml induced culture volume of OD_{600} 0.5 – 1.0 resulted in a wet pellet mass of approximately 2 g. Pellets, containing the insoluble PCV-2 CP, underwent a first round of partial purification, using BugBuster followed by multiple washes with 1 x PBS (pH 7.4). Partially purified protein samples were then analysed using 12.5% SDS-PAGE gels that were Coomassie stained. Destained gels showed that full length CP was expressed only in *E.coli* harbouring the pProEX-HTc-PCV-2 vector. Analysis showed that the protein of approximately 27kDa was seen in the lane loaded with induced cell lysate of pProEX-HTc-PCV-2, while no band of that size was seen in cell lysate of the empty vector (Figure 2.1 A). Samples were further purified, using a second round of BugBuster and ultra filtration. Clearer banding patterns can be seen (Figure 2.1 B) in the lanes of the Coomassie stained gels.

To further confirm the expression of PCV-2 CP, the cell lysates were analysed by probing the gels with anti-PCV-2 antibodies obtained from previously immunized mouse sera. A band, similar to the size as seen in the Coomassie stained SDS-PAGE gel, of approximate size 27kDa

can also be seen on the western blot, with no band of that size seen in the lane of the empty vector. Figure 2.2 A shows the cell lysates before further purification, using just one round of BugBuster. Many non-specific bands were filtered out resulting in purer samples, as seen in Figure 2.2 B. Thick bands in both the Coomassie stained gel and western blot can be seen for the PCV-2 CP samples at 27kDa, while other lighter bands may likely be due to reactivity of the antibody to *E.coli* proteins. The PCV-2 CP specific band did not seem to be thinner or lighter in intensity after further purification, suggesting minimal loss of protein during ultrafiltration.

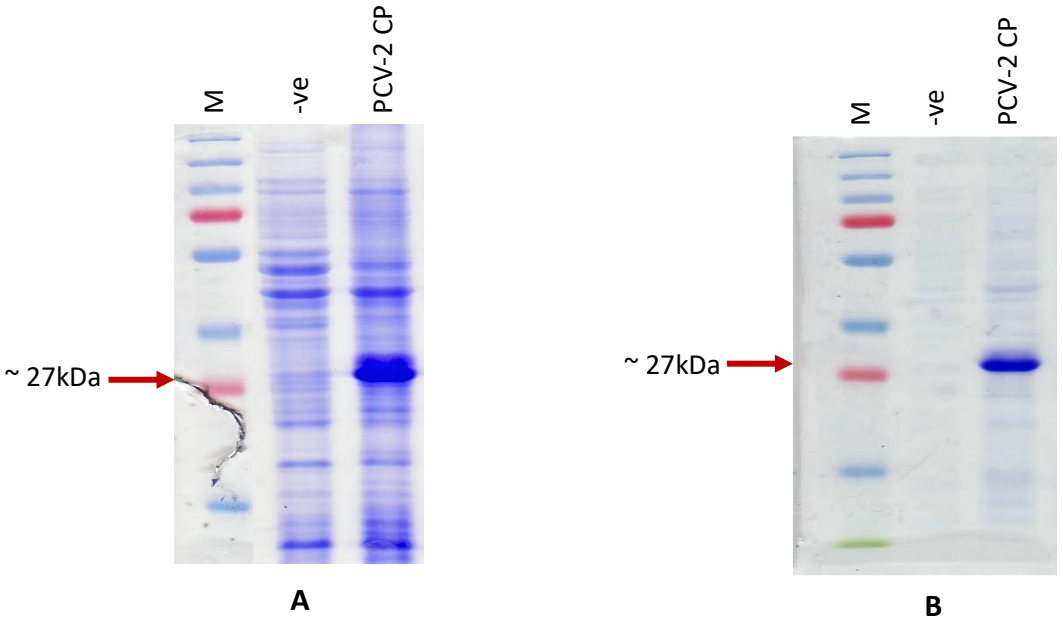

Figure 2.1: Expression of *E. coli*-produced PCV-2 CP. Coomassie-stained SDS-PAGE gel of pProEX-HTc-PCV-2 and pProEX-HTc empty vector (-ve). A band of approximately 27kDa can be seen in the PCV-2 CP lane. No band at approximately 27kDa can been seen in the empty vector negative control. M: pre-stained protein standard (kDa). **A:** bands after partial purification using BugBuster. **B:** bands after further purification using second round of BugBuster and ultrafiltration.

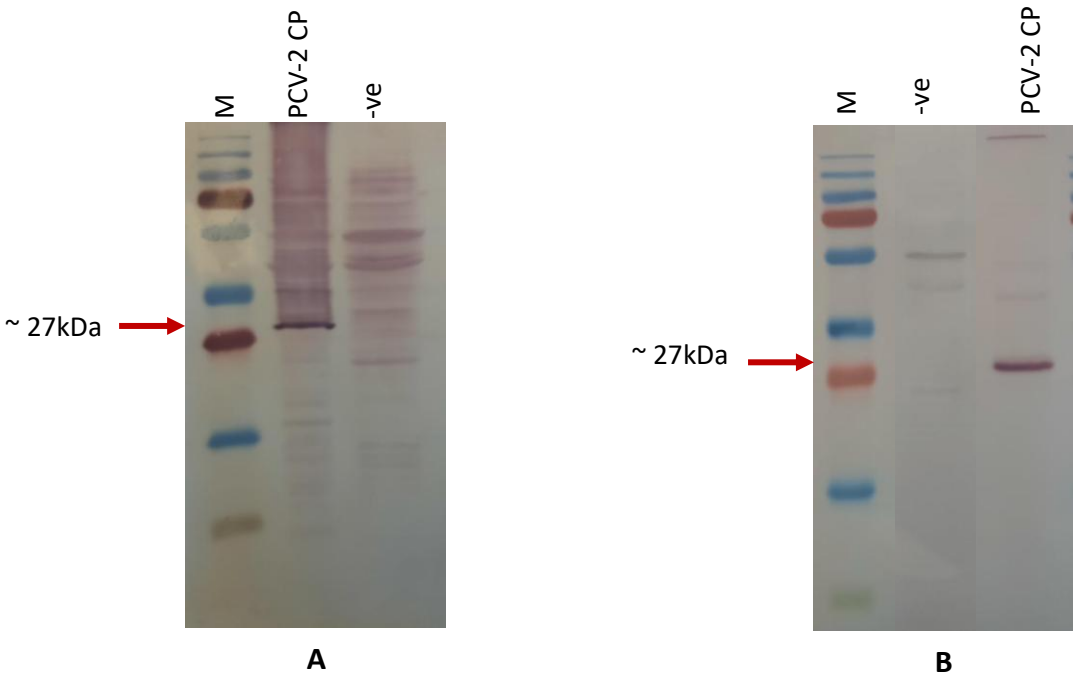

Figure 2.2: Western blot of pProEX-HTc-PCV-2 and pProEX-HTc empty vector. A band of approximately 27kDa was present in the PCV-2 lane. No band was seen in the empty vector negative control. M: pre-stained protein. Probed with mouse PCV-2 antisera (1:1000 dilution) and goat anti-mouse alkaline phosphatase-conjugated secondary antibody (1:5000 dilution). **A:** bands after partial purification using BugBuster. **B:** bands after further purification using using second round of BugBuster and ultrafiltration.

2.3.2 Quantification of *E.coli* produced recombinant PCV-2 CP

Determining the concentration of partially purified PCV-2 CP was conducted using gel densitometry analysis. Creating a standard curve of BSA protein starting at 1.0 $mg.ml^{-1}$ and completing at 0.125 $mg.ml^{-1}$, allowed for the calculation of PCV-2 CP concentration by means of a Coomassie stained gel and band absorbance. As can be seen in Figure 2.3A, the PCV-2 CP band was detected at approximately 27kDa, with no band detected in the pProEX-HTc empty vector (negative control). A calculated yield of 0.541 $mg.ml^{-1}$ of PCV-2 CP was determined using the formula obtained from Figure 2.3B, based on the values from the standard curve. Further calculations showed that the PCV-2 CP made up 54% of the total soluble protein (TSP) after purification. A 500 ml induced culture of *E.coli* pProEX-HTc-PCV-2 resulted in 2 g TSP and 1.082 g PCV-2 CP.

A

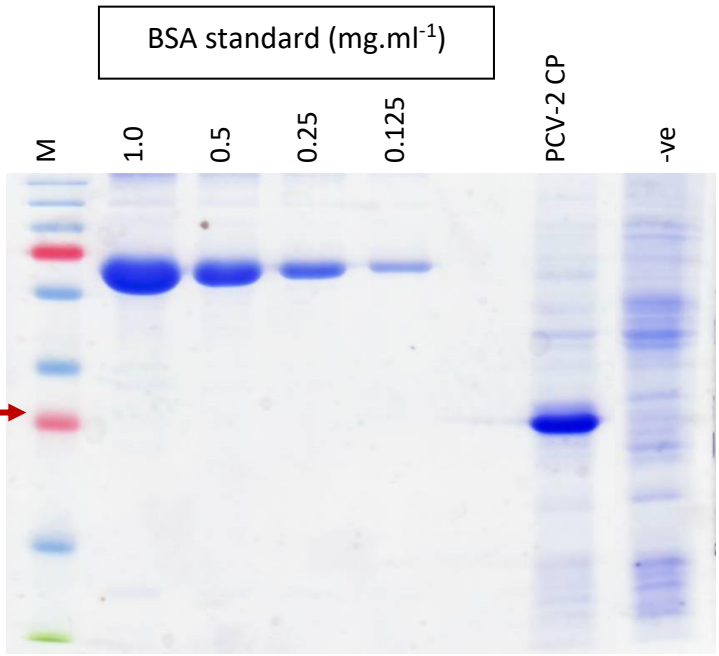

B

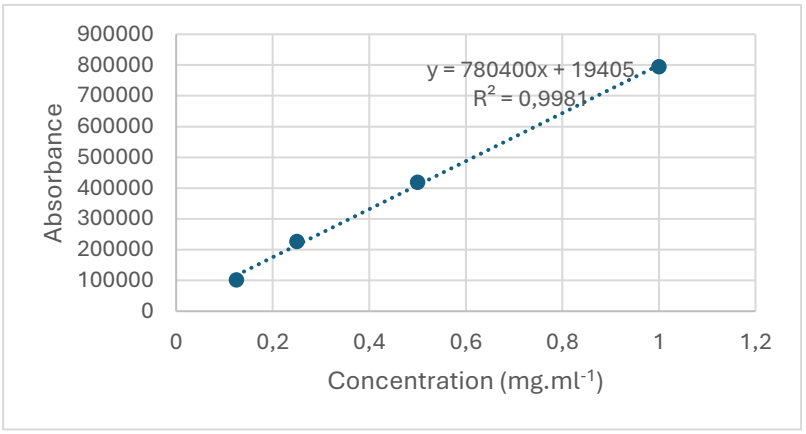

C

	Absorbance	**mg.ml^{-1}**
BSA	794147	**1**
	418754	**0,5**
	226657	**0,25**
	101310	**0,125**
Sample (PCV-2 CP)	**441812**	0.541

Figure 2.3: Quantification of PCV-2 CP. Quantification using gel using densitometry analysis of the appropriate band at approximately 27kDa. **A:** various BSA protein standards, partially purified PCV-2 CP and empty vector (-ve) resolved on a Coomassie stained SDS-PAGE gel for densitometry analysis. **B:** absorbance showing BSA standard curve and equation used for determining PCV-2 CP concentration. **C:** Absorbance values and subsequent protein concentrations for BSA standards and PCV-2 CP

2.3.3 Assembly of *E. coli* produced PCV-2 CP into VLPs

The correct assembly of PCV-2 CP proteins were verified by TEM analysis. Spherical particles, with diameters between 11 to 17 nm, was observed using the transmission electron microscope, confirming the formation of PCV-2 VLPs. This proved that the capsid protein self-assembled into VLPs. No spherical particles can be seen in the empty vector samples. Samples shown in Figure 2.4 were diluted 1:20 and showed little to no sign of contaminating particles.

A: PCV-2 VLPs

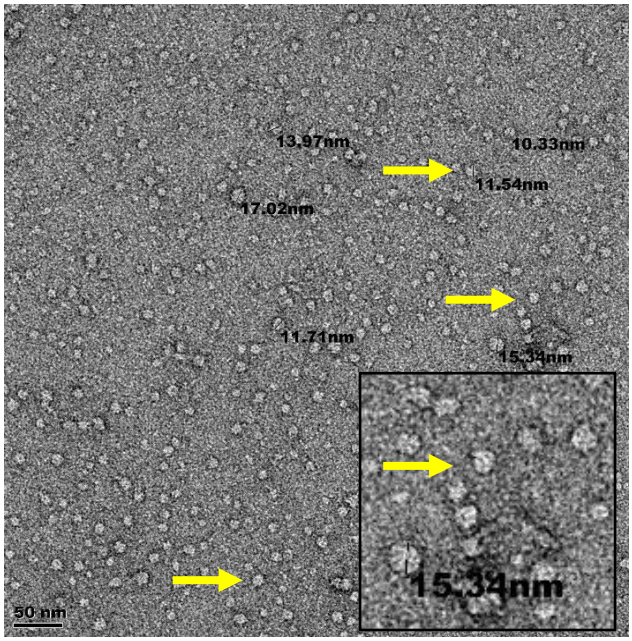

B: Negative Control

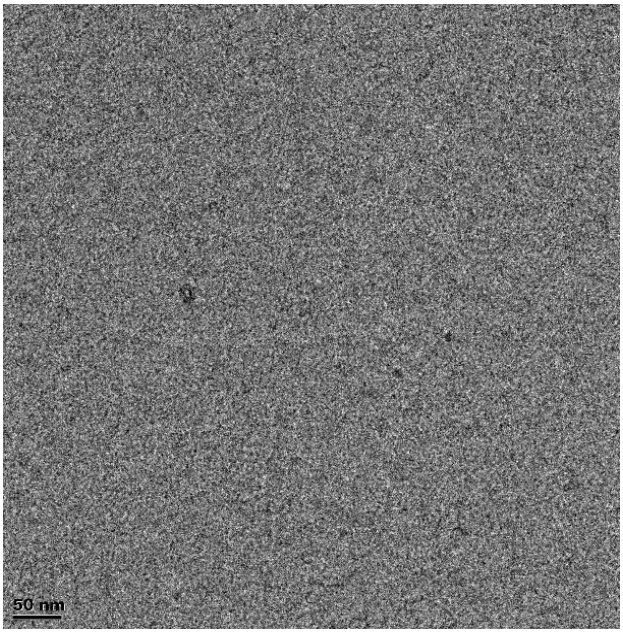

Figure 2.4: Transmission electron microscopy analysis and size distribution of *E. coli* produced PCV-2 VLPs. A: Virus-like particles of PCV-2 CP visualised under TEM with scale bars are 50 nm. Particles are indicated by yellow arrows. **B:** Lack of virus-like particles from pProEX-HTc empty vector.

2.4 Discussion

VLPs mimic the structure of the native virus and induce a similar immune response. Their ability to do this as well as elicit large quantities of antibodies within a host, make them suitable vaccine candidates (Guo et al., 2022). Additionally, their ability to elicit both an innate and adaptive immune response, make them great candidates for studying immunological processes of a host. In comparison to other expression systems, such as yeast, plants or insects, *E.coli* proves highly beneficial (Yang et al., 2021). This is because of its potential for expressing large protein outputs at a low cost, ease to upscale and its fast growth rate. However, expression of foreign genes in *E.coli* may be difficult due to the nuclear localization signal (NLS) found in the N-terminus of the PCV-2 capsid protein which is rich in arginine residues and may result in problems for full length PCV-2 CP expression. It is, therefore, important that codons are optimized to overcome this difficulty and ensure best protein expression (Liu et al., 2001).

Work conducted by past Biopharming Research Unit student Gunter 2017, optimized the full-length CP gene for *E.coli* codon to ensure efficient protein expression. The subsequent recombinant protein contained an N-terminal 6 x His, spacer region and recombinant tobacco etch virus (rTEV) protease cleavage sites fused as part of the pProEX-HTc expression system. The affinity tags were added to either detect the PCV-2 CP or aid in its purification. However, due to the improved purification technique shown in this work, by completing an additional round of BugBuster and ultrafiltration, the affinity tags were not utilized for its intended purpose. The gene codon optimisation preserved the N-terminus to ensure correct protein folding. Addition of the affinity tags did not show any interference with the protein folding process.

The recombinant PCV-2 CP was successfully expressed by *E.coli,* evident by the thick band seen at approximately 27kDa on both the Coomassie stained gels and western blots (Figure 2.1A and 2.2A). However, many non-specific bands can be seen cluttering the gels for both the PCV-2 CP sample and negative control (empty vector). The additional purification steps resulted in a sample that was less contaminated by *E.coli* specific proteins (as seen in Figure 2.1B and 2.2B). BugBuster is a protein extraction reagent that offers a gentle, non-

mechanical extraction of proteins from bacterial cells (Grabski et al., 1999). This simple and low-cost approach to extract and recover protein, denatures the bacterial cell wall without disrupting the proteins. The addition of ultrafiltration also proved beneficial in purifying the sample, as this process removed many unwanted proteins both larger and smaller in size than the PCV-2 CP. Ultrafiltration does not involve the use of heat or phase change, protecting proteins from exposure to harsh conditions, thus preserving the native structure of the protein (Berthelot et al., 2024). The PCV-2 CP proved to be insoluble and formed as inclusion bodies. This was evident by the formation of insoluble particles. Inclusion bodies are known to consist of a pool of proteins, cell debris, misfolded proteins and nucleic acid. Inclusion body formation may be associated with high rates of protein expression due to the use of efficient expression vectors that contain strong promotors, such as the *lac* (lactose) operon or optimizing codon usage (Bhatwa et al., 2021). Despite the presence of inclusion bodies, high PCV-2 CP yield and quality was obtained (as seen in the TEM image of Figure 2.4A).

Bredell et al., 2016 showed that the pProEX-HT vector was highly efficient in being translated in *E.coli* expression systems. The pProEX expression vector is a suitable choice for *E.coli* as it allows for the *lac* operon-derived promotor to regulate expression of the gene of interest. The addition of IPTG, a lactose metabolite, triggers transcription of the *lac* operon, as it induces protein expression (Gomes *et al.,* 2020). This popular system is mainly used due to its high expression levels, where up to 50% of total protein can be the protein of interest (Rosano and Ceccarelli, 2014). This was evident from the concentration of PCV-2 CP calculated in Figure 2.3A-C, which showed a yield of approximately 0.541 $mg.ml^{-1}$ that made up approximately 54% of the total proteins expressed. This was greater than the yields of a past study, conducted by past student Gunter 2017, who obtained yields of 0.25 – 0.35 $mg.ml^{-1}$ from the *E.coli* expression of PCV-2 CP. These lower yields, however, may be attributed to further purification steps that included nickel affinity purification. This study, therefore, shows that the purification process followed in this work, yields good product of higher concentrations. Choosing appropriate *E.coli* strains for protein expression is important in achieving optimal protein yields. The BL21 (DE3) and K-12 strains of *E.coli* are widely used for protein expression (Rosano and Ceccarelli, 2014). The BL21 strain lack the Lon protease, which degrades many foreign proteins. Plasmid loss in this strain is also

prevented due to the *hsd*SB mutation and as a result DNA methylation and degradation is disturbed (Gottesman, 1996). The K-12 strain has shown to have plasmid stability as it is a *recA* mutant, where the recombination system of the bacteria causes instability. As can be seen, various benefits exist in the use of specific strains (Rosano and Ceccarelli, 2014). In this study the *E.coli* DH5α strain was used for PCV-2 CP expression. The protein yield may therefore be improved if other strains of *E.coli* are tested. Also, the many wash steps conducted in the purification process may have resulted in some protein loss. Despite the many washes and further purification steps, the final pellet cannot be considered pure despite a large portion of the pellet being expressed as PCV-2 CP. Of the total protein (inclusion body), nearly 46% is non PCV-2 CP.

With a higher percentage of total protein being PCV-2 CP and the observed purity of particles seen under the transmission electron microscope, the inoculation of Japanese quails with the protein was in order. Spherical VLPs of approximate size 11 to 17 nm in diameter can be seen in the TEM images in Figure 2.4A. The average size and shape of the particles are in line with other studies that also used the *E.coli* expression system as well as other systems. An average diameter of 17 nm spheres expressed in *E.coli* was shown in a study conducted by Mo et al., 2019. Li et al., 2023, showed PCV-2 spherical particles of approximately 17 nm in diameter when expressed in baculovirus expression system. Gunter et al., 2019, showed the same particles of approximately 16 nm in diameter expressed in plants.

From all analyses, it was obvious that the PCV-2 CP was at a much higher concentration that the other non-specific proteins and the partially purified protein was fit to be used as an antigen for the animal studies. Following injection of the antigen into quails, the immunological transcriptome could be analysed.

3. Chapter 3: Quail immunisation and PBMC isolation

3.1 Introduction

Japanese quails (*Coturnix japonica*) are the smallest member of the poultry group. Quails have an egg-to-body weight ratio greater than chickens. They have a growth mortality rate of 5 - 20 %, hatch ability rate of 60 - 70 % and fertility rate of 75 – 90 % (Caetano-Anolles et al., 2015). Quail farming requires lower capital investment in comparison to chicken or duck farming and quails have become a favourable source of nutrition due to their high egg quality which, boasts a higher nutritional value than chicken eggs and their meat is usually a delicacy amongst many communities (Nasar et al., 2016).

Their use as a laboratory animal model has been explored (Morris et al., 2020). Due to their many beneficial characteristics, quails have shown to have several advantages as scientific animal models as compared to chickens (Morris et al., 2020). They also adapt easily to artificial environments and perform better while undergoing surgery or clinical procedures. Unlike chickens, their cardiovascular system functions well while under anaesthesia, enabling them to endure greater levels of stress, thus providing greater scientific insights (Flores-Santin and Burggren, 2021). Quails have been shown to be an important model in disease research and have been used to study many human diseases such as necrotizing enterocolitis in neonates or albinism (Homma et al., 1968; Waligora-Dupriet et al., 2009). They have also been used to study avian influenza affecting other birds and humans (Morris et al., 2020).

Molecular mechanisms related to the immunity of the *Coturnix japonica* is poorly understood and is imperative in understanding the management of this species. With Japanese quails being regarded as a useful animal model for disease biology, identifying and studying the immune cells can provide great understanding into the functioning of the quail's ability to fight foreign invaders and recover from it. Peripheral blood mononuclear cells (PBMCs) are white blood cells that form a critical part of the immune system in fighting infection and defending the host from negative effects of pathogens or foreign bodies. This system consists of many cell types. Understanding their subclasses, classification and function are both limited and incomplete for avian species (Qu et al., 2022a). PBMCs are

isolated from whole blood samples and can either be used immediately or cryopreserved for downstream assays, such as scRNA-seq, to understand disease biology, amongst other things. It is imperative that factors that may affect the integrity of isolated PBMCs are well considered. Such factors may include the method of isolation, storage time and temperature of whole blood before isolation and anticoagulant used in blood collection (Yi et al., 2023). Navas et al., 2019, showed that the time taken from blood collection to PBMC isolation is one of the most important factors in immunological type studies as extended periods may result in changes in cytokine secretion, gene expression and T cell counts. An increase in neutrophils or granulocyte contamination has also been shown in prolonged blood storage ahead of PBMC isolation (Jerram et al., 2021). Yi et al., 2023, found that delayed PBMC processing had a greater impact on immune-related pathways, where inflammatory pathways were upregulated and IFN-γ and metabolic pathways were downregulated, which were shown in scRNA-seq data. PBMCs are important in studying various scientific aspects including vaccine development, disease biology, disease modelling and biomarker identification (Eschke et al., 2023).

Along with gaining a better understanding of the immunological responses by immunization, one can successfully raise antibodies in a suitable animal model as a by-product. Antibodies obtained from quail egg yolk is referred to as IgY and can move from the serum to the egg yolk in large quantities to provide passive immunity to their offspring (Kovacs-Nolan and Mine, 2004). Producing polyclonal antibodies by immunization creates lasting antibody titres in birds, lowering the need for regular booster injections. This reduces costs associated with animal welfare and continuous injections as well as less antigen needed (Esmailnejad et al., 2019). Due to the phylogenetic distance between mammals and avian, bird antibodies do not mediate inflammatory responses or interact with mammalian Fc receptors. Avian species are therefore good models for production of therapeutic antibodies (Esmailnejad et al., 2019).

This chapter focuses on inoculating two groups of Japanese quails with either partially purified PCV-2 VLPs expressed in *E.coli* or with PBS as the experimental and control groups, respectively. The purpose of conducting this animal study was to stimulate an immune response as well as raise antibodies against PCV-2 in Japanese quails. To study the immune

response, PBMCs were isolated from each group of quails to perform transcriptomic analyses. This was to gain an understanding of gene expression profiles, functions and pathways in Chapter 4. The purpose of this chapter was to ensure that the quail immune system was correctly stimulated against PCV-2 by specifically looking at anti-PCV-2 antibodies. Isolation of anti-PCV-2 antibodies was verified using western blot and ELISA and anti-chicken secondary antibody to confirm specificity. The PBMC isolation and purification was conducted using the Ficoll-Paque density gradient technique. Following a quality check, consisting of cell count and viability, cells were immediately prepared for use in the 10X Genomics single cell protocol.

3.2 Materials and Methods

3.2.1 Inoculation and sample collection schedules of Japanese Quails

To stimulate a PCV-2 specific immune response in quails, 7 weeks old, female Japanese quails (*Coturnix japonica*) were used. The birds were housed in pens at the Animal Unit at the Health Science Faculty, University of Cape Town. Following a 7-day acclimatization period, the first round of inoculations took place, as shown in Figure 3.1. To do this, equal volumes of Polygen Adjuvant and *E.coli* produced PCV-2 VLPs was combined to a final concentration of 20 $ug.ml^{-1}$ PCV-2 VLPs. Two hundred microlitres of the mix was injected into the breast muscle of each animal. For the study, nine quails were used as the experimental group. The same number of quails (from the same hatch group, were injected in the same way, with 1 x PBS (pH 7.4) instead of PCV-2 VLPs, as the control group. Birds were injected twice, fourteen days apart. Eggs were collected for a full week after two weeks from the second injection. Eggs were labelled appropriately and stored at 4 °C for further analysis. The external surface, yolk and albumin of the eggs were also inspected visually and eggs were weighted. For the bleeds, 400 µl of blood per quail was withdrawn from the wing veins on day 37 (16 days after booster injection) and pooled (per group) into EDTA purple top tubes (BD Vacutainer) for PBMC isolation. Additionally, 100 - 200 µl of blood per quail was withdrawn for serum isolation. All protocols were approved by the University of Cape Town Animal Ethics Committee (AEC protocol number: 022-031) as well as the South African Department of Agriculture, Land Reform and Rural Development (Section 20, reference number 12/11/1/7/2 (2761NT).

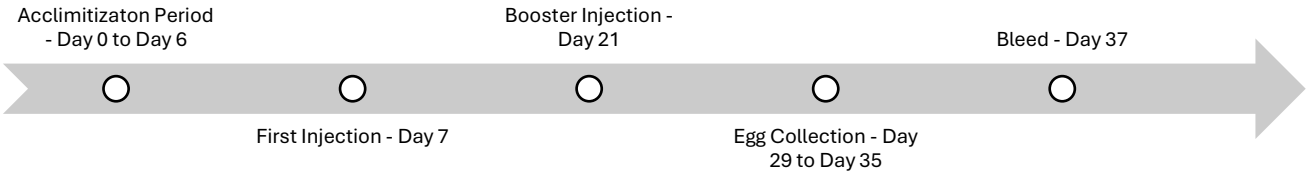

Figure 3.1: Inoculation and sample collection schedules of Japanese Quails. Timeline shows the acclimitization period, injection frequency and egg and blood sample collections during the duration of the experiment.

3.2.2 Serum isolation from whole blood

For serum isolation, 100 - 200 µl blood per quail was withdrawn into separate serum gold top collection tubes (BD Vacutainer). An additional tube was filled with pooled blood from each quail group. This was conducted on day 37 (16 days after booster injection). For pooled samples, approximately 100 µl blood per quail was pooled into one serum gold top collection tube. Separate and pooled samples were conducted for both PCV-2 and control quail groups. The gold top tubes, containing the whole blood samples, were then left to clot at room temperature for at least 30 minutes. Tubes were then centrifuged at 2000 x g for 10 minutes using the benchtop Eppendorf Centrifuge 5424. Supernatant (or serum) was then collected into separate, sterile, 1.5 ml tubes and stored at -20 °C for western blot and ELISA.

3.2.3 IgY isolation and purification from quail eggs

IgY was isolated and purified from quail eggs. This was done using 5 eggs that were collected, from both the PCV-2 and control groups, over a period of 1 week and stored at 4 °C. To isolate IgYs, yolks, from each group, were separated and pooled together. Yolks were diluted (1:7) with sterile tap water, pH adjusted to 5.0 with 0.5M HCl and then stored overnight at -20 °C. Frozen samples were then thawed at room temperature and filtered using Whatmann filter paper, Grade 1 (Merck). Thereafter, NaCl was added to the filtrate to 8.8%, pH readjusted to 4.0 using 0.5M HCl and precipitated for 2 hours at room temperature. Samples were then centrifuged at 3 700 x g for 20 minutes at 4 °C (Beckman Coulter, Avanti J-25I) and supernatant collected (protocol as per Hodek *et al*., 2013). Total IgY protein from the supernatant was then quantified using a Nanodrop (Model ND-1000) and stored at -20 °C for western blot and ELISA.

3.2.4 Antibody detection by western blotting

For antibody detection, recombinant PCV-2 VLPs, expressed in *E.coli,* was transferred to nitrocellulose membranes (as per protocol in Chapter 2). Membranes were then cut into strips according to each lane and separately probed with either **(a)** quail PCV-2 antisera or control group antisera (1:10 000) or with **(b)** IgY samples from experimental or control group (0.25 $mg.ml^{-1}$) by diluting in blocking buffer overnight at 4 °C. Blots were washed (as per protocol stated in Chapter 2) and incubated with anti-chicken alkaline phosphatase-conjugated secondary antibody (1:5000 dilution). Following an additional 4 x 15 minute washes in blocking buffer lacking milk, blots were developed for 30 minutes using NBT/BCIP substrate.

3.2.5 Antibody detection by indirect ELISA

For anti-PCV-2 antibody detection, indirect ELISA was performed. First, 100 µl of 0.2 $ug.ml^{-1}$ of *E.coli* produced PCV-2 VLPs, diluted in coating buffer (10 mM Tris pH 8.5), was coated onto a 96 well microtiter plate (Microwell MaxiSorp flat bottom plate, Sigma Aldrich). The plate was incubated at 4 °C, overnight with gentle agitation. The plate was then blocked with 200 µl of blocking buffer (6.05 g Tris, 8.76 g NaCl, dH_2O, 5% long life fat-free milk, pH 7.5) at 37 °C for 1 hour. Thereafter, 100 µl of primary antibody was added using either **(a)** quail PCV-2 antisera or control group antisera (between 1:312.5 to 1:10 000 dilutions) or **(b)** IgY samples from experimental or control group (between 0.03 $mg.ml^{-1}$ to 1 $mg.ml^{-1}$ dilutions) by diluting in blocking buffer at 37 °C for 1 hour. ELISA controls were conducted with wells that lacked either PCV-2 VLP (antigen) or primary antibody. All wells were conducted in triplicate and plates in duplicate. Plates were then washed 4 times with 200 µl of wash buffer (6.05 g Tris, 8.76 g NaCl, dH_2O, 0.05% Tween-20, pH 7.5), incubated at 37 °C for 1 hour with 100 µl of anti-chicken alkaline phosphatase-conjugated secondary antibody (1:5000 diluted in blocking buffer) and washed 4 x with 200 µl of final wash buffer (6.05 g Tris, 8.76 g NaCl, dH_2O, pH 9.0). Plates were then incubated in the dark, at room temperature for 30 minutes with 200 µl of SIGMAFAST™ p-Nitrophenyl phosphate substrate (Sigma Aldrich). Absorbance was finally read at 405 nm using a Bio-Tek Powerwave XS spectrophotometer.

3.2.6 PBMC isolation and purification

For PBMC isolation, fresh, whole blood samples were removed from EDTA purple top tubes (BD Vacutainer) into sterile 10 ml tubes. To ensure cells of a high quality were obtained, PBMCs were harvested from blood samples within 2 to 4 hours of blood draw. Blood was diluted with equal volumes of 1 x PBS (pH 7.4) then carefully overlayed on Ficoll-Paque Plus medium (Cytiva) by adding the dilute blood to the wall of a tilted centrifuge tube, to prevent the blood from mixing with the Ficoll medium. The Ficoll-Paque Plus is a sterile medium used for PBMC isolation by separating whole blood into its different components based on density gradient through centrifugation. All work was done at room temperature. Tubes were then immediately centrifuged at 400 x g for 30 minutes at 20 °C, using an Ultra centrifuge (Beckman Coulter, Opyima L-100 XP). After separation of the diluted blood, the PBMC layer appeared at the Ficoll and plasma interface (evident in Figure 3.2). The layer was carefully removed (by not disturbing the Ficoll layer) into sterile 2 ml Eppendorf tubes. At least 3 volumes of 1 x PBS (pH 7.4) were gently mixed with the PBMC sample and centrifuged at 100 x g for 10 minutes at room temperature using a benchtop centrifuge (Eppendorf Centrifuge 5424). Supernatant was removed and resulting cells (pellet) resuspended again in 3 volumes 1 x PBS (pH 7.4). Wash steps were conducted a total of 3 times and cells finally resuspended in 1 x PBS (pH 7.4) to reach desired concentration of approximately 1000 cells.ul^{-1} for single cell generation in Chapter 4. Cell count and viability was performed immediately after PBMC isolation. This was done by mixing an aliquot of PBMCs with an equal volume of trypan blue (Gibco Trypan Blue Stain 0.4%) (10 µl of cells + 10 µl of trypan blue, dilution factor = 2) for 1 minute at room temperature. Ten microliters of the stained sample was then added to a haemocytometer (Neubauer-improved, Superior Marienfeld) and viewed under a light microscope at 200X magnification. Both living and dead cells were counted. Cells that appeared blue were deemed as dead cells, while cells that appeared transparent were deemed as viable cells. The number of cells per millilitre was calculated using the following equation based on counts from each quadrant on the haemocytometer:

$$\text{Number of cells per ml} = (\text{quadrant 1} + \text{quadrant 2} + \text{quadrant 3} + \text{quadrant 4}) \div 4 \times 10\,000 \times \text{Dilution Factor}$$

Following cell count and viability determination, PBMCs were immediately used in the next step for single cell isolation (Chapter 4).

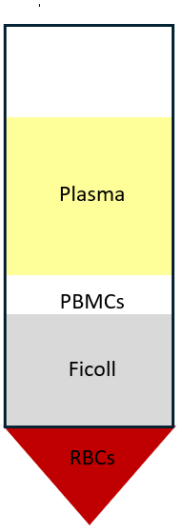

Figure 3.2: Representation of blood components separated after centrifugation using the Ficoll Paque Plus density gradient medium and centrifugation. This separation allows for PBMC retrieval from whole blood. The PBMC layer appears between the Ficoll and Plasma layers (evident as the white layer).

3.3 Results

3.3.1 Verification of elicited immune response by detecting antigen specific antibodies in serum and total IgY

To assess the presence of anti-PCV-2 antibodies in the quail blood and eggs, SDS-PAGE and western blot was conducted. Quails were split into two experimental groups, namely the PCV-2 and control groups. Quails injected with two rounds of *E.coli* produced PCV-2 VLPs formed the PCV-2 group while the control group consisted of quails that did not receive PCV-2 VLPs, but 1 x PBS instead. Quails were housed (as shown in Figure 3.3A) according to details stipulated in the approved Animal Ethics protocol.

Sera was collected on Day 37 (16 days after the booster injection). These samples were collected on the same day that blood samples were collected for PBMC isolation. Blood samples were collected from the wing vein of each bird, as shown in Figure 3.3B. Sera was isolated from fresh blood samples obtained from each individual bird as well as a pooled sample for both the PCV-2 and control groups. One bird of the PCV-2 group (bird identity number 22) had died on day 22 of the experiment (1 day after the booster injection). The

bird was found dead during the morning welfare check. It was recorded, following a post-mortem, that the bird had most likely died due to an adverse reaction from the injection the day before, as bruising at the injection site was noted. No other bird died for the remainder of the experiment due to this reason. It was therefore an isolated case, and no further action was necessary to safeguard the birds. One bird from the control group (bird identity number 14) was found dead on Day 5 of the experiment, during the acclimatization period. The post-mortem results stated that the death was most likely due to a burst crop abscess that was found on the animal which led to an empty gut and subsequent emaciation. This was also an isolated incident, with no other bird having presented a similar problem. These two deaths brought the number of birds to 8 birds per group. Additionally, eggs from both groups were weighed and was found to be between 10.2 to 12.8 g. No major difference in egg weight or visual quality of egg yolk or albumin was noted between the two groups, suggesting that the quails in the PCV-2 group may have experienced only mild levels of stress.

A

B

Figure 3.3: Animal studies involved the use of Japanese quails (*Coturnix japonica*) for antibody and immunological investigations. **A:** Nine Japanese quails per group were inoculated with *E.coli* produced PCV-2 VLPs or PBS. Quails were housed in separate groups according to the detailed protocol stated in the approved Animal Ethics. **B:** For sera and PBMC isolation whole blood was collected from the wing vein of each quail.

Confirmation of anti PCV-2 antibodies raised in quails, in the serum samples can be seen in Figure 3.4A. Each lane of the western blot in Figure 3.4 was cut and individually probed with the various sera from each quail. As noted in Figure 3.4A, a clear band at approximately 27 kDa was visible in lanes 4, 6, 8, 10, 12, 16 and 18 representing birds' number 20, 21, 23, 24, 25, 27 and pooled, respectively. A very faint band can be seen at the correct size in lane 14 representing bird number 26. This indicated that 7 of the 8 birds in the experimental group elicited the specific antibody response, thus showing that the two injection doses stimulated an immune response specific to PCV-2. The darkest band at the 27 kDa position, can be seen in lane 4, representing bird number 20. This may imply that bird number 20 elicited the highest level of anti-PCV-2 antibody. No bands at 27 kDa can be seen in Figure 3.4B, proving that none of the birds in the control group produced anti-PCV-2 antibodies either naturally or by injection. The pooled sample in the control group also showed no band at 27 kDa.

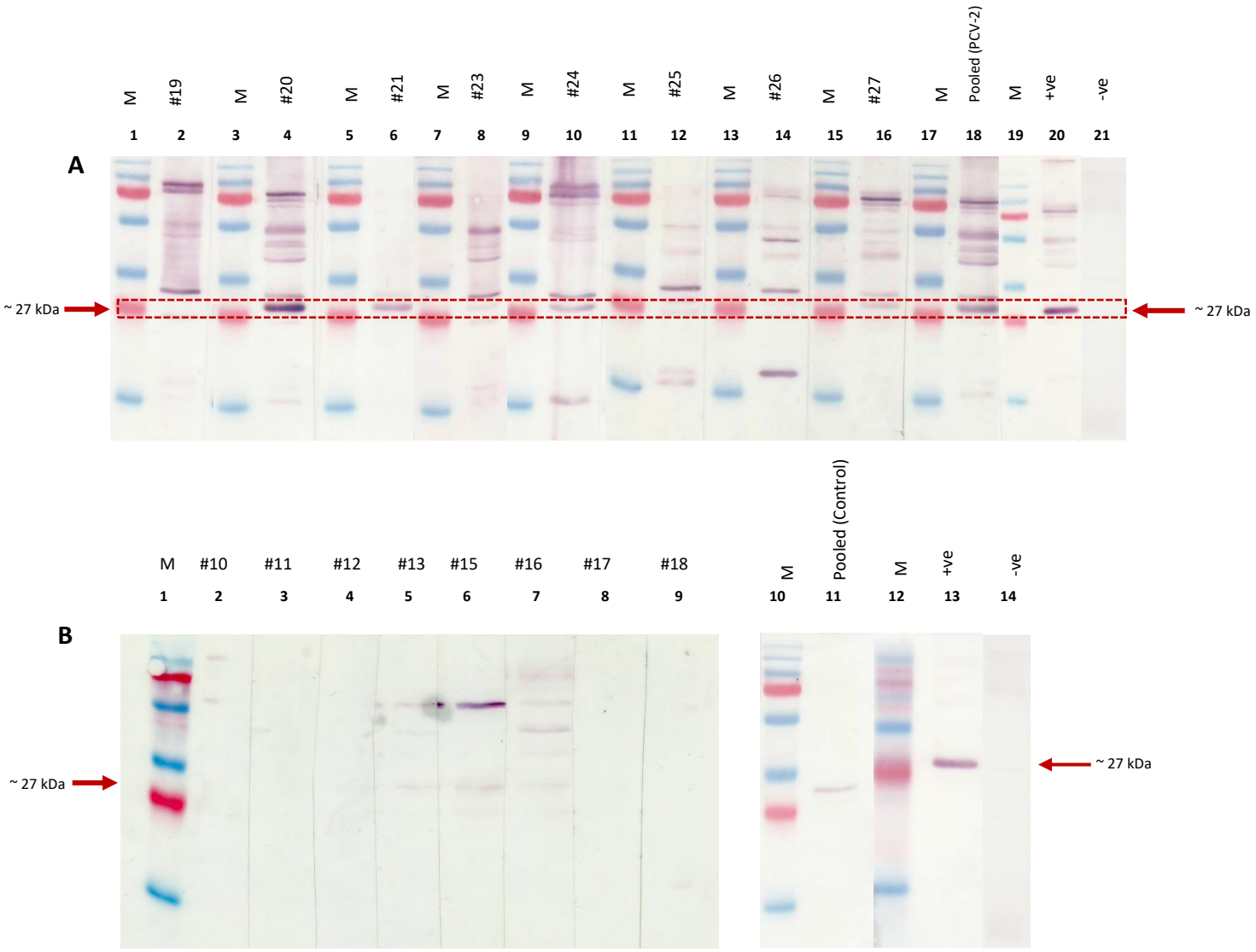

Figure 3.4: Confirmation of anti PCV-2 antibodies raised in quails (sera samples). Western blots of *E.coli* produced PVC-2 VLPs, probed with diluted sera from quails immunised with either PCV-2 VLPs or PBS (control group). Each lane of the western blots were cut and individually probed with the different sera. A band of approximately 27 kDa was present in lanes representing the individual quail sera samples as well as pooled sera sample of PCV-2 group. No band was seen in the individual quail sera samples or pooled sera sample of the control quail group. **A:** Probed with quail antisera from PCV-2 group (1:10000 dilution) and anti-chicken alkaline phosphatase-conjugated secondary antibody (1:5000 dilution). **B:** Probed with quail antisera from control group (1:10000 dilution) and anti-chicken alkaline phosphatase-conjugated secondary antibody (1:5000 dilution). **M:** pre-stained protein ladder. **+ve:** Probed with mouse PCV-2 antisera (1:1000 dilution) and goat anti-mouse alkaline phosphatise-conjugated secondary antibody (1:5000 dilution). **-ve:** Immunoblot of protein from pProEX-HTc empty vector, probed with mouse PCV-2 antisera (1:1000 dilution) and goat anti-mouse alkaline phosphatise-conjugated secondary antibody

A western blot with *E. coli* produced PCV-2 VLPs was also probed with IgY isolated from quail eggs, collected during the same time for a period of one week. The total IgY was isolated from 5 pooled egg yolk samples per group and tested for the presence of anti-PCV-2 antibodies. Similar results can be seen in Figure 3.5, where anti-PCV-2 antibodies were detected in eggs of the PCV-2 group. This can be noted in a band present at approximately 27 kDa. No band of a similar size were detected in the lanes representing IgY from the eggs of the control group or the empty vector negative control. The diluted serum samples and diluted IgY samples were able to bind to the *E.coli* produced PCV-2 VLP confirming the successful production of anti-PCV-2 antibodies in the quails injected with the PCV-2 VLPs. The antibody binding was specific to the *E.coli* produced PCV-2 VLPs, with detection at approximately 27 kDa and few non-specific binding of other proteins. Some unwanted, background proteins with non-specific binding was present in both the serum and IgY samples, with more bands seen in the serum samples than IgY sample. Some non-specific binding was noted in the serum and IgY control group samples too, but no PCV-2 signal was noted.

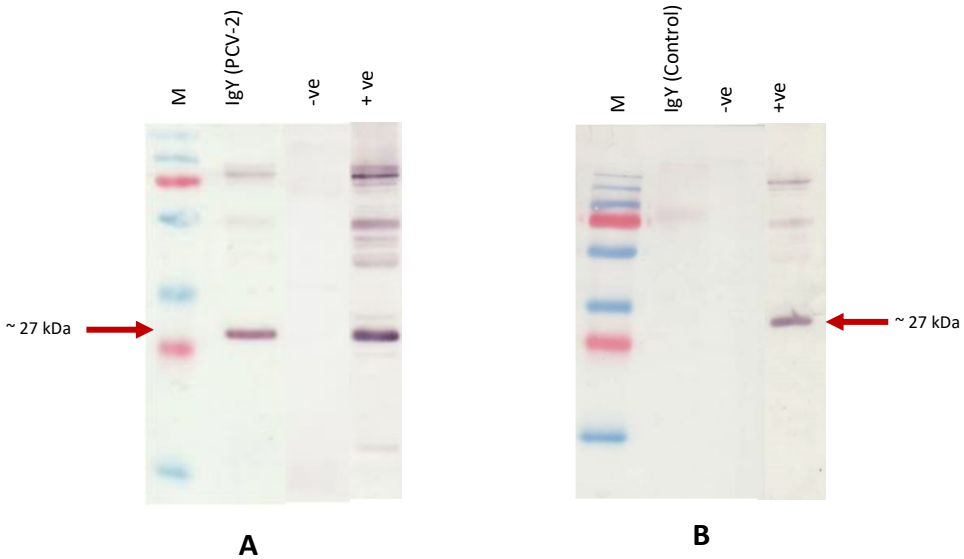

Figure 3.5: Confirmation of anti-PCV-2 antibodies raised in quails (IgY samples). Western blots of *E.coli* produced PVC-2 VLPs, probed with diluted IgY from quails immunised with either PCV-2 VLPs or PBS (control group). Each lane of the western blots was cut and individually probed with the different antibody. A band of approximately 27 kDa was present in lanes representing IgY from eggs of the PCV-2 group. No band was seen in the lane representing IgY from eggs of the control quail group. **A:** Probed with quail IgY from PCV-2 group (0.25 $mg.mL^{-1}$ dilution) and anti-chicken alkaline phosphatase-conjugated secondary antibody (1:5000 dilution). **B:** Probed with quail IgY from control group (0.25 $mg.mL^{-1}$ dilution) and anti-chicken alkaline phosphatase-conjugated secondary antibody (1:5000 dilution). **M:** pre-stained protein ladder. **+ve:** Probed with mouse PCV-2 antisera (1:1000 dilution) and goat anti-mouse alkaline phosphatise-conjugated secondary antibody (1:5000 dilution). **-ve:** Immunoblot of protein from pProEX-HTc empty vector, probed with mouse PCV-2 antisera (1:1000 dilution) and goat anti-mouse alkaline phosphatise-conjugated secondary antibody (1:5000 dilution).

3.3.2 Verification of elicited immune response by ELISA

Determination of a PCV-2 specific adaptive immune response, from individual quails, immunized with the *E.coli* produced PCV-2 VLPs, was tested by indirect ELISA. Ninety six well plates were coated with the *E.coli* produced PCV-2 CP, and were finally incubated with various serum or IgY dilutions. This was conducted for samples from the PCV-2 and control groups from individual quails, pooled samples and IgYs. The ELISA was conducted to examine the presence and specificity of anti PCV-2 antibody in both blood and eggs. From the results depicted in Figure 3.6A, the antibody was detected in the serum samples from each individual quail in the PCV-2 group, albeit in low concentrations in the blood samples. No cross reactivity was observed in the control wells, with higher absorbances noted in the PCV-2 group. At a dilution of 1:312 quail number 20 showed to have the greatest absorbance (OD_{405} ~0.270) followed by quail number 26 (OD_{405} ~0.252). This is in accordance with the high intensity of the band in the western blot for quail number 20. From the blood samples, it can be noted that antibody levels of the individual quails, as well as pooled samples, from the PCV-2 quail group, was higher than the control group. Absorbance levels across all the samples in Figure 3.6A and Figure3.6B were corrected by subtracting the absorbance value of the blank wells. Samples of each individual quail was greater than the control quail group which showed that every quail in the PCV-2 group elicited an immune response specific to PCV-2. No anti-PCV-2 response was noted in the control quail group. Similar results can be seen in Figure 3.6B showing absorbance readings of samples obtained from the quail eggs of the PCV-2 and control groups. The absorbance readings of the IgY sample from the PCV-2 group (OD_{405} ~ 0.511 at a concentration of 1 $mg.ml^{-1}$), was greater than absorbance readings from IgYs in the control quail group. These absorbance reading were also greater than all the serum samples including the pooled serum samples (also at the lowest dilution). The anti-PCV-2 antibody binding titre was determined as the reciprocal of the maximum dilution that shows an immune response with absorbance readings greater than the corresponding PBS control at a 1:312 dilution for sera and a 1 $mg.ml^{-1}$ dilution for IgY. A titre of 5000 was observed for anti PCV-2 sera.

A

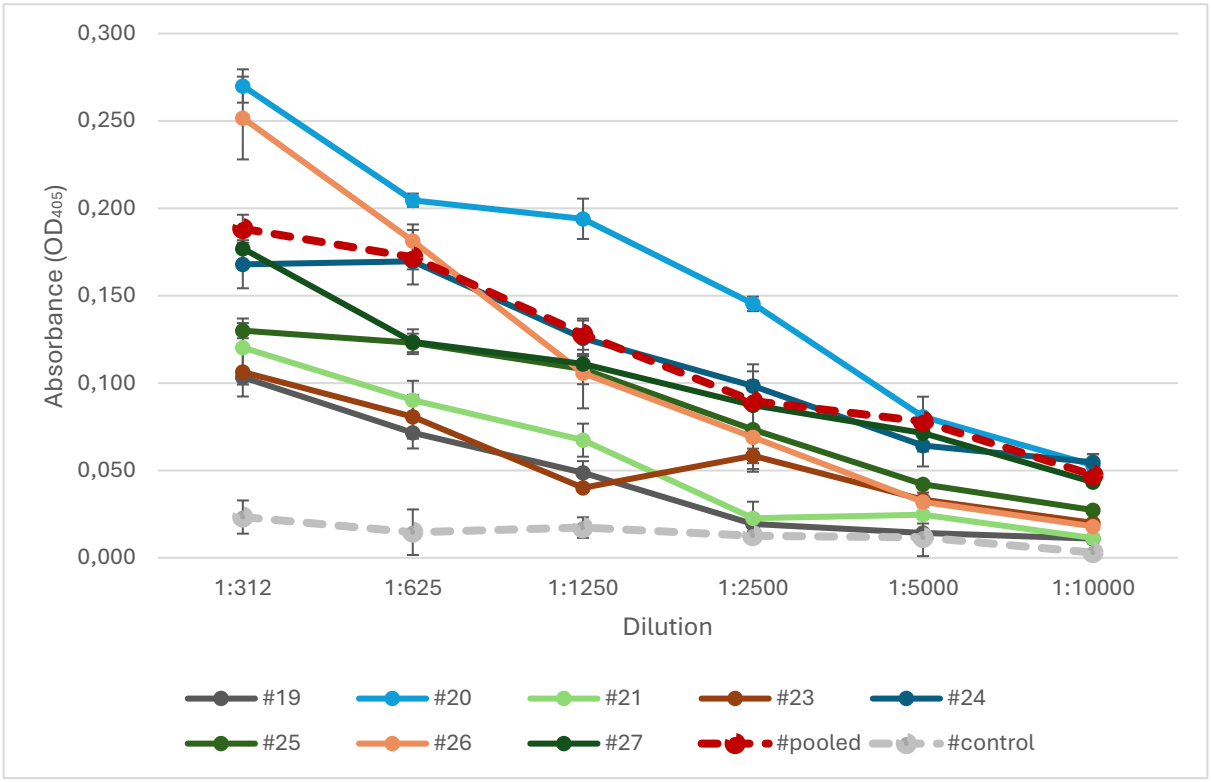

B

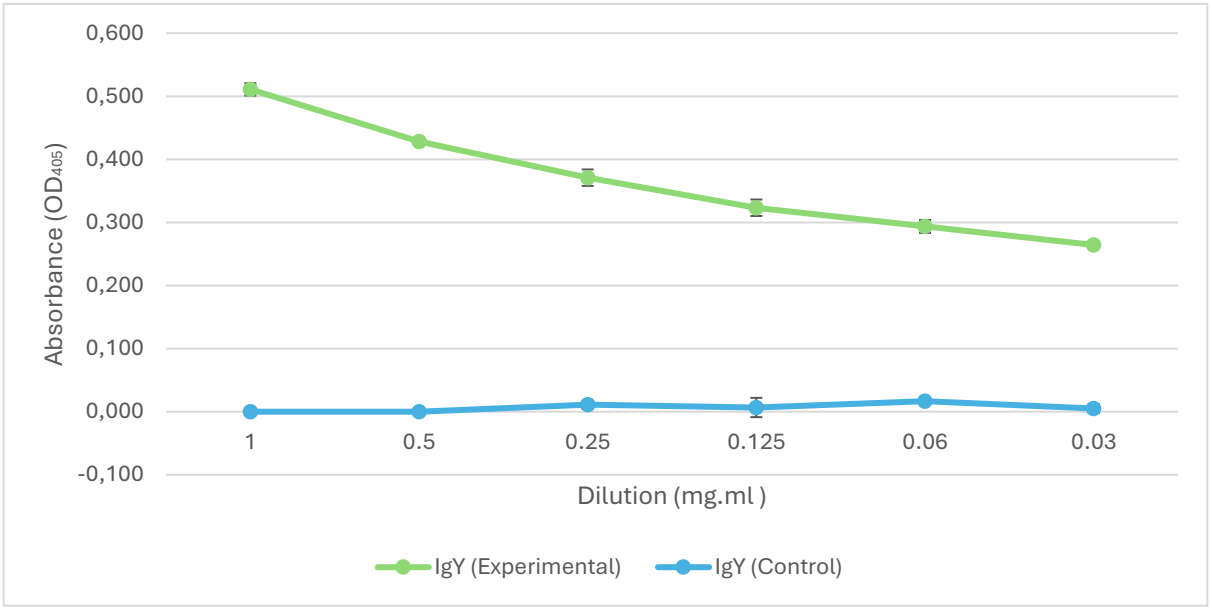

Figure 3.6: Indirect ELISA using quail sera or IgY from experimental (PCV-2) and control groups. Plates were coated with PCV-2 VLPs as the antigen, diluted sera or IgY (as primary antibody) and anti-chicken secondary antibody (1:5000). **A:** Dilutions of individual quail sera samples and pooled sera samples from experimental (PCV-2) and control groups. **B:** Dilutions of IgY from experimental (PCV-2) and control groups.

3.3.3 Cell viability and quality

PBMCs were isolated from fresh, pooled blood samples of 8 quails per group. The PBMCs were isolated within 3 hours of blood draw to ensure cells of a high quality were obtained for the subsequent scRNA-seq steps in Chapter 4. PBMCs were isolated using density gradient medium centrifugation that allowed for clear separation of white blood cells (immune cells) from undesirable blood components as indicated by the white layer in Figure 3.7.

To determine cell viability, Trypan blue stained cells were counted on a haemocytometer placed in a light microscope. Both viable and dead cells were counted. As per Table 3.1, the number of viable cells recovered for the PCV-2 group was 1 500 000 cells.ml^{-1} and 1 347 500 cells.ml^{-1} for the control group. The percentage viability of recovered cells was 92.2% and 90.3% for the experimental and control groups, respectively.

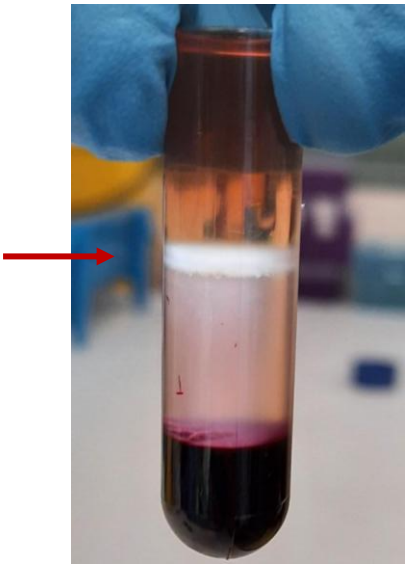

Figure 3.7: Separation of fresh, whole blood into its various components. Peripheral blood mononuclear cells isolated using density gradient medium centrifugation. The white layer (indicated by the red arrow) is the PBMC layer found at the Ficoll and plasma interface.

Table 3.1: Total number of viable PBMCs and percent viability of recovered cells for each quail group following PBMC extraction from whole blood.

Sample	Number of samples	Number of viable cells recovered (per ml)	Percentage viability of recovered cells
PCV-2 group	1 pooled sample	1 500 000	92.2 %
Control group	1 pooled sample	1 347 500	90.3 %

3.4 Discussion

Many animal species are used in research to enhance developments in the medical and scientific fields (Domínguez-Oliva et al., 2023). Fields including therapeutics, vaccine development and immunology are popular targets for animal models and address current threats to humans and animals. Animals popularly used include rabbits, mice, pigs, rats, horses, monkeys, hamsters, fish, frogs, fruit flies and birds, among others (Jota Baptista et al., 2021). Birds have been a key model in understanding biological and genetic functions in many medical fields involving immunological functions and infectious disease (Flores-Santin and Burggren, 2021; Wu et al., 2016).

In this study, Japanese quails were injected with *E.coli* produced PCV-2 VLPs to produce PCV-2 specific antibodies in quail egg yolks and serum and thereby elicit an immune response that was studied with immunoassays (such as western blot and ELISA) and later scRNA-seq (Chapter 4). Two injections were administered to each bird in the breast muscle to stimulate a specific, adaptive immune response towards PCV-2. Following immunization, quails appeared well, albeit one quail in the PCV-2 experimental group, died following the first injection. It was reported in the post-mortem results that the bird had most likely died due to an adverse reaction from the injection, as bruising at the injection site was noted. No other bird died for the remainder of the experiment due to this reason. It was noted that birds in the PCV-2 experimental group laid fewer eggs (within the research period) compared to the control group. This may have been due to stress caused by the combination of antigen and adjuvant specifically, as that combination was the only difference between the two groups. Quails from both groups were housed and fed in the exact same manner but in separate pens adjacent to each other. All birds were handled by the same person each

time in the exact same manner and received the same amount of light, ambient temperature and ventilation. Injection composition, for both groups, were the same except for the PCV-2 VLP antigen that was added to injections of the PCV-2 experimental group. Many of the eggs from quails in the PCV-2 group displayed a white residue on the shells, which was most likely a calcium coating (Gautron et al., 2021). This may occur when eggs remain in the gland for too long when hens hold on to the egg for a longer period due to stress. For these reasons, it appeared that quails in the PCV-2 group may have experienced more strain or unknown health issues compared to quails in the control group A possible reason for this strain is the combination of the PCV-2 VLP antigen and adjuvant that was injected. However, despite these two signs of possible stress, there were no other visible signs of stress such as feather pecking, weight loss or aggression, as commonly seen in stressed birds (Hedlund and Jensen, 2022). Previous research has shown that a reduction in egg quality or egg weight is a known sign of stress (Mashaly et al., 2004). Eggs from both groups showed no major difference in weight and no visual differences from the egg inspections were noted. This indicated that the birds most likely did not experience high levels of stress, as shown in research conducted by Mashaly et al., 2004.

Following immunization, sera and egg samples were collected and total IgY isolated from the eggs. The detection of a protein of approximately 27 kDa on the western blot, by serum from the PCV-2 group, revealed presence of the anti-PCV-2 antibody. Bands were visible in serum samples of majority of the quails (7 out of 8 birds) as well as the pooled sera and pooled egg yolk samples. The anti-PCV-2 antibodies were specific to the corresponding antigen with moderate cross-reactivity to other *E.coli* proteins, as seen by the darkest band at the 27 kDa size in Figure 3.4 and Figure 3.5 and other fainter bands of different sizes. The band intensity was greater in samples isolated from some birds and less visible in other birds from the PCV-2 group. The darkest band was noted in bird number 20 with no band visible in bird number 19 even when tested with varying concentrations of primary and secondary antibody (results not shown). This may have been caused by genetic differences in response to the vaccine, which indicates that the quails were not genetically identical despite being from the same hatch group and therefore elicited a different immune response. Another reason may have been because of using anti-chicken alkaline phosphatase-conjugated secondary antibody instead of an anti-quail secondary antibody. Using an anti-quail

secondary antibody may have been more specific and resulted in better binding with the primary antibodies. Unfortunately obtaining an anti-quail secondary antibody for this work, was not possible.

Overall, the presence of the band at the correct size indicated that the quails elicited an immune response specific to PCV-2. An immune response was achieved by the production of antibodies. The IgY of birds are a major type of antibody and is usually the main antibody circulating the blood system (Wang et al., 2004). To our knowledge, no previous research is available on Japanese quails injected with PCV-2 and having PCV-2 specific antibodies.

Egg and serum samples were collected approximately two weeks after the booster injection and animals received a total of two injections. This was because a previous study, injecting quails with formalin or heat-inactivated *Salmonella* immunogens, showed that antigen specific IgYs begin to increase in the egg yolks from the second week after the first injection (Esmailnejad et al., 2019). Another study showed that quails produced higher levels of specific antibody (anti-*H. pylori*) after the second immunization (Najdi, et al., 2016). These studies were used as a guide in determining the immunization regime to elicit a desirable adaptive immune response. As a result of avians protecting their offspring by passive immunity, antibodies are transferred to the egg yolk from the blood stream. A possible reason for the two-week period, after which increased levels of the specific IgY is detected in the yolk, may correspond to the time taken for specific antibodies to be transferred from the serum to the yolk (Esmailnejad et al., 2019). In the present study, anti-PCV-2 antibodies were not detected in a western blot or ELISA from eggs collected just one week after the first injection (results not shown). Bands of the correct size were only visible two weeks after the booster injection. This period of initiating the adaptive immune response coincides with the study conducted by Esmailnejad *et al.*, 2019.

Following the western blot, ELISA was conducted to confirm immunoreactivity and specificity of the isolated anti-PCV-2 antibody from both the serum and egg yolk samples. The serum and egg yolk samples were diluted in 1 x PBS to reach concentrations ranging from 1:312 to 1:10 000 for serum and 1 $mg.ml^{-1}$ to 0.03 $mg.ml^{-1}$ for the egg samples. Separate serum samples from each individual bird and a pooled serum sample, of the

experimental quail group all had the greatest absorbance (using OD_{405nm}) at the lowest dilution of 0:312. Due to the limited amount of blood withdrawn from each bird, running assays at a lower dilution was not possible because of the low sample volumes. Higher absorbance readings may have been possible if more serum was available to make lower dilutions. Obtaining higher samples volumes, by either increasing the number of animals used or using serum samples for antibody detection only and not sharing it for other tests, could be conducted in a future study to improve results. The egg yolk sample also had the greatest absorbance at the lowest dilution as expected. The absorbance levels for all samples were low, with the highest sera OD reading being ~0.270 for quail number 20, ~0.252 for quail number 26 and ~0.188 for the pooled sample. Despite there being a very light band for quail number 26 in the western blot, the ELISA results were very high. With no visible band of 27 kDa for quail number 19 in the western blot, the ELISA showed a reading greater than the control. This confirmed that all the birds elicited an immune response against PCV-2. The absorbance of the IgY (egg yolk sample) was higher at ~0.511 for the lowest dilution of 1 $mg.ml^{-1}$. Absorbance levels across all the samples in Figure 3.6A and Figure3.6B were corrected by subtracting the absorbance value of the blank wells. No readings of higher values were observed in the blank wells nor wells from the control quail group. This showed that no reactivity was noted in quails from the control group. All other samples, had a reading greater than the control, proving that all quails elicited an immune response against PCV-2. Additionally, this showed that the *E.coli* produced PCV-2 VLPs had some immunogenicity in quails but stimulated low levels of PCV-2 antibody. The light bands noted in the western blots and low absorbance readings in the ELISA, may have been as a result of using anti-chicken alkaline phosphatase-conjugated secondary antibody instead of an anti-quail secondary antibody.

The higher anti-PCV-2 antibody levels in the egg yolk compared to the serum samples may suggest that it is a better sample for antibody extraction. Extracting antibodies from eggs is non-invasive, less stressful to the animal and, cheaper. This form of antibody isolation is commonly done with chickens and ducks (Somasundaram et al., 2020). Studies have shown that chickens can produce 100-150 mg of antibodies per egg yolk (Lee et al., 2017; Rahman et al., 2013). In the present study, 7.72 mg was isolated per egg yolk using an extraction method by tap water followed by precipitation with sodium chloride (as described by Hodek

et al., 2013). A total of 6 pooled yolks were used per isolation yielding a total of 46.32 mg (or approximately 7.72 mg per egg yolk) resulting in a much lower concentration compared to that obtained in the studies done with chicken eggs. This reduction may be because the quail antibody production was low or may more likely be due to technical errors experienced during the isolation method. Additionally, no previous study has immunized Japanese quails with PCV-2 VLPs to isolate anti-PCV-2 antibodies. Therefore, a comparative quantity of specific or total IgYs are difficult to compare. From the western blot and ELISA results it must be noted that a considerable yield and specificity was achieved by production of the anti-PCV-2 antibodies. Despite chickens being able to produce bigger yolks (and possibly higher antibody concentrations) compared to quails, quails have several advantages over chickens, such as being more resistant to many diseases, reaching sexual maturity at a younger age, and are cheaper to breed, amongst other benefits (Najdi et al., 2016).

Most studies have used ELISAs to detect anti-PCV-2 antibodies (using PCV-2 VLPs) in swine and mouse models (Li et al., 2023; Wu et al., 2016). Very few studies have used bird IgYs to study immunoreactivity and specificity against PCV-2, and no study to our knowledge, have used Japanese quails as the animal model in this regard. It is, therefore, necessary to explore more animal models that may hold greater benefits than the traditionally used models.

Along with isolating serum from the pooled whole blood samples, PBMCs were also isolated. The PBMCs were isolated to study the transcriptome of the elicited immune response in quails (work shown in Chapter 4). This entailed a study of the transcriptome of the immune cells to better understand the gene expression profiles, functions and pathways associated with PCV-2.

PBMCs are heterogenous populations that comprise many cell types specific to the immune system. These cells, found in whole blood, can be isolated using density gradient centrifugation. Layering fresh, diluted blood on a density gradient medium, such as Ficoll, allows for denser cells to be separated from the less dense PBMCs, where PBMCs separate into a layer between the Ficoll and plasma. Clean removal of the PBMC layer and subsequent wash steps ensure that little contaminating cells are picked up. To ensure isolation of a superior PBMC sample with high cell viability, cells were isolated within 3 hours of blood

withdrawal. Additionally, the diluted blood was gently overlaid on Ficoll to prevent mixing and subsequent cell death. Ficoll was stored away from light and aseptic technique was followed. During centrifugation, the rotors were properly balanced to prevent unwanted vibration, thus decreasing the chance of layers mixing or cell yield being negatively affected. These steps helped improve cell yield and viability as demonstrated by work done by Tan and Lei, 2019. In the present study, the isolated viable PBMC fraction from the quail blood sample was 1.3 to 1.5 × 10^6 PBMCs.ml^{-1}. These were the viable cell proportion isolated from a total of 3.2 ml of undiluted, whole blood. Cell viability of more than 90% was achieved for both sample groups, which was within the limits needed for scRNA-seq using the 10X Genomics protocol. As per the 10X Genomics Single Cell Protocols Cell Preparation Guide (Documents CG00053), a sample viability of at least 70% is required. Due to the short storage period of the blood and maintaining the sample, as well as performing the isolation at room temperature, cell viability was high. This is in accordance with other studies that showed high cell recovery and viability when isolating PBMCs within 8 hours of blood withdrawal and storing blood at room temperature (Olson et al., 2011). Storing blood for longer than 8 hours, reduces cellular function (Bull et al., 2007).

Cell count and viability is crucial for ensuring a successful scRNA-seq workflow. For this reason, manual counting was done. Manual cell counting, using a haemocytometer, and staining with Trypan blue, is a precise method (Hanamsagar et al., 2020). Automated cell counters (using fluorescence) may be easier but generally overestimates counts thus proving less accurate.

Few studies have shown the benefit in using quails for immune response investigations against pathogens despite the many advantages that quails have over other animal models (Esmailnejad et al., 2019). From the analyses, it can be noted that Japanese quails were able to elicit a specific immune response to PCV-2 when injected with two doses of PCV-2 VLPs. Antibodies were easily studied and isolated from both blood and egg yolk and anti-PCV-2 antibody easily detected from these samples. Additionally, viable PBMCs were successfully isolated in high concentrations from quail whole blood.

4. Chapter 4: Quail PBMC transcriptomic analysis using scRNA-seq

4.1 Introduction

Immunity is a systematic response of the body to safeguard itself against harmful agents by employing lines of defence against foreign invaders such as microbes, viruses or toxins. It does this while, still able to distinguish and spare symbiotic and essential microbes and their components within the body (Swiatczak and Cohen, 2015). Innate and adaptive immunity are the two lines of defence of the immune system, as shown in Figure 4.1. These two complementary systems consist of the innate response, representing the first line of defence, and the adaptive response which is secondary and more specialised. Despite their intricacies, these systems may become defective, resulting in host vulnerability or improper reactions (Marshall et al., 2018). A clear understanding of the cellular types and their functions, in both healthy and compromised hosts are therefore important.

The innate immune response comprises of skin, mucous membranes, physiological barriers and some immune cells (Marshall et al., 2018). The skin and mucous membranes are physical barriers that protect invaders from entering the body and attaching to any internal surface. The physiological defences involve increased body temperature, lowered pH levels and increased levels of inflammation. The cellular component consists of phagocytes (neutrophils/heterophils, dendritic cells, macrophages and monocytes) and natural killer (NK) cells (Marshall et al., 2018). These cells act, if the foreign invader overcomes the physical barriers. This response is non-specific and protects against all foreign threats. With the innate immune response having no immunogenic memory, it is incapable of recognising infecting threats in recurrent interactions. This system is fast to respond by detecting and destroying the threat immediately or within a few hours (Wang et al., 2024). A large aspect of the innate immune response relates to inflammation. Inflammation occurs when immune cells release substances at the site of infection or injury, causing the blood vessels to widen. Inflammation is triggered by the production of cytokines and chemokines, which mobilize other innate defence mechanisms involving tumour necrosis factor (TNF) and various interleukin (IL) components (Wang et al., 2024). Phagocytosis, driven by macrophages and heterophils, is a mechanism where the immune cells engulf and kill pathogens or infected cells as well as remove cell debris (Turvey and Broide, 2010). The subsequent action of

phagocytosis may activate the adaptive immune response via activation of antigen-presenting cells (APCs). Lastly, NK cells induce cell apoptosis and cytokine production. NK cells are not involved in antigen presentation and therefore, do not express any receptors involved in antigen presentation. These cells are destined to kill virus-infected or cancerous cells, by releasing granzymes and perforin or initiating apoptotic pathways (Wang et al., 2024).

The adaptive immune response consists of T cells and B cells. This response is specific (to a particular invader, antigen or immunogen), may produce a variety of antibodies (to different invaders) and has memory (against recurrent invaders) (Chaplin, 2010). Aided by the innate immune response, adaptive immunity assists in pathogen elimination. Due to its specificity and dependency on an antigen, a delayed response is characteristic of adaptive immunity, from the moment of antigen exposure to its full immune reaction (Wang et al., 2024). However, the adaptive immune system has immunogenic memory, thus enabling a faster and more efficient response for future recurrences (Marshall et al., 2018). Proliferation of T cells take place via the action of the APCs, while B cells separate into plasma cells that produce antibodies or memory B cells. T cells differentiate into T helper cells (Th cells), regulatory T cells, cytotoxic T cells and memory T cells (Erf, 2004).

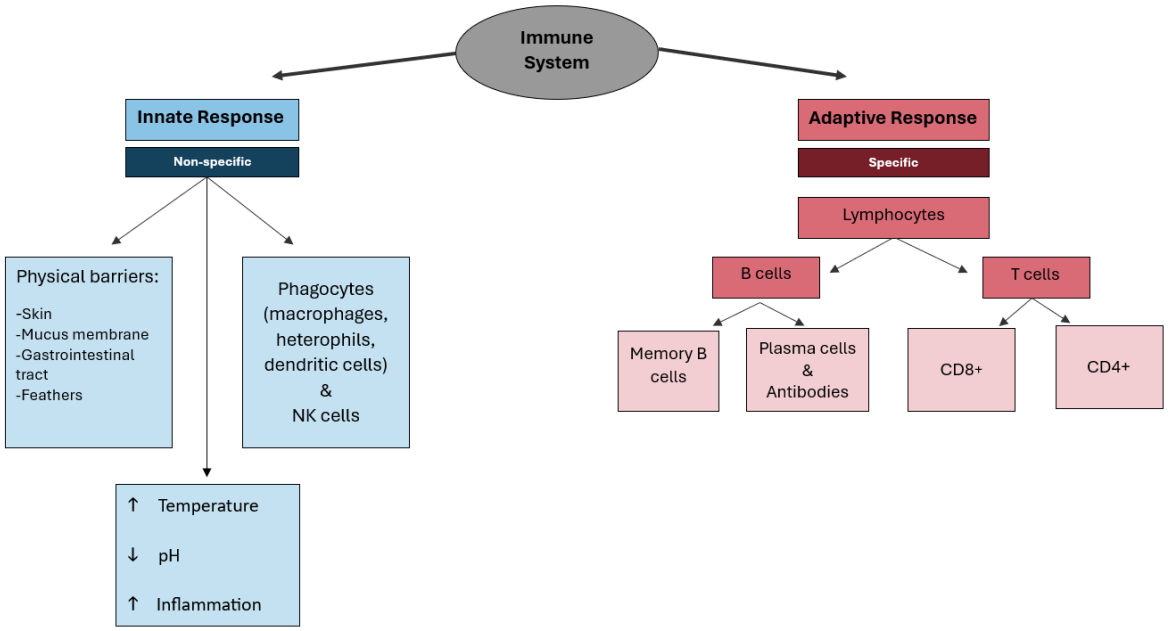

Figure 4.1: Summary of the avian immune system divided into the adaptive and innate immune responses. The innate immune response shows the non-specific reactions that occur within the body including the physical barriers, physiological reactions and cell types that respond. The adaptive immune response is a specific reaction that includes the lymphocyte cell types that are further divided into B cells and T cells.

Immune cells can be categorised into distinct groups with the aid of microscopy and flow cytometry as well as surface markers (See et al., 2018). However, with these methods alone, not all immune cell types can be fully resolved. Studying the transcriptome of an organism instead, proves to be a better option (Lawlor et al., 2021) . Transcriptomics aims to identify the current state of a cell or tissue, based on gene expression, by studying the RNA of a sample at a specific period under different experimental conditions. The discovery of new and rare cell types is occasionally possible using these techniques. However, as raised in Chapter 1 these analytical methods do not consider variability in gene expression among individual cells or the effect of mixed samples containing unrelated cell types that share overlapping surface markers. Therefore, bulk approaches for such analyses, may lead to loss of biological information (Lawlor et al., 2021).

Due to the complexity and heterogeneity of PBMCs, studying individual cells and their RNA patterns can be challenging, especially when studies rely on bulk type analyses (Derbois et al., 2023). A suitable solution to this problem is using scRNA-seq, which allows for in-depth analysis of individual cells within a mixed population. This advanced technique has been used for the study of PBMC transcriptomics in many health and disease settings related to both humans and animals (Choi et al., 2023; Derbois et al., 2023; Eschke et al., 2023). Many studies have shown that scRNA-seq is an appropriate tool for examining the heterogeneity of immune cells, their interaction with each other and other cell types (Lawlor et al., 2021; Qu et al., 2022a). As an application of next-generation sequencing, scRNA-seq relates to high-level study of the transcriptome. Quantification of the transcriptome, identification of genes and cell types, and differential gene expression is possible with this high-throughput sequencing technique.

The technique of scRNA-seq has been developed using many different approaches. These include generation of full-length cDNA transcripts (using the SMART-seq or SMART-seq2 approach) , massively parallel sequencing (MARS-seq), cell expression by linear amplification and sequencing (CEL-seq or CEL-seq2), indexing droplets (Drop-seq) (Jovic et al., 2022; Macosko et al., 2015; Picelli et al., 2014), amongst others. To aid in sample preparation and process automation, some of the approaches utilize microfluidic or droplet-based platforms,

such as 10X Genomics. The 10X Genomics Chromium platform involves droplet-based encapsulation of single cells and barcoded gel beads in an oil emulsion. The barcoded bead consists of a gel bead with oligonucleotides attached to its surface. The nucleotides code for a unique barcode, a unique molecular identifier (UMI), sequencing adapters and an oligo-dT capture site. Encapsulated cells are lysed within the nanolitre-sized droplet, the 3'poly A tail of each released mRNA molecule annealed to the poly T tail on the gel bead oligonucleotides and indexed with the cellular barcode during reverse transcription. Complementary DNA then undergoes library preparation and subsequent sequencing (See et al., 2018).

scRNA-seq plays an important role in immunological studies. This technique has been used in gaining detailed information related to infectious diseases, pathogenesis of infection, host immune responses, amongst others. The information obtained from immunological studies, using scRNA-seq, can assist in the reduction of disease transmission, treatment and therapeutic development by better understanding the immune cell landscape and host responses during infection (Jovic et al., 2022). With the first application of scRNA-seq in immunology, published in 2009 (Tang et al., 2009), many strides have been made in understanding the immune system and its responses across various species against numerous infections or disease. The technique proved valuable with the recent pandemic where many studies were performed pertaining to the immune response of people infected with SARS-CoV-2 (Jovic et al., 2022; Wilk et al., 2020; Zhang et al., 2020). These studies profiled PBMCs of healthy and infected subjects at different stages of disease, determined pathways in PBMC samples related to protective immunity, identified reconfiguration of PBMC phenotypes in diseased subjects, identified inflammatory responses and provided insights into disease severity and progression. The creation of scRNA-seq technologies has enabled a new age of immunological discovery and understanding.

This chapter focuses on performing an in-depth analysis of the transcriptome of the PBMC samples isolated from the PCV-2 and control groups of quails (as per Chapter 3). The purpose of sequencing individual cells was to better understand the immune response of quails, when injected with PCV-2 VLPs, by conducting an in-depth analysis of cell composition, as well as their differentially expressed genes. The 10X Genomics Chromium platform was used to isolate the PBMC samples into individual droplets, extract the mRNA from each cell and

synthesize barcoded cDNA. The cDNA was then prepared for sequencing and sequenced using the Illumina platform. Reads received, in a FASTQ format, were analysed bioinformatically by aligning the reads to a publicly available quail reference transcriptome (*Coturnix japonica* 2.0 (GCA_001577835.1)) (Morris et al., 2020). Datasets were then filtered to retain cells with high quality reads, normalized, clustered and finally annotated using marker genes. Pooled sample datasets were also demultiplexed into its individual samples. The demultiplexed data was then used to perform differential gene expression and gene ontology analysis. Results obtained from these analyses, enabled the identification of specific cell types and gene expression profiles, after injection with PCV-2 VLPs. Dissection of immune responses of quails against a PCV-2 immunogen in quails, were established. Additionally, the molecular functions and biological pathways, related to the immune response, were identified.

4.2 Materials and Methods

4.2.1 scRNA-seq using the 10X Genomics platform

scRNA-seq was conducted using the Chromium Next GEM Single Cell 3' kit as per the manufacturer's user guide (CG000204 Rev D). The protocol consisted of three main steps, namely, 1) GEM generation and barcoding, 2) post GEM-RT cleanup and cDNA amplification and, 3) gene expression library construction. An overview of the workflow can be seen in Figure 4.2.

Predetermined volumes of the two PBMC samples (sample details discussed in Chapter 3), along with partitioning oil, gel beads and master mix (RT Reagent B, Template switching oligo, reducing agent B, RT enzyme C) were added to the assembled Chromium Next GEM Chip G. With the aim of attaining 10,000 targeted cells, the volume of each PBMC sample, was determined using the Cell Suspension Volume Calculator Table as per the 10X Genomics user guide. Chip G was loaded into the Chromium Controller to produce gel bead-in-emulsions (GEMs) which consisted of a nanolitre oil droplet encompassing a single PBMC and a barcoded gel bead. Thousands of oligonucleotides cover the surface of the gel bead to which the 3' poly A tail of each released mRNA molecule annealed. The capture mRNA molecules were then indexed with a cellular barcode and a UMI during reverse transcription

(RT). The GEM-RT step occurred during incubation in a thermal cycler at 53 °C for 45 minutes and 85°C for 5 minutes. Post GEM-RT cleanup was done using Dynabeads and magnetic separation. Thereafter, cDNA was amplified via 11 PCR cycles, with a target of more than 6000 cells recovered. The cDNA once again underwent a cleanup step where SPRIselect reagent was used for fragment size selection.

Quality of the cDNA was then analysed for fragment size distribution and concentration using the Agilent TapeStation D 5000 (TapeStation Analysis Software 4.1.1) and Qubit, respectively. Both quality checks were conducted at the Central Analytical Facility (CAF, University of Stellenbosch).

Fragmentation, end repair and A-tailing was conducted, followed by double-sided size selection using the SPRIselect reagent This ensured cDNA molecules of optimum size was selected for subsequent Illumina sequencing. Thereafter adapters were ligated onto the fragments and post-ligation cleanup conducted using the SPRIselect reagent. Sample Indexes were then added by means of PCR. The sample concentration was determined, using Qubit analysis (as previously done). Based on the calculated cDNA yield, 13 PCR cycles were selected to amplify the libraries during the sample index PCR, after which sample cleanup, using SPRIselect reagent, and quality control were performed once more.

In the final libraries, each cDNA molecule contained the P5 and P7 primers, TruSeq reads 1 and 2 for paired-end Illumina sequencing, 10X barcode for identifying transcripts of individual PBMCs, UMI for identifying individual transcripts and the sample-index to allow multiplexing during sequencing. A final round of quality control (TapeStation and Qubit as above) was performed on the cDNA libraries prior to sequencing. Libraries were sequenced by Novogene (Singapore) using the Illumina NovaSeq 6000 platform and a paired-end 150 base pair sequencing strategy.

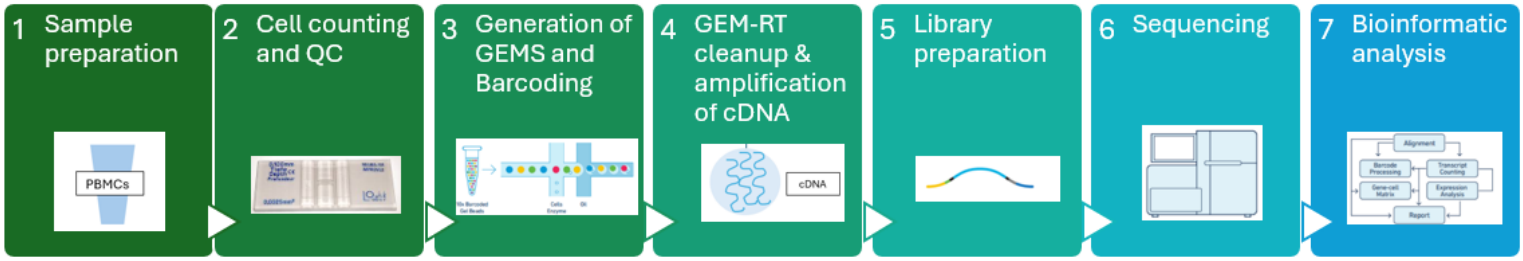

Figure 4.2: Procedural overview of scRNA-seq using the Genomics 10X Chromium platform. 1-2: PBMCs, isolated from whole blood samples, were purified, confirmed viable and counted for introduction to the 10X microfluidic device. **3:** The cells, oil and barcoded beads were then partitioned into nanolitre Gel Beads-in-Emulsion (GEMs). **4:** Following cell lysis, mRNA was captured onto the barcoded beads, reverse transcription conducted, and cDNA amplified. **5:** cDNA was then fragmented, tail ends repaired, and sequencing adapters (P5 and P7) and sample index added. **6:** Libraries were then sequenced using the Illumina sequencing platform. **7:** Finally reads were analysed with bioinformatic pipelines.

4.2.2 Bioinformatic analysis of scRNA-seq data

4.2.2.1 Pre-processing and read alignment

The FASTQ files received for the PCV-2 experimental sample and control sample, from Novogene, were processed using the 10X Genomics CellRanger (v 6.0.1) software. Reads were aligned to the *Coturnix japonica* 2.0 reference transcriptome (GCA_001577835.1) (Morris et al., 2020) and quantified using the *count* function from the 10X Genomics CellRanger software (Code available, script 1). A predetermined filtering protocol was conducted (as per CellRanger software) to eliminate barcodes with very low UMI counts and those which may represent encapsulated ambient RNA from dead or low-quality cells. These pre-filtered datasets were then used for further analysis as well as demultiplexing of samples. Outline of bioinformatic processes and pipelines used are outlined in Figure 4.3 below.

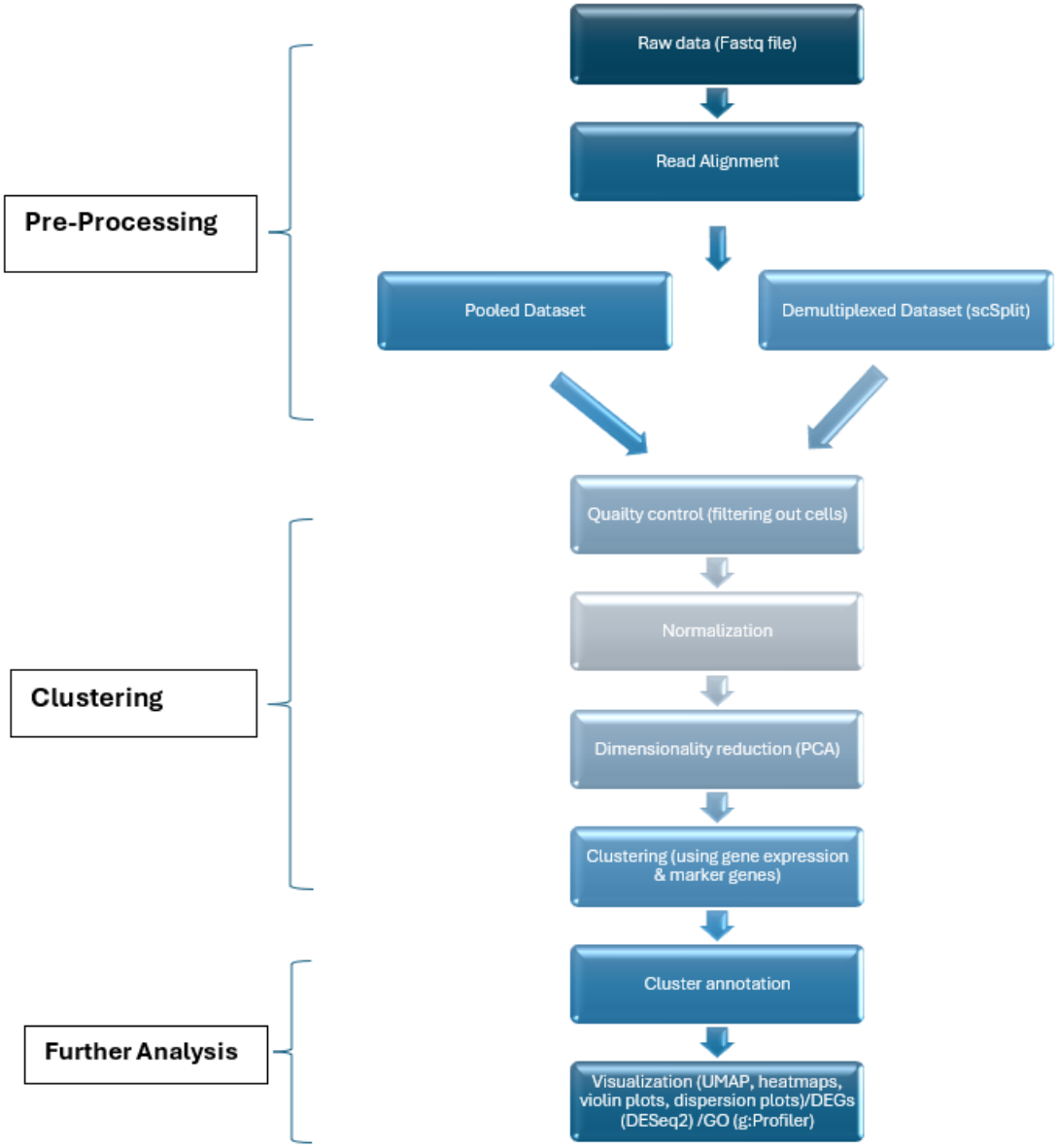

Figure 4.3: Graphical representation of analytical processes followed using bioinformatics for single-cell RNA sequencing datasets. The process began with the raw data, in a Fastq format, used as input into the CellRanger software for alignment to a reference transcriptome and count matrix created. Pooled samples were then processed further or demultiplexed. Sample datasets underwent QC, normalization, dimensionality reduction and clustering using the Seurat software in R. Specific marker genes were then used for cluster annotation and data visualized using tools in Seurat. Finally, DEG analysis was conducted using Deseq-2 and GO terms performed using g:Profiler.

4.2.2.2 Demultiplexing of pooled scRNA-seq data

A genotype-free demultiplexing pipeline was used to separate genetically distinct samples within the pooled control PBMC and pooled PCV-2 PBMC samples, respectively. The two pooled samples, representing two different conditions (control and PCV-2), were demultiplexed into its original 8 samples each, where each PBMC sample originated from a different quail. This was done to allow downstream differential expression analysis where sample replicates were needed.

The CellRanger filtered BAM files, of each pooled sample, were filtered to remove read quality below 10 using Samtools (v1.9) software (Danecek et al., 2021). The Samtools software was also used to remove duplicated reads (using *rmdup*), followed by file sorting and indexing (using the *sort* and *index* functions). Single-nucleotide variants (SNVs) were then called from the filtered BAM files using Freebayes (v1.2.0) software (Garrison and Marth, 2012). Minimum allele count and minimum base quality was set to 2 and 1, respectively. To enable more efficient processing, the BAM file was split by chromosome for this analysis and then merged afterwards. The resultant file was filtered even further, using the bcftools (v1.9) software (Danecek et al., 2021), to remove SNVs with a quality score of less than 30. Allele count matrices were then built using scSplit, pysam and PyVCF in Python (v3.7) (Xu et al., 2019). Lastly, samples were demultiplexed and a presence/absence matrix created using scSplit (Code available, script 2 - 10). Generated matrices were used to demultiplex the cells into the 16 samples (8 samples per condition) creating CSV files. Separated CSV files and the Cell Ranger filtered feature matrix was imported into R, where the demultiplexed samples were converted to Seurat Objects in R (v 4.3.0) and integrated into a single list.

4.2.2.3 Quality control

Specific parameters were used for manual filtering of barcodes in R (v 4.3.0). The raw gene barcode matrix of each sample was imported into R using the *Read10X* function from the Seurat package (version 5.1.0) (Satija et al., 2015). Features used for filtration included the number of individual transcripts (nUMIs), individual genes (nGene), number of genes detected per UMI (log10GenesPerUMI) and fraction of mitochondrial read counts to total read counts (mitoRatio). Filtering parameters, for both sample conditions, were used as stated in Table 4.1. The parameters were based on those commonly used in literature involving studies on avian PBMC samples (Dai et al., 2023; Maxwell et al., 2024; Qu et al., 2022a; Warren et al., 2023). Other features used in the filtration process included the removal of genes that had zero counts in each cell and removal of genes expressed in less than 10 cells (Code available, script 11).

Table 4.1: Parameters used to remove low quality barcodes from PCV-2 experimental sample and control sample datasets as well as demultiplexed datasets

Features	Parameters
nUMIs	≥ 8000
nGene	≤ 200
Log10GenesPerUMI	< 0.8
mitoRatio	> 0.10

4.2.2.4 Normalization, dimensional reduction by principal component analysis and clustering

Datasets were normalized and scaled using various functions within the Seurat package in R. This was done to remove technical variability related to factors associated with sequencing depth, where the number of detected molecules within each cell may vary substantially. The process began with normalization using the *NormalizeData* function. Thereafter, principal component analysis (PCA) was conducted for dimensionality reduction. This was done using 2000 of the most variable features and setting the principal component (PC) values for both the aggregated, integrated PCV-2/control, and demultiplexed

integrated dataset at 15. Datasets were then scaled using the *ScaleData* function. SCTransform was implemented to normalization data once again and regress out mitochondrial expression (Code available, script 12).

To align similar cell types across the two conditions, datasets were integrated. This was done using Seurat's *SelectIntegrationFeatures* using the 3000 most variable genes. The *FindIntegrationAnchors* function was used to perform canonical correlation analysis to identify shared sources of variation between the two datasets. The datasets were then integrated using the *IntegrateData* function and data visualized using PCA and Uniform Manifold Approximation and Projection (UMAP) (Code available, script 12).

The *FindNeighbors* function was used to cluster the cells for the datasets. This graph-based clustering method utilizes the K-nearest neighbor (KNN) approach. The *FindClusters* function then performs the final clustering. The resolution was set at 0.8 for the PCV-2/control aggregated, integrated datasets and 0.5 for the demultiplexed datasets (Code available, script 13).

4.2.2.5 Cluster annotations

Cell types within each cluster were annotated manually by 1) assessing the expression of published avian PBMC marker genes across the clusters (Table 4.2) and 2) by identifying published cell-type-specific marker genes present in the 100 most highly conserved genes (in descending order of log2FoldChange) within each cluster using the Seurat's *FindConservedMarkers* function (Supplementary Data 2). The *FindConservedMarkers* function identified genes that were differentially expressed within each condition and then identified the genes that were conserved within the same cluster across all conditions. Both these functions utilize the Wilcoxon Rank Sum test with a log2FoldChange threshold of 0.25 and specifying positive markers only (Code available, script 14).

The above-mentioned protocol (including QC, normalization, PCA, clustering and annotation) was also followed for the demultiplexed datasets (Code available, script 15).

Table 4.2: Selected marker genes used for annotation of various cell types within different scRNA-seq clusters based on literature.

Cell type	Marker gene	Reference
APC Myeloid cells	*IFI30*	(Maxwell et al., 2024)
	LY86	(Maxwell et al., 2024)
B cells	*CD79B*	(Warren et al., 2023)
	PAX5	(Maxwell et al., 2024)
	BCL11A	(Qu et al., 2022a)
Macrophages	*TPM2*	(Warren et al., 2023)
	CD9	(Warren et al., 2023)
T cells	*CD3E*	(Désert et al., 2016)
CD4+ T cells	*IL7R*	(Dai et al., 2023)
Th1-like T cells	*TBX21*	(Dai et al., 2021b)
Th2-like T cells	*GATA3*	(Dai et al., 2021b)
	CCR4	(Dai et al., 2023)
Tregs	*CTLA4*	(Maxwell et al., 2024)

4.2.2.6 Differentially gene expression analysis using DESeq2

Differentially expressed genes (DEGs) between the two experimental conditions were analysed using the DESeq2 software (v 1.40.2) in R (Piper et al., 2022). A counts matrix, with counts from the technical replicates, was created from aggregated counts for each cluster in each sample condition. Demultiplexed data (8 samples from the PCV-2 condition and 8 samples from the control condition) were used as input for the counts matrix as well as a metadata file that details information specific to the sample conditions. The counts are normalized, using size factors in DESeq2 to ensure that differences in library size between samples were accounted for. To assess variation between samples, PCA was performed. Using the counts as input, the *DESeqDataSetFromMatrix* function the DESeq2 object was created. The *DESeq* function was then used to estimate the size factors, dispersion, Wald statistic and Negative Bionomial GLM fitting on the DESeq2 object. Thereafter shrinkage of the Log2FoldChange was performed using the apeglm method (Zhu et al., 2019). An adjusted p-value is analysed as DESeq2 corrects for multiple comparisons due to the many genes that are tested at once. The fold change is also analysed for each gene as it represents the ratio of gene expression between the two sample conditions (PCV-2 and control). DESeq2 determines a Log2FoldChange to ensure better interpretation of results. A positive Log2FoldChange (FC > 1) indicates upregulation of the gene, while a negative

Log2FoldChange shows downregulation. Significant genes were extracted, using a p-adjusted threshold of 0.05 (Code available, script 16).

4.2.2.7 Gene ontology analysis

Gene Ontology (GO) analysis was used to gain insights into the biological significance and processes of DEGs within a sample. GO terms are organized by Molecular Function (MF), Cellular Component (CC) and Biological Process (BP) based on roles of known genes. MF refer to cellular actions that take place at the molecular level performed by gene products. CC refer to the locations within a cell where a gene may be active. BP are larger processes that are formed by multiple molecular functions.

g:Profiler, is a public web server, that compares large gene lists to databases to perform an enrichment analysis and provide information on Gene Ontology. The output data from DESeq-2 (list of DEGs per cell type- upregulated DEGs, downregulated DEGs, a combined list of both upregulated and downregulated DEGs, and DEGs unique to each cell type from UpSet plot) was used as input to g:Profiler to compare the DEG lists to a background selection of all genes specific to *Coturnix japonica* (Ensembl *Coturnix japonica* database). The GO terms were then output as different functional groups, while also displaying "driver terms" that were specific GO terms most significant to the enrichment score (Kolberg et al., 2023). The KEGG (Kyoto Encyclopedia of Genes and Genomes) pathways were also analysed to identify disease associations with the DEGs. KEGG pathways were also obtained using g:Profiler.

4.3 Results

4.3.1 Quality control of scRNA-seq library preparation

Two pooled scRNA-seq libraries were created from PCV-2 VLP- and PBS- injected quail PBMC samples, using the 10X Genomics platform. The PBMC samples were split into nanoliter droplets, containing individual cells and barcoded beads, via a process of GEM generation. Thereafter, cDNA was synthesized, quality control (QC) steps and library preparation conducted, and fragments sequenced. Testing fragment concentration and size (as part of the QC steps) were conducted twice during the 10X Genomics protocol. The first QC step was conducted on the cDNA, after amplification and cleanup while, the second step was conducted on the final library fragments, before sequencing. The quality of the cDNA libraries, before and after the library preparation, can be seen in Table 4.3 and Figure 4.4. Using the Qubit fluorometric quantification system, the concentration of the two libraries yielded low but acceptable concentrations of 5.82 $ng.\mu l^{-1}$ and 3.80 $ng.\mu l^{-1}$ for the PCV-2 and control samples, respectively. Following fragmentation, end repair and A-tailing of the cDNA libraries, adaptors for Illumina sequencing were added as well as a sample index for a multiplexed sequencing run. Following 13 PCR cycles for sample indexing, the concentration of the PCV-2 sample increased to 10.5 $ng.\mu l^{-1}$, but decreased for the control sample to 2.06 $ng.\mu l^{-1}$. Despite the low concentration levels, both samples were sufficient for sequencing. The other QC check used to determine library quality was fragment size (using the Agilent TapeStation D 5000). The peak fragment size for the PCV-2 sample was 1101 bp and 495 bp, before and after library preparation, respectively. While the control sample showed a peak fragment size of 1127 bp before library preparation and 456 bp after library preparation. These sizes were in line with expected results for pre- and post- library preparation.

Table 4.3: Quality control of cDNA using Qubit. cDNA concentrations before and after scRNA-seq library preparation for the two samples (PCV-2 and control).

Sample	Concentration ($ng.\mu l^{-1}$) Pre-library prep	Concentration ($ng.\mu l^{-1}$) Post-library prep
PCV-2	5.82	10.5
Control	3.80	2.06

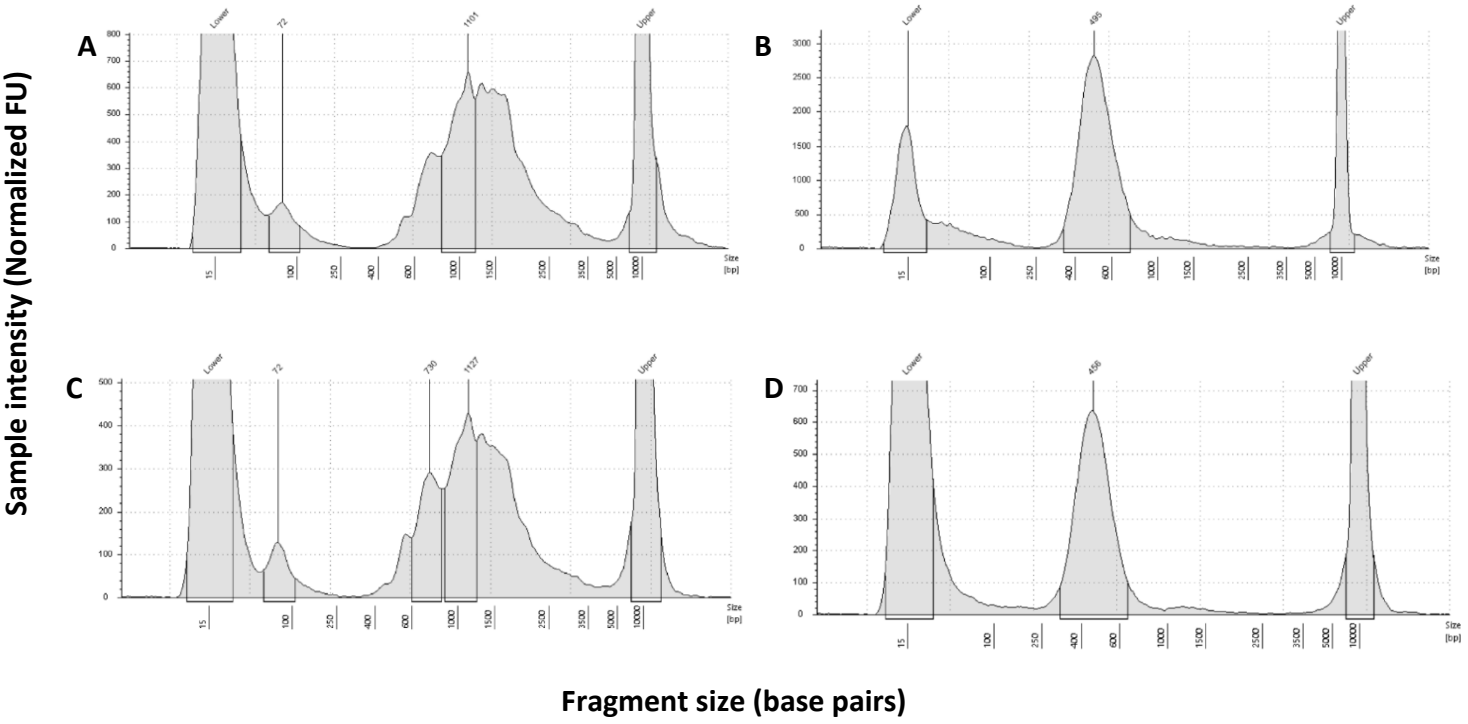

Figure 4.4: Quality control reports of cDNA using TapeStation. Graphs depicting cDNA fragment sizes for scRNA-seq libraries of each sample before and after library preparation. The peak fragment size (FU, fluorescence units) of each sample is indicated by the numbers presented above the vertical lines. **A**: Sample PCV-2, before library prep. **B**: Sample PCV-2, after library prep. **C**: Sample Control, before library prep. **D**: Sample Control, after library prep.

4.3.2 Pre-processing and QC for 10X scRNA-seq datasets

The sequenced scRNA-seq libraries underwent pre-processing and QC steps as the beginning processes of the bioinformatics analysis. Reads, obtained in a FASTQ format, were processed by alignment to the *Coturnix japonica* 2.0 reference transcriptome (GCA_001577835.1) (Morris et al., 2020) using the CellRanger pipeline (v 6.0.1). To remove transcripts with very low UMI counts, dead cells or low-quality barcodes, specific filtering parameters were employed using the Seurat package (version 5.1.0) in R (v 4.3.0) (Satija et al., 2015).

The Cell Ranger Web Summary outputs and cell numbers after Seurat filtering are shown in Table 4.4. It was noted that a total of 10716 cells were isolated from the PCV-2 group and 8426 cells were isolated from the control group. Following Seurat filtering, 8325 cells were obtained for the PCV-2 sample with 4312 cells for the control sample. The change in cell numbers was due to removing barcodes with greater than 8000 transcripts (UMIs), barcodes with fewer than 200 genes, barcodes with a fraction of number of genes detected per UMI

that was fewer than 0.8 and barcodes with a mitochondrial gene count of more than 10%. Other features used in the filtering process included the removal of genes that had zero counts and removal of genes expressed in less than 10 cells. The median UMI counts per cell after filtering was 1259 and 1122 for the PCV-2 and control samples, respectively. The median number of genes per cell for the PCV-2 sample was 518 and 448 for the control sample.

Table 4.4: Quality control statistics produced from the CellRanger and Seurat software. The statistics include the number of reads, valid barcodes, median UMI counts and genes per cell, as well as percentage of reads mapped to the genome, using the CellRanger software. It also includes the number of cells obtained per sample before and after filtering, using the Seurat Software.

Sample	Number of Reads	Valid Barcodes	Number of Cells (before filter)	Number of Cells (after filter)	Median UMI Counts per Cell	Median genes per Cell	Mapped to Genome
PCV-2	353,902,413	95.4%	10716	8325	1259	518	88.4%
Control	338,569,239	87.7%	8426	4312	1122	448	80.1%

After the preliminary processing of the pooled libraries, using CellRanger, the dataset was demultiplexed into individual samples (8 samples per experimental condition) using scSplit in Python (v3.7) and its supporting software packages (Xu et al., 2019). Details pertaining to the 16 samples can be seen in Table 4.5, which shows the distribution of cells per sample per condition. Following demultiplexing using scSplit, additional filtering in Seurat was performed as described above for the pooled samples. Before filtering (showing cell counts after scSplit filtering but no Seurat filtering), the average cell count was 604 and 320 for PCV-2 and control samples, respectively. After both scSplit and Seurat filtering, an average of 595 cells per sample was noted for the PCV-2 condition, while an average of 311 cells per sample was noted in the control group. Before Seurat filtering, the total cell count was 4829 for PCV-2 and 2561 for control. This decreased slightly to a total of 4762 cells in the PCV-2 condition and 2484 cells in the control samples, after both scSplit and Seurat filtering (Table 4.5). This is lower than the values obtained in the pooled data (Table 4.4). A slight drop in the number of cells per sample was noted after the Seurat filtering (Figure 4.5). After filtering, the median number of UMIs per cell for the PCV-2 condition was 1234 and 1098

for the control. The median number of genes per cell was 517 for the PCV-2 condition was and 454 for the control (Figure 4.6).

Table 4.5: Demultiplexed data showing the distribution of cells per quail within each condition before and after QC filtering. The cell count, before filtering, was conducted using only the scSplit filtering. The cell count, after filtering, represents values after both the scSplit and Seurat filtering. The total number of doublets and average cells per sample condition is also indicated.

Sample		Quail 1	Quail 2	Quail 3	Quail 4	Quail 5	Quail 6	Quail 7	Quail 8	Total	Total scSplit Doublets	Average cells per sample
PCV-2	**Before Filtering**	763	645	931	498	461	522	507	502	4829		604
	After Filtering	752	641	920	487	456	513	500	493	4762	444	595
Sample		**Quail 9**	**Quail 10**	**Quail 11**	**Quail 12**	**Quail 13**	**Quail 14**	**Quail 15**	**Quail 16**	**Total**	**Total scSplit Doublets**	**Average cells per sample**
Control	**Before Filtering**	222	282	270	461	291	445	271	319	2561		320
	After Filtering	217	280	265	448	287	415	262	310	2484	233	311

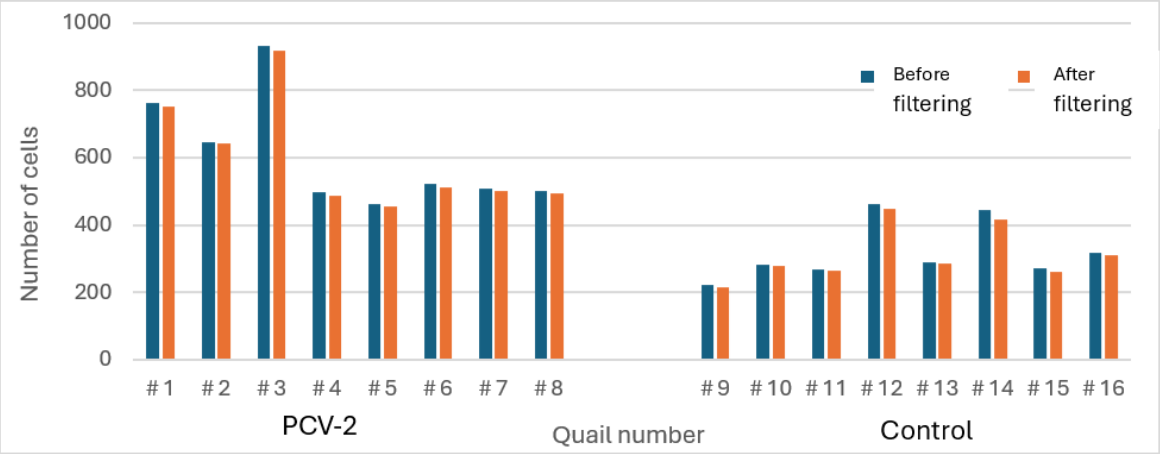

Figure 4.5: Distribution of cells before and after Seurat filtering. Number of cells per sample per experimental condition. The cell count, before filtering, was conducted using only the scSplit filtering. The cell count, after filtering, represents values after both the scSplit and Seurat filtering.

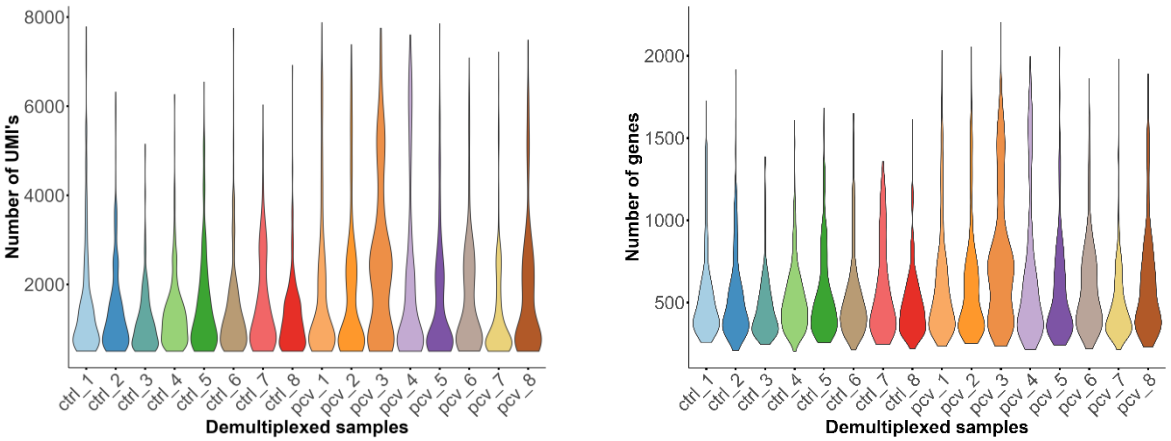

Figure 4.6: Quality control statistics per sample for each experimental condition after scSplit and Seurat filtering. Number of transcripts and number of genes per cell per sample. Key: ctrl = control samples, pcv = PCV-2 samples.

4.3.3 Data integration, clustering and annotation

4.3.3.1 Aggregated analysis of pooled samples from the PCV-2 and control conditions

The aggregated, pooled samples were processed and analysed before the demultiplexed samples, to assess the quality of the data. Upon completion of QC on the pooled sample dataset, the gene counts were subjected to normalization and scaling using Seurat. The PCV-2 and control datasets were then aggregated and integrated to allow for alignment of same cell types across the two conditions. This was done to identify cell types that were present in the samples from both conditions. Figure 4.7 shows the two integrated datasets by visual means of a UMAP. An overlay of both conditions can be seen in the UMAP, showing the similarity between the control and PCV-2 clusters (Figure 4.7A). The integrated datasets were also separated into the two conditions, and visualised by means of a UMAP (Figure 4.7B) to show that all the cells, within each condition, aligned well. The integrated datasets were then clustered resulting in 14 clusters (Figure 4.7C) when using a resolution setting of 0.8 and PC parameter of 15 (based on results obtained from the elbow plot in Supplementary Data 1, Supp Figure 1).

Annotation of the clusters was achieved by taking a manual approach of assessing the expression of published avian PBMC marker genes across the clusters and by identifying published cell-type-specific marker genes present in the 100 most highly conserved genes within each cluster using the Seurat's *FindConservedMarkers* function (Supplementary Data 2). This function allowed identification of genes that were conserved in each cluster in both conditions. The marker genes used for annotation of the 14 clusters were (as per Table 4.2): *IFI30* and *LY86* for APCs (Maxwell et al., 2024); *CD79B* (Warren et al., 2023), *PAX5* (Maxwell et al., 2024) and *BCL11A* (Qu et al., 2022a) for B cells; *TPM2* and *CD9* for macrophages Warren et al., 2023); *CD3E* for T cells (Désert et al., 2016); *TBX21* for Th1-like T cells (Dai et al., 2021a); *GATA3* and *CCR4* for Th2-like T cells (Dai et al., 2021a) and *CTLA4* for Tregs (Maxwell et al., 2024).

Based on the expression of *TPM2* and *CD9,* clusters 0, 2, 3, 4, 5, 6 and 11 were defined as macrophages (Figure 4.7D-E and Figure 4.8A-B). The tetraspanin protein, encoded by *CD9*, is found on macrophages and is involved in cell adhesion and migration, assisting in the process of phagocytosis and antigen presentation. The protein is used by macrophages to interact with extracellular matrix proteins when migrating to a site of inflammation (Reyes et al., 2018). Additionally, these clusters showed expression and up regulation of *TUBB1* (shown in top 100 conserved genes expressed within the clusters - see Supplementary Data 2 and Figure 4.7D). *TUBB1* encodes for the beta-tubulin protein, involved in microtubules, which are essential for phagocytosis, cell migration to a site of inflammation and cell division during lymphocyte proliferation (Seta et al., 2023). The microtubule structure is also needed for antigen presentation by macrophages. Another gene found in most of the macrophage clusters was *TIMP3* (Supplementary Data 2 and Supplementary Data 3, Supp Figure 3). Tissue inhibitor of metalloproteinases–3 (*TIMP3*) is expressed on macrophages and regulates cytokine production and receptors on macrophage cell surface (Gill et al., 2013). The *F13A1* gene, also found in these clusters (Supplementary Data 2 and Figure 4.7D), is a transglutaminase that alleviates blood clotting thereby assisting with wound healing. The protein initiates an immune response during infection or presence of a foreign invader (Oh et al., 2023).

The second largest combined cluster was that of T cells. The consistent presence of *CD3E* in clusters 1, 8, 10, 12, 13 and 14 (Figure 4.7D-E and Figure 4.8H) indicated the presence of total T cells. The gene is a major component of the T cell receptor complex (TCR) and essential to the overall activation and functioning of T cells throughout the immune response. The CD3 complex, along with a TCR molecule, is always present on T cells and is therefore a pan-T cell marker (Désert et al., 2016). Subclusters within the T cell cluster were identified as T helper-like T cells (Th1-like and Th2-like T cells) and T regulatory (Treg) cells, which fall under CD4+ T cells. T helper cells, mainly involved in a regulatory role within the adaptive immune system, are a subset of CD4+ T cells. T helper cells produce cytokines and express cell surface molecules that signal to the cells of the adaptive immune system (Dai et al., 2021b). The first type of helper cell, Th1-like, mediates the adaptive response towards a cell-mediated response, while Th2-like generally mediates a humoral response (Dai et al., 2021a). Cluster 13 was defined as the Th1-like T cells because of the expression of *TBX21* (Figure 4.7D and 4.8I). Due to the high expression of *GATA3*, clusters 8 and 12 were defined as the Th2-like T cells (Figure 4.7D and 4.8J-K). From the relatively high expression levels of *CTLA4* (Figure 4.7D and 4.8L), clusters 1, 10 and 14 were defined as the Tregs. Tregs maintain immune homeostasis.

Using the classical avian B cell marker genes, *BCL11A*, *PAX5* and *CD79B*, cluster 7 was defined as B cells (Figure 4.7D and 4.8E-G). B cells play a crucial role in the adaptive immune system. They are primarily responsible for antibody production and the humoral immune response, which involves the release of antibodies to neutralize pathogens (Dai et al., 2021a). They also provide immunological memory and regulate immune responses. *CD79B* forms part of the B cell receptor complex and is essential for B cell activation and antigen recognition (Maxwell et al., 2024). It helps initiate signalling that leads to antibody production and the activation of the adaptive immune response. *PAX5* is a transcription factor that regulates B cell lineage commitment and early B cell development. It ensures that hematopoietic progenitor cells differentiate into B cells and regulates B cell-specific gene expression (Chivukula and Dabbs, 2011). *BCL11A* is a transcription factor involved in B cell maturation. It plays a role in the development of plasma cells and memory B cells, affecting antibody production (Dai et al., 2021a).

The remaining cluster, cluster 9 was defined as antigen-presenting and myeloid cells (APC). This was due to the expression of *LY86* and *IFI30* (Figure 4.7D and 4.8C-D). APCs are a subset of immune cells that capture, process, and present antigens to T cells to initiate and regulate adaptive immune responses. They play a crucial role in bridging the innate and adaptive immune system (Wu and Kaiser, 2011). *IL-1B, TLR4*, *TLR6* and *TLR7* were also found in the APC cluster, and these genes inferred that a pro-inflammatory state was most likely active (Supplementary Data 2 and 3, Supp Figure 3). The three toll-like receptors, *TLR4*, *TLR6* and *TLR7*, act as pattern recognition receptors and activation of these genes results in production of inflammatory cytokines (Kawasaki, Takumi and Kawai, 2014).

Figure 4.7E shows the 6 main cell types found within the 14 clusters, namely B cells, APCs, macrophages, Th1-like T cells, Th2-like T cells and Tregs. From the cell distribution (number of cells – Figure 4.7F) and proportion (percentage of cells – Figure 4.7G), macrophages were the most dominant cell type amongst both the PCV-2 (5839 cells; 70%) and control samples (2236 cells; 52%). The second largest group was the combined T cell group, subclustered into Tregs (PCV-2: 1065 cells; 13%. Control: 901 cells; 21%), Th1-like T cells (PCV-2: 218 cells; 3%. Control: 259 cells; 6%) and Th2-like T cells (PCV-2: 302 cells; 4%. Control: 380 cells; 9%). APCs amongst the PCV-2 sample was 403 cells (5%) and 245 cells (6%) for the control sample. A similar distribution was found for the B cells at 498 cells (6%) for PCV-2 and 291 cells (7%) for the control sample.

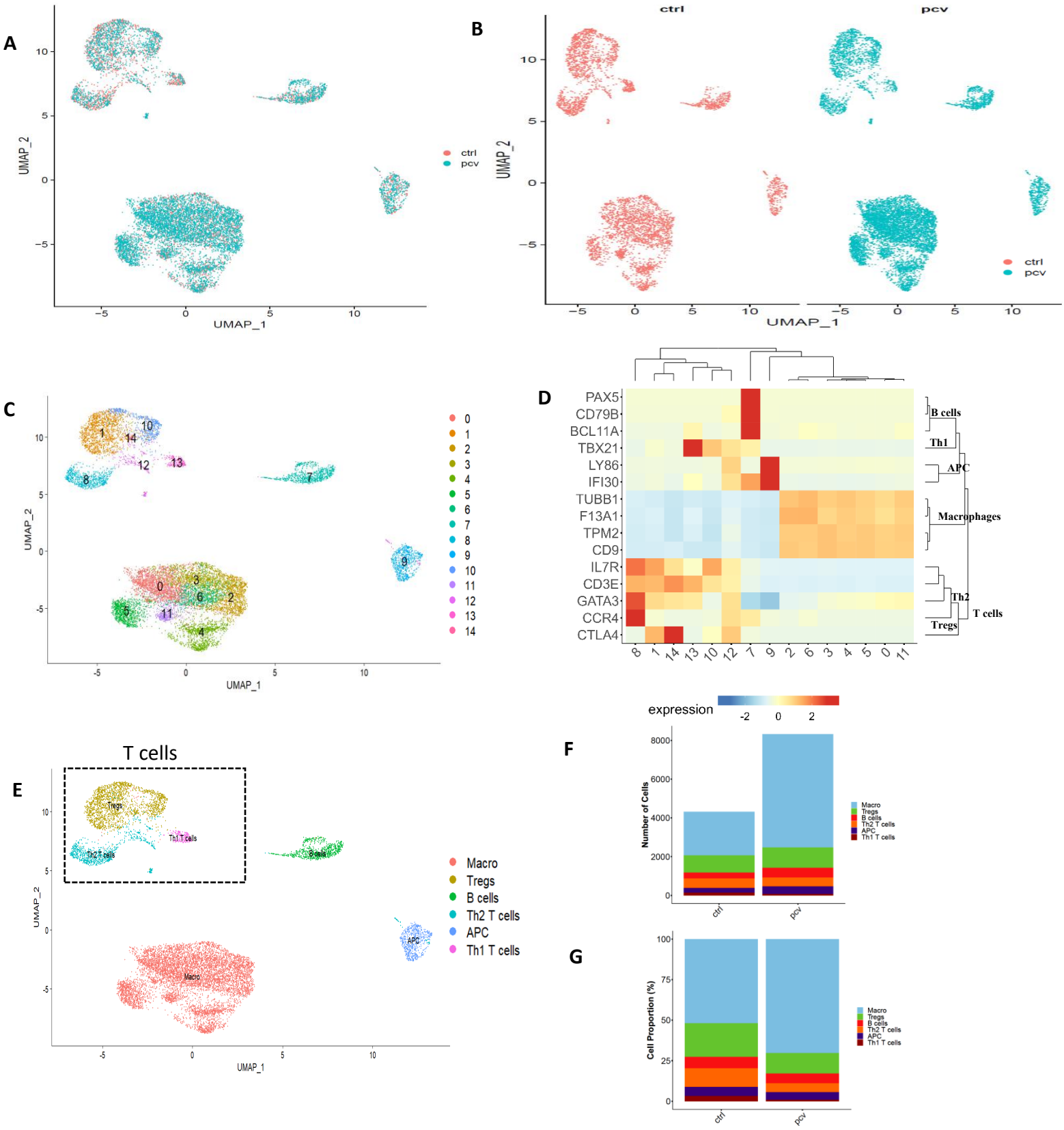

Figure 4.7: Annotation and cell distribution of 14 clusters in the integrated, pooled PCV-2 and control dataset. **A:** UMAP of the integrated clustering of the PCV-2 and control sample. **B:** UMAP showing separation of integrated datasets by condition. **C:** UMAP displaying 14 clusters of the integrated dataset. **D:** Heatmap of avian PBMC marker genes present in the dataset showing levels of relative expression per cluster. The darker the red box the more highly expressed the gene is within a cluster. The bluer a box, the less expressed it is within a cluster**. E:** Annotated UMAP of integrated dataset showing the cell types identified. **F:** Distribution of cells in each sample (after integration) showing cell numbers per cell type. **G:** Distribution of cells in each sample (after integration) showing cell type proportions in percentage per cell type. Key: Macro = Macrophages, Tregs = T regulatory cells, APC = Antigen presenting cells, Th1 = Th1-like T cells, Th2 = Th2-like T cells, ctrl = control sample, pcv = PCV-2 sample.

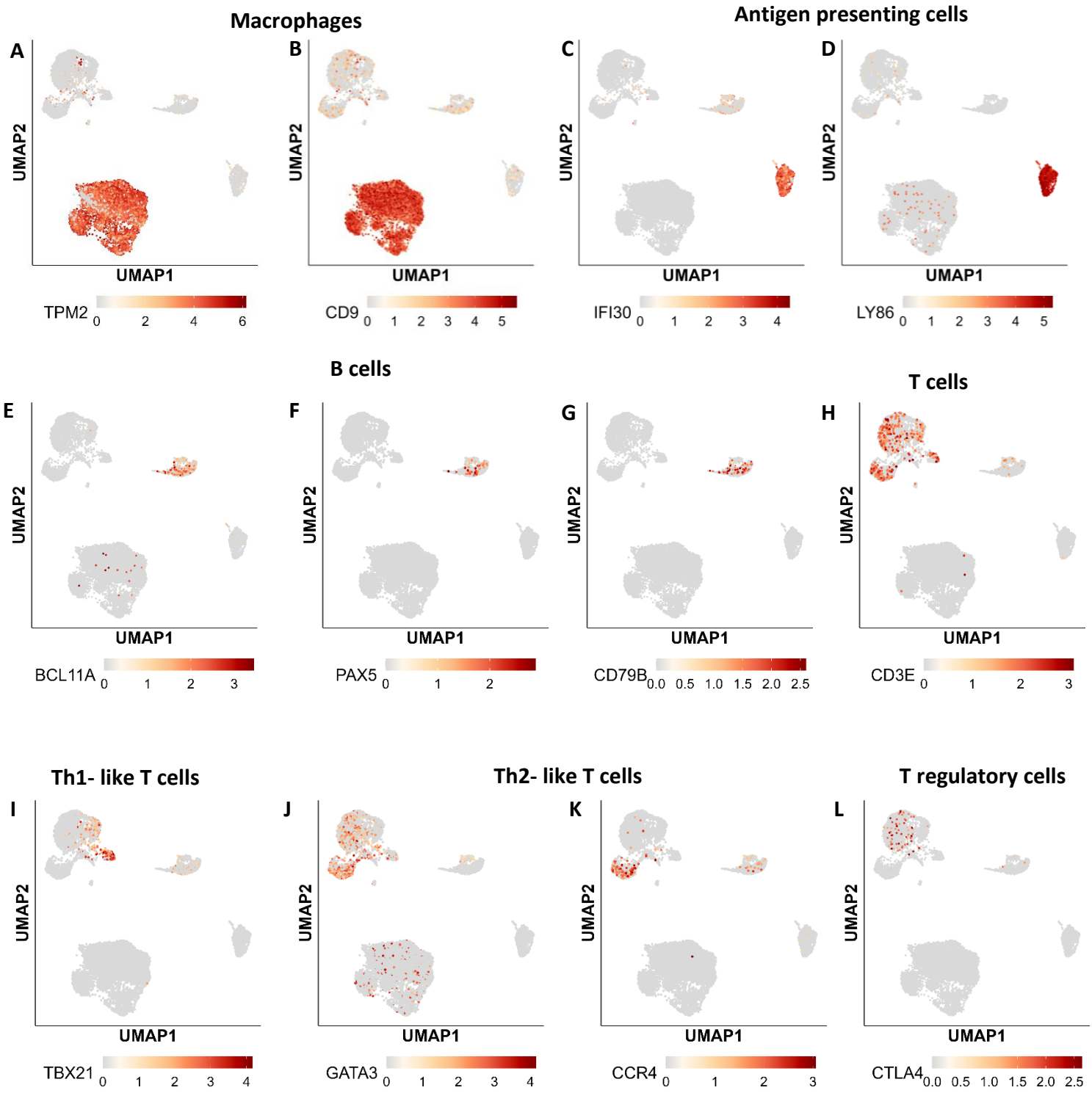

Figure 4.8: Marker genes examined across each of the 14 clusters of the pooled dataset. UMAP plots showing the expression of selected avian PBMC marker genes identified within each cluster. **A-B:** Macrophage cell type expressing marker genes *TMP2* and *CD9.* **C-D:** Antigen presenting cells (APCs) expressing marker genes *IFI30* and *LY86.* **E-G:** B cells expressing marker genes *BCL11A, PAX5* and *CD79B.* **H:** T cells expressing marker gene *CD3E.* **I:** Th1-like T cells expressing marker gene *TBX21.* **J-K:** Th2-like T cells expressing marker genes *GATA3* and *CCR4.* **L:** T regulatory T cell expressing marker gene *CTLA4.*

4.3.3.2 Demultiplexed data of samples from the PCV-2 and control conditions

Following processing of the pooled PCV-2 and control dataset, through the Seurat pipeline and annotation process, it was determined that the overall dataset consisted of sound data that could be successfully analysed and annotated. The same pipeline was then repeated on the demultiplexed data, to annotate the data and conduct downstream differential expression analysis. As described above, the pooled samples for the PCV-2 and control conditions were separated into 16 samples representing 8 quail PBMC samples for each condition, using scSplit.

Normalization, dimensionality reduction and scaling were done including integration of the PCV-2 and control datasets to determine alignment of similar cell types between the 2 conditions and across the 16 samples. Evident in Figure 4.9A, the clustering pattern showed a total of 11 clusters after using a resolution setting of 0.5 and PC parameter of 15 (based on results obtained from the elbow plot in Supplementary Data 1, Supp Figure 1).

The same marker genes that were used for the pooled samples were used to annotate the 11 clusters of the demultiplexed samples. Cluster 10, however, remained unannotated and was removed from all downstream analysis. This was because Cluster 10 consisted of very few cells and the avian PBMC marker genes were weakly expressed, making it difficult to annotate the cluster. No single well-defined cell type was distinguishable in cluster 10.

Expression of the known cell-type-specific marker genes were visualized as a heatmap (Figure 4.9B), showing 6 cell types. The relationship between the clusters by their gene expression profiles (evident in the hierarchical clustering tree on the right side of the heatmap in Figure 4.9B) showed separation into the 6 cell types. The relationship between the clusters by columns (evident in the hierarchical clustering tree above the heatmap in Figure 4.9B) showed 2 main divisions, which may indicate the two main immune responses, namely innate and adaptive immune responses.

The macrophages were annotated by expression of the *TPM2* and *CD9* genes and formed part of the innate immune system (Figure 4.9B and 4.10A-B) (Warren et al., 2023). This cell

type was present in clusters 0, 2 and 7. The other cell types that formed part of the innate immune system, APCs, were defined by *IFI30* and *LY86* expression (Maxwell et al., 2024). The presence of *LY86* and *IFI30* in clusters 5 and 11 suggests that the cells in these clusters were involved in immune activation (Figure 4.9B and 4.10C-D). Specifically, these genes are associated with inflammatory responses and pathogen recognition (Wu and Kaiser, 2011). The co-expression of these genes could point to a cluster of cells that were activated macrophages, dendritic cells, or other innate immune cells that participated in both antigen presentation (via *IFI30*) and inflammation (via *LY86*).

The two main cell types present in the adaptive immune system were the B cells and T cells. Cluster 3 was annotated as B cells based on the expression of marker genes *BCL11A, PAX5* and *CD79B* (Figure 4.9B and 4.10E-G). The presence of total T cells was identified by *CD3E* expression in clusters 1, 4, 6, 8 and 9 (Figure 4.9B and 4.10H). T cells are differentiated into CD4+ and CD8+ T cells. Differentiation of the cells is dependent on the stage of infection, tissue damage or cell repair (Dai et al., 2021a). Clusters 1, 4, 6, 8 and 9 expressed *IL7R*, which shows that majority of the T cells in those clusters were CD4+ T cells (Figure 4.9B). *IL7R* is a marker gene for the CD4+ T cell type, which has subtypes of T-helper cells and Tregs (El Helaly Goher et al., 2024; Erf, 2004). The high expression of *TBX21* in clusters 6 and 8 indicated that these clusters were likely Th1-like T cells, which are a subset of CD4+ T cells (Figure 4.9B and 4.10I). The other T cell subtypes present were Tregs, identified by the presence of the *CTLA4* gene in cluster 1 and 9 (Figure 4.9B and 4.10L), and Th2-like T cells identified by the presence of *GATA3* and *CCR4* in cluster 4 (Figure 4.9B and 4.10J-K).

Annotation of the clusters resulted in the same 6 cell types as in the pooled dataset, containing macrophages, APCs, Tregs, Th1-like T cells, Th2-like T cells and B cells as well as one cluster (cluster 10) that was unidentifiable (Figure 4.9C). Figure 4.9C and 4.9D showed the distribution of cells per quail for both conditions. The macrophages were the main cell type amongst the samples in the PCV-2 condition, with an average of 54%. This value dropped slightly in the control samples to an average of 26%, making the macrophages the second most dominant cell type in the control samples. Tregs were the second major cell type in the PCV-2 samples, with an average of 21%, and the main cell type amongst the control samples with an average of 34%. The Th1-like T cells were present in the lowest

degree amongst all the samples, with an average of 2% in the PCV-2 samples and 8% in the control samples. An average of 6% Th2-like T cells were present in the PCV-2 samples with an increased value of 14% in the control samples. B cells and APCs were present at an average of 9% and 8% in the PCV-2 samples, respectively. This increased slightly in the control samples with 10% and 11% for the B cells and APCs, respectively.

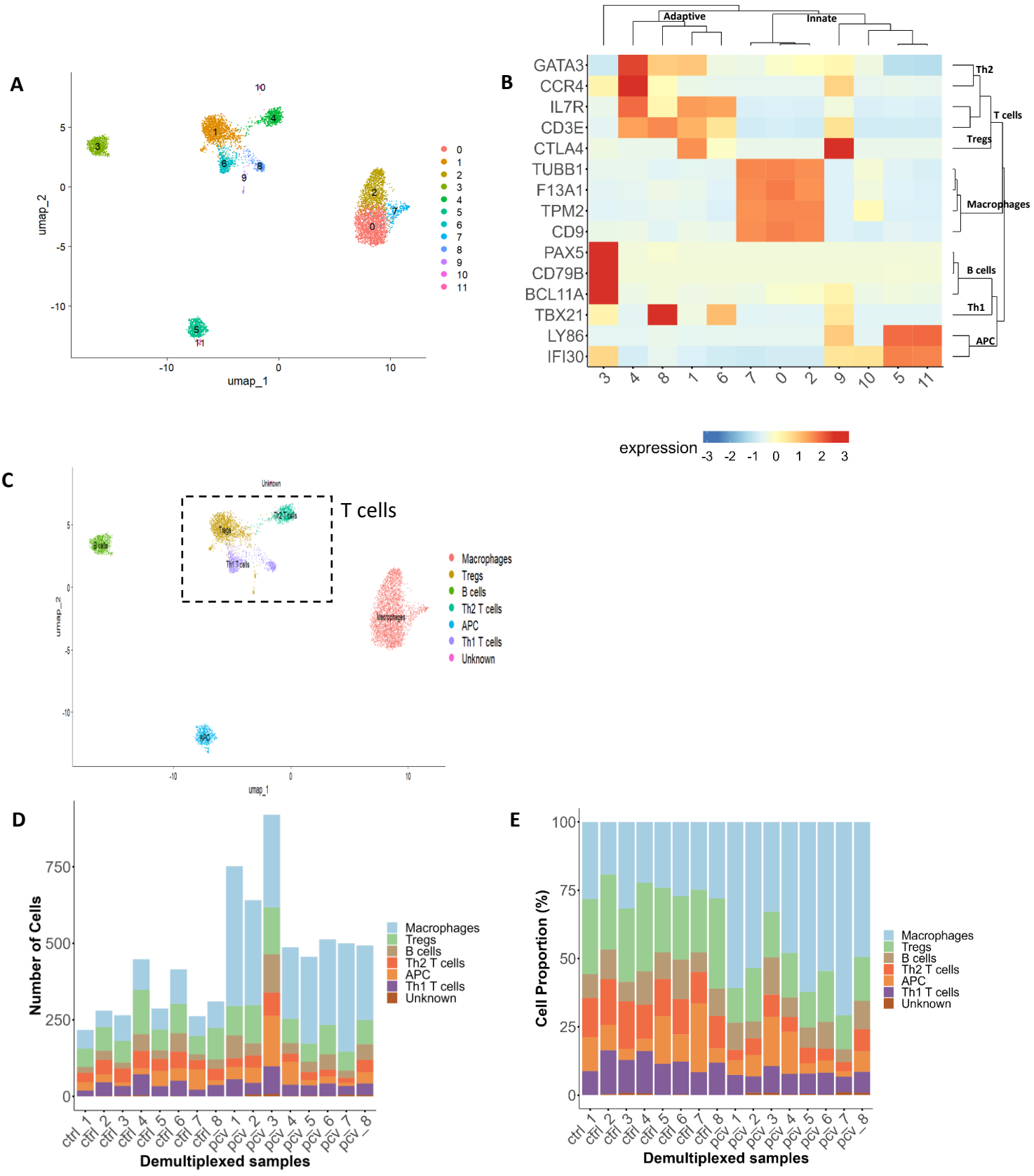

Figure 4.9: Annotation and cell distribution of 11 clusters from the demultiplexed, integrated PCV-2 and control samples. **A:** UMAP of demultiplexed, integrated clustering of PCV-2 and control samples displaying 11 clusters. **B:** Heatmap of avian PBMC marker genes present in the dataset showing relative levels of expression per cluster. The darker the red box the more highly expressed the gene is within a cluster. The bluer a box, the less expressed it is within a cluster**. C:** Annotated UMAP of the demultiplexed dataset showing the cell types identified. **D:** Distribution of cells in each sample showing cell numbers per cell type. **E:** Distribution of cells in each sample showing cell proportion in percentage per cell type. Key: Tregs = T regulatory cells, APC = Antigen presenting cells, Th1 = Th1-like T cells, Th2 = Th2-like T cells, ctrl = control samples, pcv = PCV-2 samples

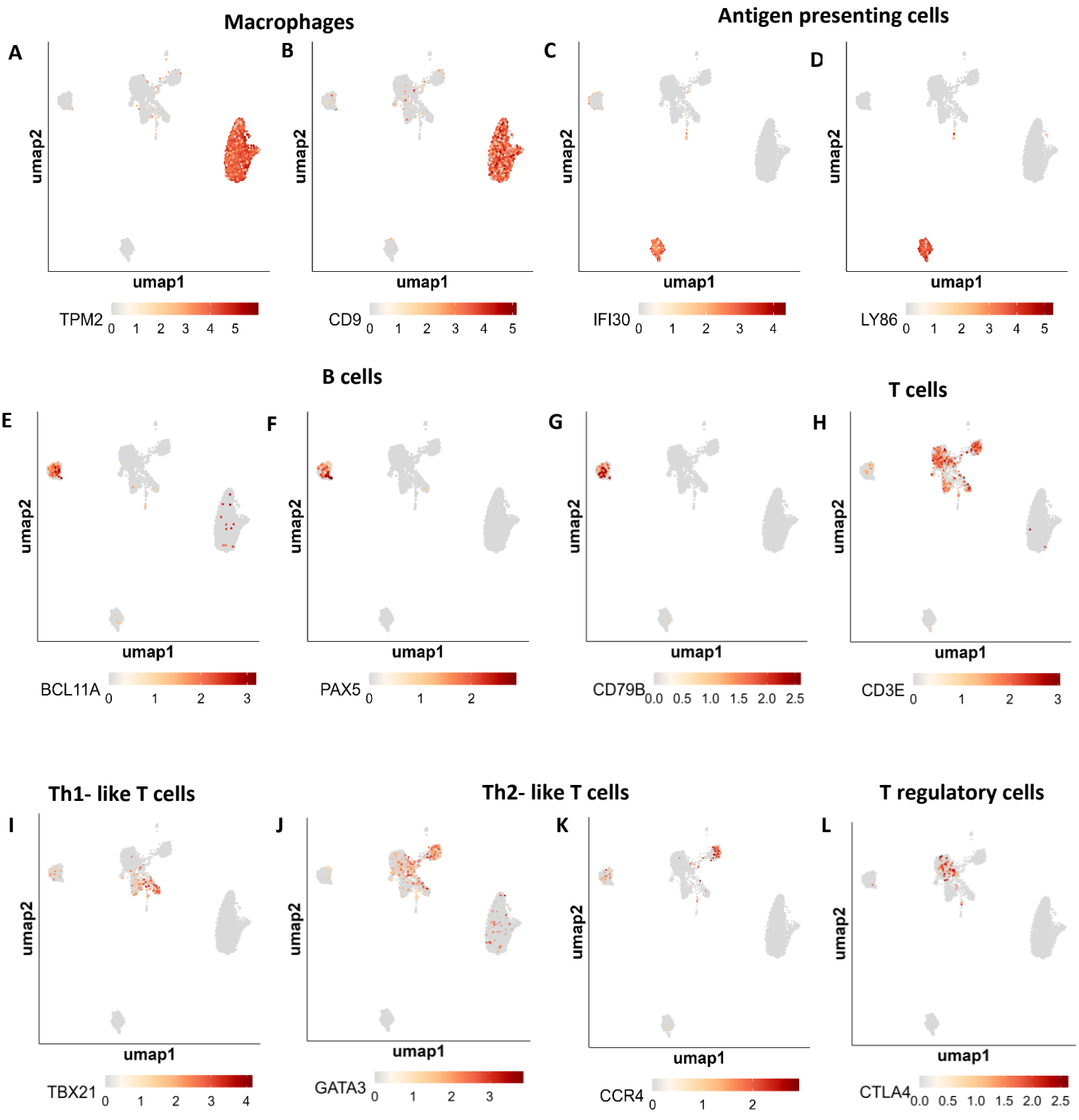

Figure 4.10: Marker genes examined across each of the 11 clusters of the demultiplexed dataset. UMAP plots showing the expression of PBMC marker genes. **A-B:** Macrophage cell type expressing marker genes *TMP2* and *CD9.* **C-D:** Antigen presenting cells expressing marker genes *IFI30* and *LY86.* **E-G:** B cells expressing marker genes *BCL11A, PAX5* and *CD79B.* **H:** T cells expressing marker gene *CD3E* **I:** Th1-like T cells expressing marker gene *TBX21.* **J-K:** Th2-like T cells expressing marker genes *GATA3* and *CCR4.* **L:** T regulatory T cell expressing marker gene *CTLA4*

4.3.4 Differential Expression Analysis

Differential expression analysis was performed using DESeq2 (v 1.40.2) in R (Piper et al., 2022). The pipeline makes use of “pseudo-bulk” values for gene expression for each cell type cluster. DESeq-2 began by normalizing the counts data to ensure that differences in library size between samples were accounted for. Thereafter, QC was performed and relevant functions conducted to perform the differential expression analysis. Differential expression analysis was performed for each cell type (macrophages, B cells, APCs and combined T cells). The T cell subtypes were combined into one cell type cluster to increase the number of cells analysed, thus increasing the number of significantly DEGs detected for the cell type. Dispersion plots showed a decrease in dispersion as the mean count increased for each cell type (Supplementary Data 4, Supp Figure 4.1). The line of best fit, on the plots, showed that the model utilized by DESeq2 was suitable. PCA analysis was conducted using the 500 most variable genes to determine the PCs for each cell type across the two experimental conditions. A clear separation between the samples on PC1 by the experimental conditions were evident for all cell types (Figure 4.11).

Heatmaps for each cell type with the significant DEGs showed a clear separation between sample conditions (Supplementary Data 4, Supp Figure 4.2). Most of the genes that were upregulated in the PCV-2 samples were downregulated in the control samples and vice versa. Significantly upregulated and downregulated DEGs were identified for each cell type (Table 4.6). T cells had the most DEGs with 149 upregulated genes and 48 downregulated genes. This was followed by the APCs, which had 74 upregulated genes and 49 downregulated genes. Macrophages and B cells had the fewest upregulated DEGs, at 57 and 58, respectively. Macrophages had 51 downregulated genes and B cells had 37 downregulated genes.

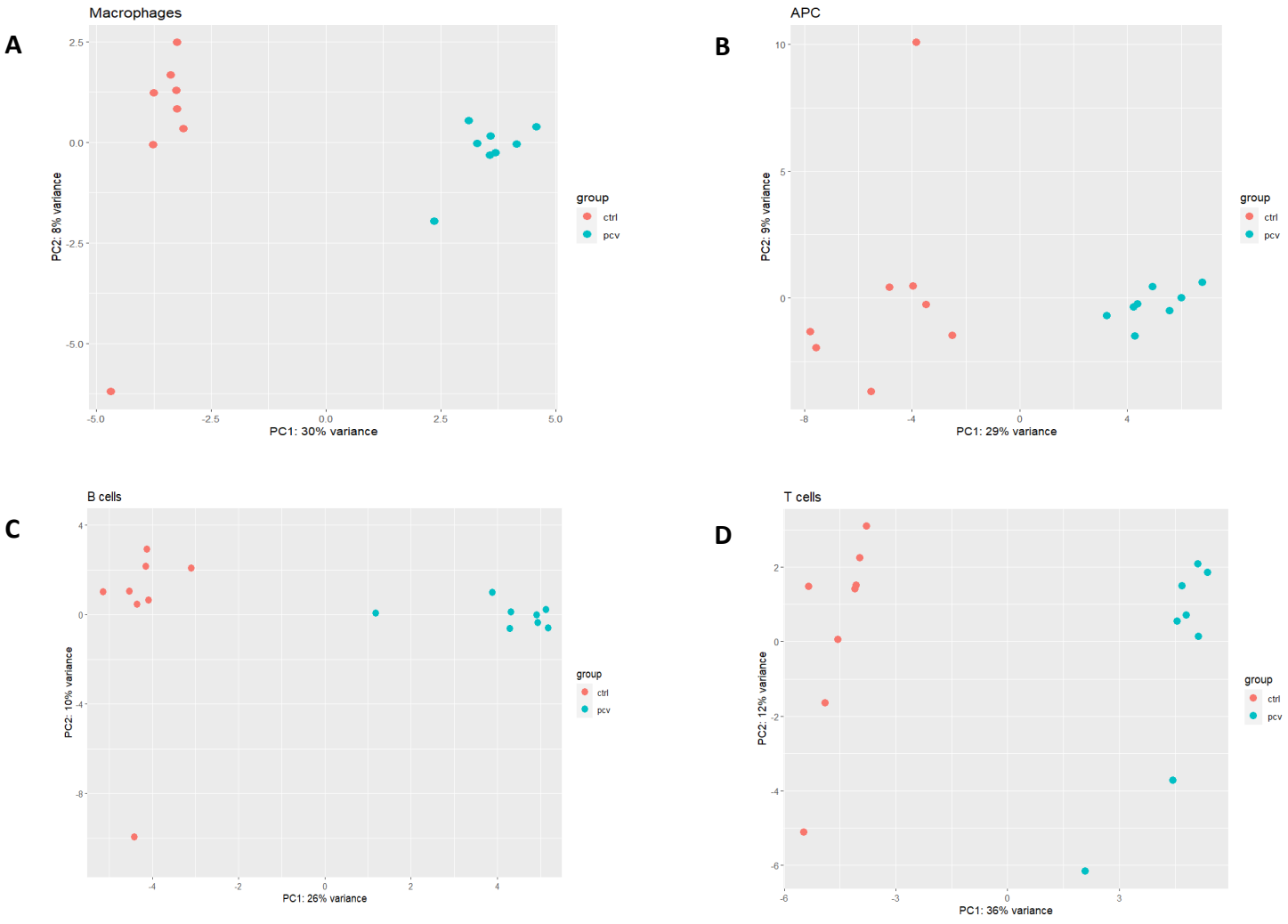

Figure 4.11: PCA analysis displaying a comparison between the PCV-2 and control samples. The first two principal components on the x- and y- axis for each quail sample from the PCV-2 and control conditions. The control samples are indicated in red and PCV-2 samples in blue. **A:** PCA plot for macrophages. **B:** PCA plot for antigen presenting cells. **C:** PCA plot for B cells. **D:** PCA plot for T cells. Key: ctrl = control sample, pcv = PCV-2 sample, APC = Antigen presenting cells

Table 4.6: Number of upregulated and downregulated DEGs for each cell type. The upregulated genes are presented in shades of blue and downregulated genes in shades of green. The intensity of the colour is proportional to the number of differentially expressed genes. Key: APC = Antigen presenting cells

	Cell Type			
	Macrophages	**B cells**	**APC**	**T cells**
Upregulated	57	58	74	149
Downregulated	51	37	49	48

The most upregulated and downregulated DEGs were ordered by Log2FoldChange as evident in Supplementary Data 5. For macrophages, B cells and T cells , the most upregulated DEG was the unannotated transcript, *ENSCJPG00005002336* (Figure 4.12A, C and D; Supplementary Data 5). This gene is orthologous to *ACTN1,* according to the Ensembl Genome Database of 2024 (Harrison et al., 2024). The top 3 annotated upegulated genes for the macrophages were *EEF1D, SDHC* and *USP45*, for B cells they were *MAGOH*, *SF3B5* and *EEF1D* and for T cells they were *DAD1*, *MPC2* and *EEF1D*. While, the top 3 most upregulated (annotated) DEGs for APC were *ASS1, MAGOH* and *EEF1D*. *EEF1D* was shared in the group of the top 3 annotated upregulated genes, between all four major cells types. *MAGOH* was shared between B cells and APCs as the second most upregulated gene.

The most downregulated DEG for the macrophages, was *ENSCJPG00005003476,* for B cells it was *ENSCJPG00005016409* and for T cells it was *ENSCJPG00005019442*. *ENSCJPG00005016409 was* orthologous to *Hbb-bh1,* according to the Ensembl Genome Database of 2024 (Harrison et al., 2024). Orthologues for the other 2 unannotated genes could not be found on the Ensembl Genome Database. The top 3 annotated downregulated DEGs for macrophages were *HMGN1, KTN1* and *CTNNAL1*, for B cells they were *RASGEF1A, LRP12 and SACM1L* and for T cells they were *EML5, RNF41* and *DOT1L*. The top 3 annotated downregulated genes for APCs were *DOT1L, DTX2 and BUD13*. The *DOT1L* gene was shared, as part of the top 3 downregulated genes, between T cells and APCs. Many of the DEGs in Supplementary Data 5 are represented by Ensembl codes as they are novel quail genes and have not yet been annotated.

The DEGs were also analysed by means of an UpSet plot, which shows the number of DEGs that were uniquely differentially expressed in one cell type or shared between more than one cell type (Figure 4.12E). From this plot, it can be seen that 73 genes were uniquely upregulated in T cells, while 17 genes, 15 genes and 11 genes were uniquely upregulated in APCs, macrophages and B cells, respectively. Higher values for the uniquely downregulated genes in macrophages, APCs and B cells were noted at 42, 36 and 28 genes, respectively. Twenty nine genes were uniquely downregulated in T cells. Seventeen upregulated genes were shared amongst all the cell types with only 1 gene commonly downregulated amongst them. B cells, APCs and T cells shared 15 upregulated genes, while macrophages, APCs and

T cells had 10 upregulated genes in common. T cells and APCs shared 13 upregulated genes and 6 downregulated genes. T cells and B cells shared 8 upregulated genes between them and 3 downregulated genes. The DEGs were further analysed by means of Gene Ontology to determine cellular processes that may be involved within each cell type.

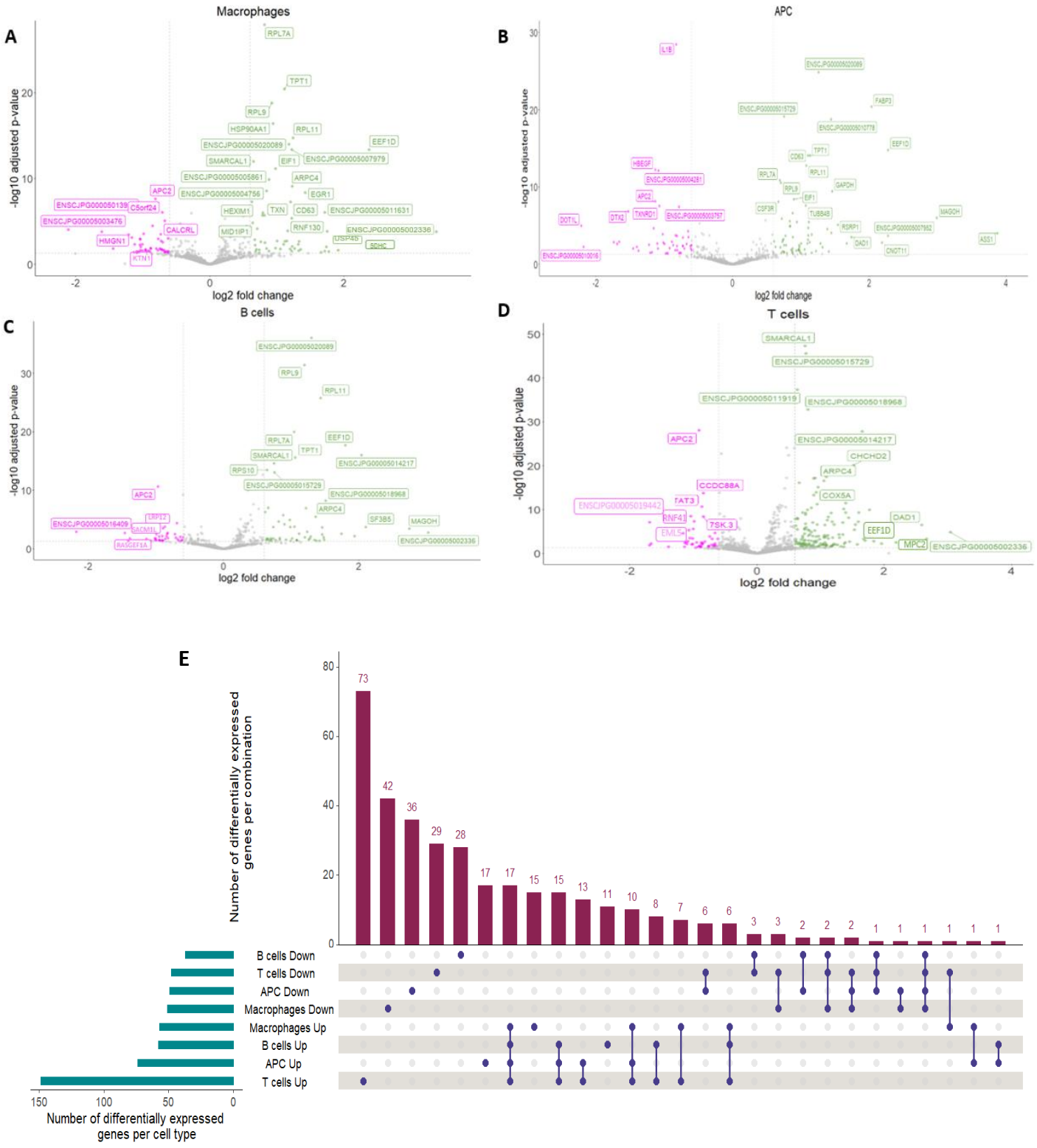

Figure 4.12: Differential expression gene results, using Deseq-2 to compare the PCV-2 and control conditions across the different cell types. A-D: volcano plots showing upregulated and downregulated DEGs for each indicated cell type. Data is plotted with a log2 fold change on the x-axes with the – log10 adjusted p-value on the y-axes. The upregulated genes were filtered (log2FC > 0.6 and adjusted p value < 0.05) and represented in green, while the downregulated genes (log2FC < - 0.6 and adjusted p value < 0.05) are represented in magenta. **E:** Upset plot showing total number of DEGs upregulated or downregulated per cell type (represented by blue bars) and number of DEGs that are either unique to a cell type or are shared across cell types (represented by maroon bars and blue dots connected by lines). Key: APC = Antigen presenting cells

4.3.5 Gene Ontology Analysis

Gene ontology (GO) describes terms that connect cells to one another based on the expression of certain genes. GO terms are organized by Molecular Function (MF), Cellular Component (CC) and Biological Process (BP) based on roles of known genes. GO terms and KEGG pathway analysis were conducted by first inputing the annotated DEG lists (combined upregulated and downreglated DEGs) for each cell type into g:Profiler, as well as separate upregulated and downregulated DEG lists for each cell type (Supplementary Data 5). The analysis was also conducted on unique DEGs of each cell type obtained from the UpSet plot (Supplementary Data 8). Analysis of the combined upregulated and downreglated DEG lists (Figure 4.13) allowed for a broader look at the processes, pathways and regulatory networks that were potentially affected in the experimental condition without any bias in the interpretation. Looking at both the upregulated and dowregulated genes, in a combined list, allowed for a wider scope of analysis rather than focusing only on activation or repression of enriched pathways and processes that may have been involved.

The GO terms shown in Figure 4.13, represent selected terms from a longer list of driver terms determined by g:Profiler (full gProfiler results in Supplementary Data 6). The dominant MF terms, present in all the cell types, were “protein binding” and “catalytic activity”. Selected terms such as “biological regulation”, “ immune system process”, “response to stimulus”, “cellular response to stimulus”, “cell differentiation” and “response to stress” were the dominant BP terms selected across the cell types. The CC terms selected, for all the cell types, were “cytoplasm”, “membrane” and “nucleoplasm”.

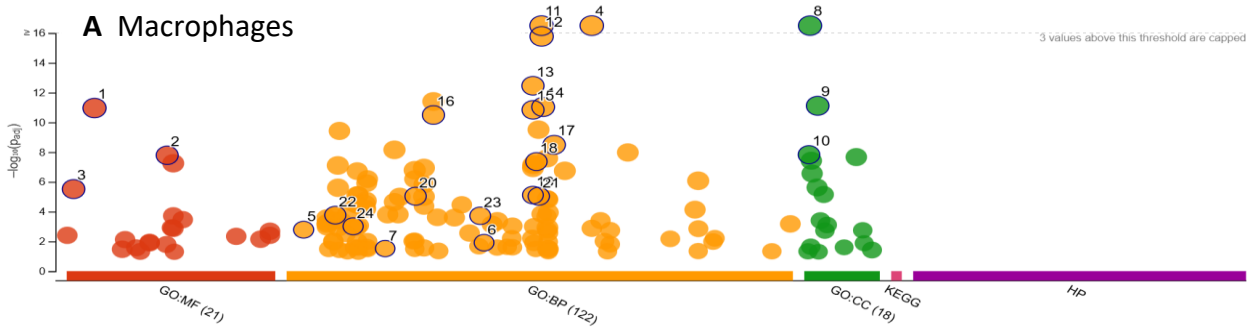

ID	Source	Term ID	Term Name	p_{adj} (query_1)
1	GO:MF	GO:0005515	protein binding	1.092×10^{-11}
2	GO:MF	GO:0036094	small molecule binding	1.638×10^{-8}
3	GO:MF	GO:0003824	catalytic activity	3.052×10^{-6}
4	GO:BP	GO:0065007	biological regulation	2.358×10^{-19}
5	GO:BP	GO:0002376	immune system process	1.645×10^{-3}
6	GO:BP	GO:0042592	homeostatic process	1.230×10^{-2}
7	GO:BP	GO:0016477	cell migration	3.040×10^{-2}
8	GO:CC	GO:0005737	cytoplasm	8.305×10^{-19}
9	GO:CC	GO:0016020	membrane	7.710×10^{-12}
10	GO:CC	GO:0005654	nucleoplasm	1.492×10^{-8}
11	GO:BP	GO:0050789	regulation of biological process	5.299×10^{-18}
12	GO:BP	GO:0050794	regulation of cellular process	1.660×10^{-16}
13	GO:BP	GO:0048518	positive regulation of biological process	3.479×10^{-13}
14	GO:BP	GO:0050896	response to stimulus	9.239×10^{-12}
15	GO:BP	GO:0048522	positive regulation of cellular process	1.442×10^{-11}
16	GO:BP	GO:0032502	developmental process	3.201×10^{-11}
17	GO:BP	GO:0051716	cellular response to stimulus	3.249×10^{-9}
18	GO:BP	GO:0048731	system development	4.322×10^{-8}
19	GO:BP	GO:0048513	animal organ development	7.718×10^{-6}
20	GO:BP	GO:0030154	cell differentiation	9.245×10^{-6}
21	GO:BP	GO:0048869	cellular developmental process	9.245×10^{-6}
22	GO:BP	GO:0006950	response to stress	1.719×10^{-4}
23	GO:BP	GO:0042221	response to chemical	1.908×10^{-4}
24	GO:BP	GO:0009605	response to external stimulus	9.739×10^{-4}

version	e111_eg58_p18_f463989d
date	1/13/2025, 4:22:36 PM
organism	cjaponica

g:Profiler

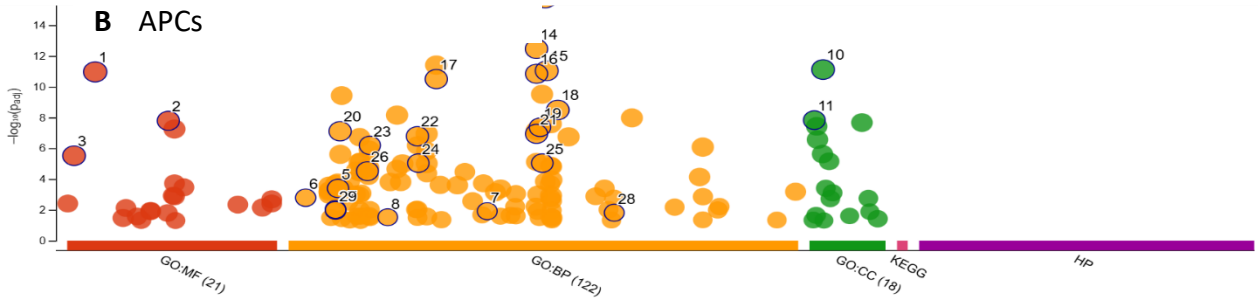

ID	Source	Term ID	Term Name	p_{adj} (query_1)
1	GO:MF	GO:0005515	protein binding	1.092×10^{-11}
2	GO:MF	GO:0036094	small molecule binding	1.638×10^{-8}
3	GO:MF	GO:0003824	catalytic activity	3.052×10^{-6}
4	GO:BP	GO:0065007	biological regulation	2.358×10^{-19}
5	GO:BP	GO:0006996	organelle organization	4.096×10^{-4}
6	GO:BP	GO:0002376	immune system process	1.645×10^{-3}
7	GO:BP	GO:0042592	homeostatic process	1.230×10^{-2}
8	GO:BP	GO:0016477	cell migration	3.040×10^{-2}
9	GO:CC	GO:0005737	cytoplasm	8.305×10^{-19}
10	GO:CC	GO:0016020	membrane	7.710×10^{-12}
11	GO:CC	GO:0005654	nucleoplasm	1.492×10^{-8}
12	GO:BP	GO:0050789	regulation of biological process	5.299×10^{-18}
13	GO:BP	GO:0050794	regulation of cellular process	1.660×10^{-16}
14	GO:BP	GO:0048518	positive regulation of biological process	3.479×10^{-13}
15	GO:BP	GO:0050896	response to stimulus	9.239×10^{-12}
16	GO:BP	GO:0048522	positive regulation of cellular process	1.442×10^{-11}
17	GO:BP	GO:0032502	developmental process	3.201×10^{-11}
18	GO:BP	GO:0051716	cellular response to stimulus	3.249×10^{-9}
19	GO:BP	GO:0048731	system development	4.322×10^{-8}
20	GO:BP	GO:0007154	cell communication	7.862×10^{-8}
21	GO:BP	GO:0048519	negative regulation of biological process	1.160×10^{-7}
22	GO:BP	GO:0023052	signaling	1.653×10^{-7}
23	GO:BP	GO:0010646	regulation of cell communication	6.474×10^{-7}
24	GO:BP	GO:0030154	cell differentiation	9.245×10^{-6}
25	GO:BP	GO:0048869	cellular developmental process	9.245×10^{-6}
26	GO:BP	GO:0010468	regulation of gene expression	3.090×10^{-5}
27	GO:BP	GO:0006793	phosphorus metabolic process	9.448×10^{-3}
28	GO:BP	GO:0071705	nitrogen compound transport	1.551×10^{-2}
29	GO:BP	GO:0006796	phosphate-containing compound metabolic proce...	1.095×10^{-2}

version	e111_eg58_p18_f463989d
date	1/13/2025, 4:28:34 PM
organism	cjaponica

g:Profiler

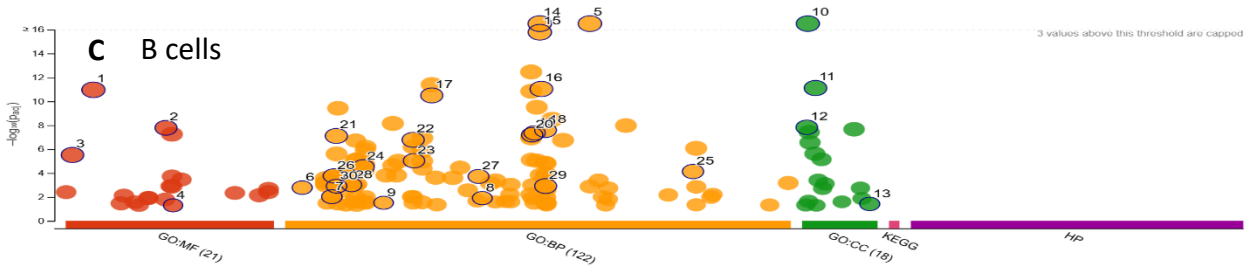

ID	Source	Term ID	Term Name	p_{adj} (query_1)
1	GO:MF	GO:0005515	protein binding	1.092×10^{-11}
2	GO:MF	GO:0036094	small molecule binding	1.638×10^{-8}
3	GO:MF	GO:0003824	catalytic activity	3.052×10^{-6}
4	GO:MF	GO:0043565	sequence-specific DNA binding	4.997×10^{-2}
5	GO:BP	GO:0065007	biological regulation	2.358×10^{-19}
6	GO:BP	GO:0002376	immune system process	1.645×10^{-3}
7	GO:BP	GO:0006793	phosphorus metabolic process	9.448×10^{-5}
8	GO:BP	GO:0042592	homeostatic process	1.230×10^{-2}
9	GO:BP	GO:0016477	cell migration	3.040×10^{-2}
10	GO:CC	GO:0005737	cytoplasm	8.305×10^{-19}
11	GO:CC	GO:0016020	membrane	7.710×10^{-12}
12	GO:CC	GO:0005654	nucleoplasm	1.492×10^{-8}
13	GO:CC	GO:1902494	catalytic complex	3.814×10^{-2}
14	GO:BP	GO:0050789	regulation of biological process	5.299×10^{-18}
15	GO:BP	GO:0050794	regulation of cellular process	1.660×10^{-16}
16	GO:BP	GO:0050896	response to stimulus	9.239×10^{-12}
17	GO:BP	GO:0032502	developmental process	3.201×10^{-11}
18	GO:BP	GO:0051171	regulation of nitrogen compound metabolic proce...	2.587×10^{-8}
19	GO:BP	GO:0048731	system development	4.322×10^{-8}
20	GO:BP	GO:0048583	regulation of response to stimulus	6.204×10^{-8}
21	GO:BP	GO:0007154	cell communication	7.862×10^{-8}
22	GO:BP	GO:0023052	signaling	1.653×10^{-7}
23	GO:BP	GO:0030154	cell differentiation	9.245×10^{-6}
24	GO:BP	GO:0010468	regulation of gene expression	3.090×10^{-5}
25	GO:BP	GO:1901362	organic cyclic compound biosynthetic process	7.380×10^{-5}
26	GO:BP	GO:0006950	response to stress	1.719×10^{-4}
27	GO:BP	GO:0042221	response to chemical	1.908×10^{-4}
28	GO:BP	GO:0009605	response to external stimulus	9.739×10^{-4}
29	GO:BP	GO:0051179	localization	1.220×10^{-3}
30	GO:BP	GO:0007166	cell surface receptor signaling pathway	1.242×10^{-3}

version e111_eg58_p18_f463989d
date 1/13/2025, 11:30:34 PM
organism cjaponica

g:Profiler

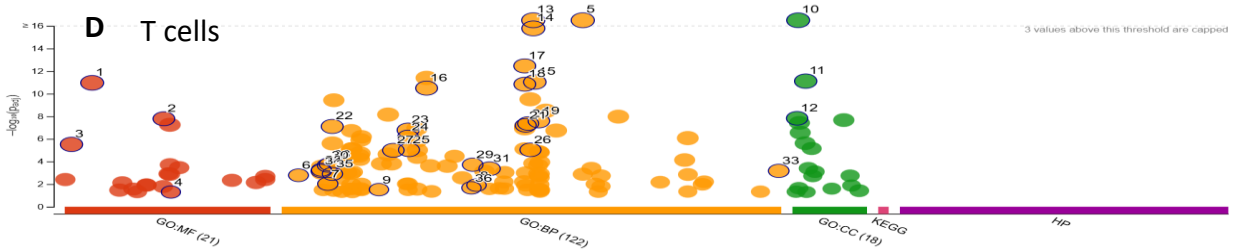

ID	Source	Term ID	Term Name	p_{adj} (query_1)
1	GO:MF	GO:0005515	protein binding	1.092×10^{-11}
2	GO:MF	GO:0036094	small molecule binding	1.638×10^{-8}
3	GO:MF	GO:0003824	catalytic activity	3.052×10^{-6}
4	GO:MF	GO:0043565	sequence-specific DNA binding	4.997×10^{-2}
5	GO:BP	GO:0065007	biological regulation	2.358×10^{-19}
6	GO:BP	GO:0002376	immune system process	1.645×10^{-3}
7	GO:BP	GO:0006793	phosphorus metabolic process	9.448×10^{-5}
8	GO:BP	GO:0042592	homeostatic process	1.230×10^{-2}
9	GO:BP	GO:0016477	cell migration	3.040×10^{-2}
10	GO:CC	GO:0005737	cytoplasm	8.305×10^{-19}
11	GO:CC	GO:0016020	membrane	7.710×10^{-12}
12	GO:CC	GO:0005654	nucleoplasm	1.492×10^{-8}
13	GO:BP	GO:0050789	regulation of biological process	5.299×10^{-18}
14	GO:BP	GO:0050794	regulation of cellular process	1.660×10^{-16}
15	GO:BP	GO:0050896	response to stimulus	9.239×10^{-12}
16	GO:BP	GO:0032502	developmental process	3.201×10^{-11}
17	GO:BP	GO:0048518	positive regulation of biological process	3.479×10^{-13}
18	GO:BP	GO:0048522	positive regulation of cellular process	1.442×10^{-11}
19	GO:BP	GO:0051171	regulation of nitrogen compound metabolic proce...	2.587×10^{-8}
20	GO:BP	GO:0048731	system development	4.322×10^{-8}
21	GO:BP	GO:0048583	regulation of response to stimulus	6.204×10^{-8}
22	GO:BP	GO:0007154	cell communication	7.862×10^{-8}
23	GO:BP	GO:0023052	signaling	1.653×10^{-7}
24	GO:BP	GO:0023051	regulation of signaling	6.543×10^{-7}
25	GO:BP	GO:0030154	cell differentiation	9.245×10^{-6}
26	GO:BP	GO:0048869	cellular developmental process	9.245×10^{-6}
27	GO:BP	GO:0019538	protein metabolic process	1.012×10^{-5}
28	GO:BP	GO:0006950	response to stress	1.719×10^{-4}
29	GO:BP	GO:0042221	response to chemical	1.908×10^{-4}
30	GO:BP	GO:0006810	transport	2.147×10^{-4}
31	GO:BP	GO:0044271	cellular nitrogen compound biosynthetic process	4.331×10^{-4}
32	GO:BP	GO:0006366	transcription by RNA polymerase II	5.361×10^{-4}
33	GO:BP	GO:2001141	regulation of RNA biosynthetic process	6.700×10^{-4}
34	GO:BP	GO:0006355	regulation of DNA-templated transcription	6.888×10^{-4}
35	GO:BP	GO:0007166	cell surface receptor signaling pathway	1.242×10^{-3}
36	GO:BP	GO:0042127	regulation of cell population proliferation	2.131×10^{-2}

version e111_eg58_p18_f463989d
date 1/13/2025, 11:36:38 PM
organism cjaponica

g:Profiler

Figure 4.13: GO driver terms for DEGs of each cell type for combined DEG lists. A-D: GO terms for macrophages, APCs, B cells and T cells. Terms are sorted by GO categories and adjusted p values (Padj) with data points depicted by circles. Red, orange and green circles represent GO terms related to molecular function (MF), biological process (BP) and cellular component (CC), respectively. Key APC = Antigen presenting cells

GO terms were then analysed for the upregulated and downregulated DEGs separately, for each cell type. This was done to determine the biological meaning and functions associated with genes that were specifcally upregulated or downregulated (Supplementary Data 7, Supp Figure 7). GO terms for each cell type were selected from the full list of 'driver terms' obtained from g:Profiler (Supplementary Data 6). In the case where many driver terms were identified for molecular functions, biological processes and cellular components, only the top 3 terms were selected based on adjusted p-values from g:Profiler. The genes related to each GO term were also compared to the top 20 upregulated and downregulated annotated DEGs per cell type. Those DEGs, ordered by Log2FoldChange, that were related to the GO terms, are highlighted in bold in the sections that follow.

Macrophage DEGs

DEGs that were upregulated in macrophages were related to the MF "structural molecule activity" (*H1-0, RPL7A, RPL9,* ***RPL11****,* ***ARPC4****,* ***H2AZ2****, ARPC1B*). The top 3 CC terms, based on the adjusted p-values, were "respiratory chain complex", "respirasome" and "mitochondrial respiratory chain complex IV" (common genes amongst the 3 terms were: *NDUFA4, COX5A and COX7C*, *NDUFB4,* ***SDHC***). No BP were detected in the upregulated DEGs for this cell type. The 2 KEGG pathways identified were "oxidative phosphorylation" and "glycolysis/ gluconeogenesis".

No GO terms were detected in the downregulated DEGs of the macrophages. One KEGG pathway was found which was related to the "NOD-like receptor signaling pathway".

APC DEGs

The upregulated DEGs of the APCs were related to CC terms and KEGG pathways only. The top 3 CC terms, based on the adjusted p-values, were "respiratory chain complex", "respirasome" and "membrane protein complex" (common genes amongst the 3 terms were: *COX6A1,* ***SDHD****, NDUFB4, NDUFAB1)*. The 2 KEGG pathways identified were "oxidative phosphorylation" and "spliceosome".

The top 3 MF terms identified in the downregulated APC DEGs were "chemokine activity", "cytokine activity" and "chemokine receptor binding" (common gene amongst the 3 terms

was: *IL1B*). The "immune system process" (***IL1B***, *SDC4,* ***PDE4B***, ***YWHAE***, ***PLSCR1***), "regulation of calcium ion transport" and "regulation of monoatomic ion transport" (common genes between the 2 terms were: ***PDE4B***, ***YWHAE***, ***CHD7***, ***RRAD***) were the BP terms identified. The 2 KEGG pathways found were "NOD-like receptor signaling pathway" and "toll-like receptor signaling pathway".

B cells DEGs

Within B cells, "structural molecule activity" and "structural constituent of ribosome" (common genes between the 2 terms were: ***RPL9***, ***RPL11***, *RPL7A, RPS10*) were identified as the MF terms of the upregulated DEGs. The BP terms identified as the 3 most upregulated were "aerobic respiration" and "cellular respiration" as well as "energy derivation by oxidation of organic compounds" (common genes amongst the 3 terms were: ***CHCHD2***, ***SDHD***, *COX5A, ATP5F1D, COX7A2L,* ***FH***, *ATP5MF*). "Respiratory chain complex", "inner mitochondrial membrane protein complex" and "respirasome" (common genes amongst the 3 terms were: *COX5A, NDUFB4, COX7A2L,COX6A1*) were identified as the top 3 CC terms, with "oxidative phosphorylation" identified as the KEGG pathway.

The downregulated DEGs resulted in the top 3 MF terms being "histone H3 methyltransferase activity", "lysine N-methyltransferase activity" and "protein-lysine N-methyltransferase activity" (common genes amongst the 3 terms were: ***ASH1L***, ***SETD1B***, ***SETD2***). The only CC term identified was "hemoglobin complex" and KEGG pathway identifed was "lysine degradation".

T cells DEGs

DEGs that were upregulated in the T cells that were related with the MF, were "structural molecule activity" and "structural constituent of ribosome" (common genes between the 2 terms were: *RPL7A, RPL11, RPL9, ARPC4,* ***H2AZ2***, *TUBB4B, ARPC1B, H1-0,* ***RPL39***). BPs that were enriched in the upregulated T cell DEGs were "oxidative phosphorylation", "aerobic respiration" and "cellular respiration" (common genes amongst the 3 terms were: ***CHCHD2***, *COX5A,* ***SDHD***, *ATP5F1D, COX7C, ATP5MF, NDUFB6, NDUFC2, NDUFA8)*, amongst others. "respiratory chain complex", "respirasome" and "inner mitochondrial membrane protein complex" (common genes amongst the 3 terms were: *COX6A1, COX5A,* ***SDHD***, *COX7C,*

NDUFB4, NDUFA4, NDUFB6, NDUFAB1, NDUFC2, UQCRC1, NDUFA8) were the top 3 CC terms listed. The KEGG pathways identified were “oxidative phosphorylation” and “RNA polymerase”.

No MF terms were identified for the downregulated T cell DEGs. The one BP term was “regulation of signal transduction” (*APC2,* ***CCDC88A****,* ***STAT3****, EGR1, RGS2,* ***HMGCR****,* ***ATF3****,* ***DDX60****, DOT1L,* ***RSAD2****,* ***SMAD5****,* ***ITPR1****, RNF41,* ***GID8***) and CC term was “hemoglobin complex” with KEGG pathway being “NOD-like receptor signaling pathway”.

DEGs shared across cell types

The MF term identified in the upregulated DEGs for macrophages, B cells and T cells, was “structural molecule activity”. “Structural constituent of ribosome” was the other MF term expressed by the B cells and T cells, which highlights the upregulation of structural integrity of molecules that form part of the ribosome. Shared CC terms between the upregulated DEGs, of all the cell types, were related to “respiratory chain complex”, “respirasome” and “mitochondrial respiratory chain complex”. The CC terms unique to the upregulated B cell DEGs included terms such as “MHC protein complex” and “MHC class II protein complex”. “Oxidative phosphorylation” was the KEGG term present for all cell types.

For the downregulated DEGs, the only shared term, was that of the cellular component between B cells and T cells, which related to “hemoglobin complex”. No other terms, for the downregulated DEGs, were shared between cell types. The KEGG pathway present for macrophages, APCs and T cells was “NOD-like receptor signaling pathway.

Comparison of GO terms and the top 20 DEGs

Many of the top 20 upregulated DEGs in all the cell types were related to “structural molecule activity”. B cells and T cells contained a few DEGs that were associated with “aerobic respiration” and “cellular respiration”. The other GO terms showed a poor correlation with the top 20 upregulated DEGs having just one gene in common or none at all.

APCs had many of the top 20 downregulated DEGs associated with “immune system process”, “regulation of calcium ion transport” and “regulation of monoatomic ion transport. B cells also shared a number of the top 20 downregulated DEGs with terms related to “histone H3 methyltransferase activity”, “lysine N-methyltransferase activity” and “protein-lysine N-methyltransferase activity”. “Regulation of signal transduction” had many genes in common with the top 20 downregulated DEGs for T cells.

GO terms from unique UpSet plot gene groups

GO analysis was performed on unique DEGs of each cell type obtained from the upset plot. Only GO terms for the upregulated T cells and downregulated APCs, B cells and T cells were identified, when using g:Profiler (Supplementary Data 8 and 9, Supp Figure 9). The MF term identified in the upregulated T cell DEGs was “DNA-directed 5'-3' RNA polymerase activity”, the BP terms were related to “mitochondrial respiratory chain complex assembly” and “formaldehyde catabolic process” and the KEGG pathway identified was “RNA polymerase”. For APC downregulated MF terms, “cytokine activity” and “chemokine activity” were identified, with two of the identified KEGG pathways related to “Toll-like receptor signaling pathway” and “RIG-I-like receptor signaling pathway”. Many of the MF terms identified in the downregulated B cells DEGs were related to “histone and lysine methyltransferase activity”, while the identified KEGG pathway was “lysine degradation”. Only BP terms were identified from the downregulated T cell DEGs. These mainly related to interleukin 2- and 15- response.

Summary

From the GO results, it can be noted that the four cell types share similar gene products that have similar functions. This analysis enabled the identification of the different pathways shared between the cell types. All cell types were involved in structural molecular activities, as well as actively involved in respiratory activities. This may imply that cells were rapidly dividing, which lead to increased mitochondrial activity to support the high energy requirements. The response to stress may have also lead to the upregulation of the respiratory chain complex. From the downregulated pathways, it would appear that there was a reduced immune response and general inflammation amongst all the cell types.

4.4 Discussion

The potential of infection to both humans and animals continues to pose a major threat in today's world (Dei Giudici et al., 2023). Diseases common to certain animal groups, such as PCV-2 to pigs, can result in great damage and loss of life and business (Fan et al., 2023). While human intervention, in reducing the effects of the PCV-2 disease may be possible, elimination of infection, once already present, remains a challenge (Sagrera et al., 2024). The one system capable of eliminating the threat and protecting the host is the immune system. By sequencing the transcriptome of PBMCs, obtained from PCV-2 injected or control groups of quails, and analysing their genetic profile at the level of individual cells, this chapter provides the first insights into the immunological responses of the experimental quails to this VLP. This study built an understanding of the types and functions of quail immune cells that may be involved when responding to PCV-2 antigens in quails, following their exposure to the stimulus. In particular, the molecular functions and biological pathways involved in the quail immune system, when injected with the VLPs, were investigated using scRNA-seq.

Quality of scRNA-seq datasets

The intention to obtain 10 000 cells per sample, following completion of the 10X Genomic protocol, was conducted by inputting specified volumes of PBMC sample at the onset of the experiment. The capture efficiency of the platform is approximately 60% (Yamawaki et al., 2021). Therefore, achieving 10 716 cells and 8 426 cells for the PCV-2 and control groups, respectively, was satisfactory. These values dropped to 8325 cells for the PCV-2 group and 4312 cells for the control group, following Seurat filtering. The PCV-2 sample had a higher median gene per cell count (518) compared to the control sample (448). This increase may be due to the activation of the immune system, caused by the PCV-2 VLP, that resulted in an increase in gene expression diversity. Qu et al., 2022b, made a similar finding in PBMC samples of chickens that were infected with Avian leukosis virus subgroup J (ALV-J). They found that the ALV-J infected samples had a greater median gene count compared to the control samples at 337 and 312 genes per cell, respectively (Qu et al., 2022b). Similar results were also found in other studies, where infected PBMC samples had higher values than the control samples, due to increased cellular activation markers and responding proteins

caused by an infection (Lagumdzic et al., 2023; Vahey et al., 2002). The percentage of valid barcodes in the current study was over 75% for both samples (95.4% for PCV-2 and 87.7% for control), which indicated adequate sequencing with no sequencing issues. Overall, these initial statistics revealed the expected trends and, therefore, indicated that the data was suitable for further bioinformatic analyses.

To allow for DEG analysis, using the DESeq-2 software, sample replicates were needed (Piper et al., 2022). For the scRNA-seq protocol, small aliquots of blood samples from 8 individual quails (per experimental group) were pooled to achieve enough blood volume to isolate PBMCs, while also reducing costs and technical variability during library preparation and limit the number of animals utilized for the experiment. Using scSplit, the pooled datasets were bioinformatically separated into samples of the individual quails (Xu et al., 2019). Other demultiplexing tools include Freemuxlet, Demuxlet, Souporcell, Vireo, Demuxafy, amongst others (Neavin et al., 2024). Pooled samples have been successfully demultiplexed using the various tools, allowing for separation of samples having only partial or no genotype information (Huang et al., 2019; Nassiri et al., 2024; Neavin et al., 2024; Zhu et al., 2024). In this study, pooled sample datasets were demultiplexed using the hidden state model of scSplit as well as identifying variant sites and modeling the allelic counts by assigning cells to clusters utilizing an expectation-maximization framework (Xu et al., 2019). This tool allowed for the separation of the pooled blood samples into samples from each individual quail, thus increasing the number of samples that could be analysed. Through the demultiplexing protocol, further filtering was conducted by scSplit, resulting in an average cell count per quail of 604 and 320 cells for PCV-2 and control samples, respectively. To maintain uniformity between the pooled dataset and the demultiplexed datasets, Seurat filtering was also employed to remove barcodes greater than 8000 transcripts (UMIs), barcodes with fewer than 200 genes, barcodes with a fraction of number of genes detected per UMI that was fewer than 0.8 and barcodes with a mitochondrial gene count of more than 10%. The filtering parameters used were chosen based on those commonly used in literature involving studies on avian PBMC samples (Dai et al., 2023; Maxwell et al., 2024; Qu et al., 2022a; Warren et al., 2023). Other features used in the filtering process included the removal of genes that had zero counts in each cell and removal of genes expressed in less than 10 cells. Prior to Seurat filtering, PCV-2 samples had a total cell count of 4829 and

2561 for the control. After both scSplit and Seurat filtering, the PCV-2 samples had a total of 4762 cells and the control samples had 2484 cells. The cell numbers were far lower, in the demultiplexed samples, than in the pooled samples. This reduction may most likely be due to scSplit using the CellRanger BAM file as input, which was already filtered, followed by additional filtering (by scSplit and Seurat) as well as removal of doublets. The scSplit and Seurat filtering most probably provided a more stringent filter and subsequently removed more low-quality barcodes which may have been GEMS containing cell debris. After filtering, the median number of UMIs per cell for the PCV-2 condition was 1234 and 1098 for the control. The median number of genes per cell was 517 for the PCV-2 condition and 454 for the control (Figure 4.6). These values were in line with previous studies conducted on avian PBMC samples, making the results of this study consistent with studies performed on other birds and thus suggesting good quality data (Qu et al., 2022a; Warren et al., 2023). For example, analysing chicken PBMCs, Qu et al., 2022a, obtained a median number of genes per cell ranging from 312 to 372 and median UMIs per cell from 450 to 503. Warren et al., 2023, obtained a median of 478 genes per cell.

Thereafter, data normalization was conducted to account for variations in sequencing depth and over-dispersed counts to enable comparison across genes and samples. The counts of the mapped reads of every gene are relative to the RNA expression (Satija et al., 2015). Taking the sequence depth into account is important to compare gene expression levels amongst cells. The length of sequenced genes were also accounted for to enable comparison of gene expression within the same cell (Satija et al., 2015). Normalization began with scaling, where every UMI count was multiplied by the cell specific factor to ensure that every cell contained the same UMI count. Due to different cells containing varied amounts of mRNA (because of variation between cell types or success of the scRNA-seq experimentation between individual droplets), scaling is necessary. Secondly, data was transformed during normalization. This process facilitated the data being more comparable across cells by eliminating biases and technical variation such as technical noise, cell size and sequencing depth.

The pooled PCV-2 and control datasets were then aggregated and integrated to allow for alignment of same cell types across the two conditions. Similar clustering patterns of both

conditions were noted, when aggregated and integrated. This implied that the cell types, in every cluster, were present in both conditions. The quails used in the experiment were brought from a local farm to the laboratory at 7 weeks old. This meant that the quails used in both experimental groups (PCV-2 and control) were previously exposed to the outside environment, may have suffered infection from pathogenic and non-pathogenic microorganisms, had exposure to beneficial and commensal organisms as well as toxins and allergenic substances. As a result of this, both groups of quails would have had an immune system that was in the innate and adaptive phase. This may be why the integrated dataset showed similar clustering patterns, and therefore, similar cell types in both experimental quail groups. To determine the sole effect of PCV-2 on the immune system, germ-free or specific pathogen-free quails should be used. Obtaining germ-free or specific pathogen-free quails for the current study was not possible due to cost and time constraints, however, this can be a consideration for future studies.

To assess the quality of the data, the pooled, integrated dataset was processed and analysed ahead of the demultiplexed datasets. The high quality normalized and scaled data was then clustered using Seurat. Clustering of cells was achieved based on the PCA value of cells obtained from the expression of the most variable genes. Using the K-nearest neighbor approach for clustering, Seurat groups cells together into different clusters. The clustering of cells was possible using the Euclidean distance in PCA space and the Louvain algorithm (in Seurat), to create a graph with a set resolution parameter that determined the number of clusters produced (Macosko et al., 2015). Fourteen clusters were obtained for the pooled, integrated dataset.

Thereafter, the identity of the clusters was determined using marker analysis to establish the types of cells found in the samples and their gene expression patterns. Seurat's *FindConservedMarkers* allowed the detection of the conserved markers that were differentially expressed across clusters within both conditions. Along with this form of analysis, the expression of cell-specific, avian PBMC marker genes were used to assign identities to each cluster. A manual approach was implemented for the annotations due to the lack of an appropriate quail reference atlas to map to. Alternate methods for annotation may include the use of gene sets or reference expression profiles that may exist for certain

species, well curated reference datasets and cell type databases, such as *PanglaoDB*, *MapMyCells, CellMarker,* and other sample specific atlases (Franzén et al., 2019; Hu et al., 2023; MapMyCells (RRID:SCR_024672). Artificial intelligence tools, such as *Pluto AI* (https://pluto.bio) can also be used, or machine learning-based tools that compares the gene expression data to reference datasets (such as *scMatch* or *CellTypist*) (Pasquini et al., 2021; Quan et al., 2023). These methods can be efficient and time-saving when a well-curated, detailed reference dataset exists (Pasquini et al., 2021). Tools that have been used, in previous studies, for chicken PBMC dataset analyses included *PanglaoDB* and *CellMarker* (Dai et al., 2023, 2021a; Warren et al., 2023). However, these tools were used for comparison against human and mice biomarkers as reference and cell type databases for avian species are not widely available.

Four major cell types were present in the sample, namely macrophages and APCs that made up the innate immune response and B cells and T cells (further subclustered into Tregs, Th1-like T cells and Th2-like T cells) that formed the adaptive immune cells. The published avian, PBMC marker genes used for annotation, produced clear expression patterns in the feature plots (Figure 4.8 and 4.10) and heatmaps (Figure 4.7D and 4.9B), which allowed for a convincing identity of clusters for both the pooled and demultiplexed datasets. VLPs have been shown to induce an adaptive immune response in animals (Crisci et al., 2013). Crisci et al., 2013, published that VLPs can induce a humoral and cell mediated response with high presence of B cells, CD4+ T cells and cytotoxic T lymphocytes, which is the goal of any vaccine. They also reported that birds immunized with Newcastle disease virus VLPs, elicited an adaptive immune response with the production of specific antibodies, B cells and T cells (Crisci et al., 2013). The presence of APCs are also common with VLP immunization as these cells effectively take up the VLP for antigen presentation to other cells (Schädler et al., 2019). VLPs have the ability to elicit both an innate and adaptive immune response in birds, and thus lead to the presence of cells pertaining to both types of responses (Schädler et al., 2019). Therefore, the four major cell types found in this study, are in line with what was expected.

The proportion of cells, in the pooled dataset, showed that macrophages were the most dominant in both the PCV-2 and control samples. The second largest cell type was T cells for

both samples, with the subgroup of Tregs, Th1-like and Th-2 like T cells being higher in the control samples compared to the PCV-2 samples. B cells and APCs were the smallest groups between both samples when compared to the 4 major cell types. Similar cell proportions were obtained for the demultiplexed dataset. In this dataset, macrophages were also the largest cell type for samples in both experimental conditions, with samples in the PCV-2 condition having more macrophages than the control condition. T cells were the second largest combined group for samples in both conditions. All subtypes of the T cell group were more dominant in the samples of the control condition than the PCV-2 condition. APCs and B cells were also higher in the control condition than the PCV-2 condition. The greater proportion of cells belonging to the combined groups of macrophages and APCs, as compared to the combined groups of T cells and B cells, showed that more cells of the innate immune system were present in all the samples. The T helper cells and Tregs are subtypes of CD4+ T cells. A study conducted by Dai et al., 2023, had similar findings where virus-infected avian samples had a greater macrophage proportion. They also found that the control samples had a greater proportion of T cells (specifically CD4+ T cells) than the infected samples (Dai et al., 2023). The macrophage dominance, followed by a T cell prevalence may indicate that the PCV-2 birds were still in an innate immune response state and early adaptive immune state as macrophages are usually the first responders and assist in activating other components of the immune system (Jin et al., 2018). Macrophages also present antigens to T cells, thus initiating T cell proliferation (Jin et al., 2018). The lower levels of T cells in the PCV-2 samples compared to the control samples may also indicate that the PCV-2 birds were experiencing an innate immune response and early adaptive immune response, as the innate immune response (dominated by macrophages) take precedence initially (in infected samples) while non-infected samples experience normal immune surveillance (Mehrzad et al., 2024). The small proportion of B cells in the PCV-2 samples may also indicate that the birds were in an early stage of the adaptive immune response and thus producing low levels of antibodies. This result correlates with the low anti-PCV-2 antibodies isolated from the egg and blood samples in Chapter 3.

Differential gene expression and gene ontology

Differential expression analysis was performed, using DESeq2 to determine the most upregulated and downregulated genes in the demultiplexed samples of each experimental condition. The differential expression analysis, using DESeq2, made use of "pseudo-bulk" values for gene expression for each cell type cluster. This approach aggregated the gene expression across the cells within each cell type cluster, treating all the cells within that cluster as if they were part of a single "bulk" sample. To reduce the influence of individual cell variability and noise, aggregation is necessary. This pseudo-bulk method is superior to other single cell methods in terms of their sensitivity and specificity (Murphy and Skene, 2022). DESeq2 uses a negative binomial distribution to model the count data allowing statistical comparisons between experimental conditions across samples (Love et al., 2014). Following PCA, the PC 1 verse PC2 plots showed distinct separation between samples of the two experimental conditions (Figure 4.11). The clear separation was noted for plot of all the cell types. This showed that samples within each condition were similar to one another, resulting from a good separation between the experimental groups.

GO analysis was conducted on the DEGs to allow for the connections between cells to be described looking specifically at molecular functions, cellular components and biological processes. The GO terms and KEGG pathways of upregulated and downregulated DEGs of each cell type were analysed.

Macrophages

Macrophages are responsible for phagocytic activity and cytokine production (Qureshi, 2003). Phagocytosis is possible via different mechanisms. Most commonly, specific receptors present on the macrophage surface, bind to specific targets, enabling phagocytosis. They also have scavenger receptors that internalize pathogens and kill via the production of nitric oxide (Chaplin, 2010; Mehrzad et al., 2024). Following degradation of the foreign threat, the macrophage presents the antigenic components to other immune cells such as B cells and T cells (in either class I or class II major histocompatibility complex molecules, MHC) (Qureshi, 2003). Macrophages persist at sites of infection or chronic inflammation for long periods of time (Chaplin, 2010). While they attack during the innate immune response phase, they may also form part of the adaptive immune response via their

regulatory role in the production of certain cytokines and presentation of antigens (Chaplin, 2010).

The most upregulated DEG in the macrophage, B cell and T cell groups, was the unannotated transcript, *ENSCJPG0000500233,* which is orthologous to *ACTN1.* This gene codes for *actinin alpha 1*, which plays a role in immunology as an actin cytoskeleton (Sun et al., 2022). The actin cytoskeleton assists with the formation of the immune synapse, which is the interface between cells such as macrophages and T cells or B cells. The synapse is involved in T cell activation and maturation. With B cells, actin regulates B cell receptors (Sun et al., 2022). The cytoskeletal adjustments by actin result in changes in cellular structure that affect T cell and B cell development and activity (Dustin and Cooper, 2000; Sun et al., 2022). Therefore, due to the high number of macrophages and lower numbers of T cells and B cells, identifying *actinin alpha 1* as being highly upregulated, may indicate that T cells and B cells were most likely in the earlier stages of activation and maturation.

EEF1D, SDHC and *USP45* were the top 3 annotated upregulated genes for the macrophages. The *EEF1D* gene is responsible for elongation during protein synthesis (Gao et al., 2020). *SDHC* (*Succinate Dehydrogenase Complex Subunit C*) faciltates the conversion of succinate to fumerate in the Krebs cycle, thereby assisting in mitochondrial function, cellular respiration and energy production (Esteban-Amo et al., 2024). Lastly, *USP45* codes for an enzyme that removes ubiquitin molecules from proteins (Sun et al., 2022). Ubiquitin is a small protein that attaches to other proteins, marking them for degradation. The enzyme, encoded for by *USP45,* stabilizes certain proteins and regulates their activity by removing the ubiquitin molecule, thus saving them from being degraded or altering their function (Sun et al., 2022). Therefore, the upregulation of these 3 genes, may indicate that their protein cellular functions were involved in proliferation and differentiation of cells, cellular metabolism which was important for immune cell activation and differentiation, and ubiquitin-mediated protein regulation. From the high macrophage cell numbers, it was obvious that this cell type was in a high state of proliferation. Due to this state, there would have been greater levels of cellular metabolism to allow the macrophages to engage in possible cytokine production and antigen presentation during the immune response (Esteban-Amo et al., 2024; Gao et al., 2020; Sun et al., 2022).

The top 3 annotated downregulated DEGs for macrophages were *HMGN1, KTN1* and *CTNNAL1. HMGN1* encodes for a nuclear protein that stimulates cytokine and chemokine production during activation of the innate immune response (Arts et al., 2018). Therefore, downregulation of this gene would mean that there was a reduction of cytokine and chemokine production and a subsequent weakened inflammatory response. Downregulation of pro-inflammatory responses may indicate that a regulatory process is at play to protect the host (against tissue damage) and regulate the progression of the immune response (Chen et al., 2018). Downregulation of the *KTN1* gene could lead to reduced antigen presentation and cytokine secretion. This is because the resultant protein is involved in vesicular trafficking allowing for efficient transport of intracellular components (such as antigens) (Gao et al., 2021). *CTNNAL1* is linked to cell migration allowing cells to move to sites of infection (Guerra et al., 2023). Downregulation of this gene, may mean that the migration of the macrophages to the sites of infection or their ability to present antigens to T cells were reduced.

The MF term “structural molecule activity” was upregulated . The upregulation of genes that are invovled in ribosomal proteins and actin production (*ARPC4*), indicate that ribosome synthesis was increased, which may indicate an increase in cell growth and proliferation, and cell signalling (Sun et al., 2022). Macrophages form part of the innate immune system and are responsible for phagocytosis, and regulation and initiation of other immune cells. From the upregulated genes, such as those discussed above, as well as the upregulation of ribosomal proteins, it would appear that the macrophages were in a state of phagocytosis (Mylvaganam et al., 2021). Phagocytosis is made possible with an intricate cytoskeleton composed of actin filaments (genes encoding for this was upregulated). Phagocytosis, however, results in excessive inflammation (Mylvaganam et al., 2021). With the downregulation of cytokine related genes, it would appear that a pro-inflammatory state was active but reduced in this cell type, possibly as a protection mechanism or regulatory function. The activities of the cells would require high levels of energy (by the mitochondria), which explains the upregulation of the cellular component terms “respiratory chain complex” and “mitochondrial respiratory chain complex IV”. It would therefore appear that the macrophages were in the early stages of phagocytosis and also involved in initiating the adaptive immune response.

T cells

The combined T cell cluster was the second largest cluster identified. The demultiplexed samples, within this cluster, expressed *DAD1*, *MPC2* and *EEF1D* as the top 3 annotated upregulated DEGs. *DAD1* encodes for a protein that improves cell survival, by regulating programmed cell death, homeostasis and cell proliferation (Hong et al., 1999). Upregulation of the *MPC2* gene increases the subunit of the mitochondrial pyruvate carrier, to regulate the transport of pyruvate into the mitochondria (Ramstead et al., 2020). Pyruvate must be transported into the mitochondria to create ATP. During activation, T cells enhance aerobic glycolysis to support the requirements for cell proliferation and cytokine production. Therefore, upregulation of *MPC2* signifies rapid expansion of immune cells in response to an infection by means of oxidative metabolism (Buchanan and Taylor, 2020). Upregulation of these genes, including *ACTN1* and *EEF1D* as discussed above, implies the proliferation, activation and differentiation of the T cells within the sample.

Downregulation of *EML5, RNF41* and *DOT1L,* was noted in the T cells. *EML5* (*Echinoderm Microtubule-Associated Protein-Like 5*) is mainly expressed in the brain and is involved in regulating microtubules. The function of this gene has been primarily established in brain samples and therefore its role in immune cells is unknown (Sun et al., 2015). The involvement of the gene in cytoskeletal rearrangement, as a result of regulating microtubules, include cell division, motility and signaling (Sun et al., 2015). It can, therefore, be speculated that these functions may be similar to the functions of the T cells. Downregulation of the cytoskeletal rearrangement in the T cells would indicate reduced cell division, motility and cell signaling. *RNF41* encodes a protein that prevents the production of pro-inflammatory cytokines and assists with anti-inflammatory responses (Moreno-Lanceta et al., 2023). Downregulation of this gene indicates that a pro-inflammatory response was most probable amongst the T cells. Downregulation of *DOT1L,* which codes for an enzyme that is involved in methylation, showed that the cells were in a pro-inflammatory state, as this gene represses such a response (Kwesi-Maliepaard et al., 2020). It has been shown that CD4+ T cells attract a pro-inflammatory response to ensure optimal activation of T cell antigenic receptors (Moro-García et al., 2018). Differentiation of T cells also results in the production of high pro-inflammatory levels (Moro-García et al., 2018). The most prevalent T cell subtype was the Tregs and it may appear that this cell type was

most active. Tregs form from naïve T cells in order to control the immune response preventing harm to the host, yet still ensuring elimination of the foreign invader. Tregs naturally reduce inflammation to protect the host and regulate immune responses (Sun et al., 2023). Therefore, an upregulation of inflammation would not be expected. This upregulation may indicate development in the adaptive immune system, moving from a regulatory role to a more responsive role (Sun et al., 2023). It can be noted that T cells had the highest number of upregulated and downregulated DEGs compared the the other cell types. This may be because this group of cells consisted of three sub groups, namely Th1-like and Th2-like T cells and Tregs.

As with the macophages, the MF term “structural molecule activity”, was also upregulated. The increase in ribosomal and actin related genes (*RPL7A, RPL11, RPL9, RPL39, ARPC1B, ACTN1*), indicated an increase in cell proliferation activity and cell differentiation (Sun et al., 2022). With the T cells being split into 3 subtypes, it can be expected that cell differentiation and proliferation would be high. The upregulated MF term, that was unique to T cells as per the UpSet plot, indicated an increase in catalytic activity related to transcription where more RNA molecules were being synthesized using the DNA template. With the increase in cell proliferation, an increase in mRNA would be required for protein synthsis. Oxidative phosphorylation and respiration biological processes were also upregulated. This could be as a result of glycosis allowing for increased cell proliferation and cytokine production as shown by the upregulation of *MPC2* (Ramstead et al., 2020). The KEGG pathways identified were “oxidative phosphorylation” and “RNA polymerase”. Based on the results, it is most likely that the T cells were in the early phase of activation and differentation.

B cells

In avians, B cells develop in the bursa of Fabricius and form part of the adaptive immune response (Warren et al., 2023). Their functions include the humoral response (where antibodies are produced to neutralize pathogens), their immunological memory and regulatory response (Dai et al., 2021a). However, unlike with mammals, identifying the developmental stages of B cells in avians is difficult as few gene markers are available for avian species (Warren et al., 2023). It has been shown, that avian lymphocytes, consisting of T cells and B cells, are able to eliminate viral infections (Dai et al., 2021a).

The top 3 annotated upregulated genes were *MAGOH*, *SF3B5* and *EEF1D*. The *MAGOH* gene encodes a protein that regulates mRNA splicing, which is a process that assists with mRNA maturation and subsequent protein translation (Barreiro et al., 2023). This process regulates gene expression, and in immune cells, where proliferation and differentiation is generally high, it is expected that alternative splicing would be high (Schaub and Glasmacher, 2017). In this study, IgY antibodies were isolated from egg and blood samples. This showed that the quails' immune system were in a cell mediated state, where antibodies were being produced and secreted. Therefore, the B cells were proliferating and differentiating in order to produce the antibodies and alternative splicing would therefore be upregulated (Schaub and Glasmacher, 2017). The *SF3B5* gene, encodes for a component of the spliceosome, which is responsible for RNA splicing (Chen et al., 2023). This gene also plays a role in the regulation of gene expression by ensuring correct maturation of RNA. The upregulation of *MAGOH*, *SF3B5* and *EEF1D* (function stated above for macrophages and T cells), may indicate the activation of B cell signalling pathways that lead to plasma cell differentiation and subsequent antibody production. This process is important for the adaptive immune response, as B cells must undergo these processes in order to synthesise high-affinity antibodies, as was evident by the anti-PCV-2 antibodies shown in Chapter 3. Newly formed B cells do not secrete the first antibodies that are made. These antibodies are inserted into the plasma membrane to act as a receptor for antigens. B cells may have up to one hundred thousand receptors in the plasma membrane. Transmembrane proteins interact with the receptors to initiate intracellular signalling pathways upon contact with an antigen (Alberts et al., 2002). As stated above in macrophages, *ACTN1* was also upregulated in B cells. The function of this gene also points to antibody production, as a result of its role in the immunological synapse, where B cells and T cells interact to initiate antibody synthesis (Sun et al., 2022).

The most downregulated DEG in the B cell groups, was the unannotated transcript, *ENSCJPG00005016409,* which is orthologous to *Hbb-bh1.* This gene codes for *hemoglobin Z, beta-like embryonic chain*, which is expresssed during early stages of life before adult hemoglobin (HbA) becomes the main hemoglobin component (Nebor et al., 2016). While, not being actively involved in immune cells, downregulation of this gene may indicate that the quails were developing into a different stage of adulthood, where the Hbb hemoglobin

(common during adolescence) was reducing within the body. *RASGEF1A*, *LRP12* and *SACM1L* were annotated genes that were downregulated in the B cells. *RASGEF1A* and *LRP12* are genes involved in cell migration, while *SACM1L* is a suppressor of actin mutations (Bhuin and Roy, 2014; Huang et al., 2023; Liu et al., 2021). *RASGEF1A* are guanine nucleotide exchange factors, that control cell migration, compartmentalization and movement of proteins in and out of cell membranes (Bhuin and Roy, 2014). Cell migration is critical during immune responses as immune cells must navigate through the body. Immune cells must patrol and circulate to respond to sites of inflammation. This is common of monocytes, dendritic cells, naïve T cells and plasma B cells (Pereira et al., 2010). Downregulation of genes asscociated with cell migration may indicate that movement of the B cells from the bursa of Fabicus to the site of infection were reduced. During the adaptive immune response, B cells must encounter the antigen by interacting with helper T cells, then proliferate and diferentiate into plasma cells followed by memory cells (Pereira et al., 2010). Reduced movement may indicate that few B cells were already at the site of infection producing antibodies and additional B cells were not being recruited from the bursa of Fabicus. This may be due to a regulatory process where plasma B cell migration was still in its infancy. This may also indicate the reason for the low numbers of B cells identified in the PBMC samples.

The MF terms upregulated, as with macrophages and T cells, were also related to “structural molecule activity” and “structural consituent of the ribosome”. This was as a result of the many ribosomal related genes found in these GO terms. The biological processes upregulated in the cell type and KEGG pathway identified, verify that respiration levels and ATP creation had increased. From the GO analysis, terms related to MHC class II protein complex was identified. The MHC protein complex is essential for immune recognition and response, particularly in antigen presentation. The MHC class II molecules present peptides that are obtained from extracellular proteins to T cells (particularly CD4+ T helper cells), as they enable T cells to recognize and respond to the foreign invader (Erf, 2004). B cells commonly carry the MHC Class II complex. The most highly expressed CC term amongst all the cell types was “respiratory chain complex”. This complex is involved in the the electron transport chain of the cell and is essential for the production of ATP by means of oxidative phosphorylation for cell energy production (He et al., 2024). This complex may be

upregulated when cells are rapidly dividing and subsequently increases mitochondrial activity to support the high energy requirements. The response to stress may also lead to upregulation of the respiratory chain complex. Oxidative stress, associated with the complex, may also upregulate mitochondrial function, which is evident by the upregulated CC term “mitochondrial respiratory chain complex”. “Oxidative phosphorylation” was the KEGG term present for all cell types. This reiterates the above mentioned terms involving ATP production via the electron transport chain in the mitochondria. This too may be a sign of cellular stress, requiring increased energy demands (He et al., 2024).

These GO terms expressed by the B cells were similar to a study conducted by Maxwell et al., 2024, who described B cells as “activated” (active in protein synthesis and antigen presentation) due to high expression of ribosomal proteins in conjunction with upregulation of the associated GO terms. It is not conclusive at what stage of maturity the B cells were, but from the DEGs and GO terms that were upregulated, it appears that the B cells may be mature naïve B cells (as they were isolated from the peripheral blood and not from the bursa of Fabricus), due to the proliferation, differentation and presence of IgYs (from Chapter 3), the cells were most likely plasma B cells. Therefore, cellular energy, created by the mitochondria, would be upregulated.

APCs

The myeloid APCs are a group of cells that belong to the innate immune system and respond early to viral infections (Warren et al., 2023). This cell group is made up of macrophages, T cells, B cells or dendritic cells that are specifically involved in antigen presentation. Upregulation of *ASS1, MAGOH* and *EEF1D* show that the cells within this group were also most likely experiencing high states of proliferation and differentiation. The main function of APCs is to present antigens to T cells and B cells. They also regulate the immune system, via cell surface receptors, to distinguish pathogenic antigens from self (non-pathogenic) antigens (Maxwell et al., 2024; Warren et al., 2023). Upregulation of *ASS1* results in an increase in the synthesis of arginine, which is a precursor for nitric oxide production that aids in APC activation (Mao et al., 2022). Mao et al., 2022, found that *ASS1* is a pro-inflammatory gene. The upregulation of this gene indicates that the main APC cell type being expressed are macrophages. This agrees with the proposed stage of the innate immune

system, because macrophages (as discussed above) were the most dominant cell type and responsible for most of the immunological functions at the innate and early adaptive immune stages. Upregulation of *MAGOH* and *EEF1D* (as discussed above) indicates cell proliferation. This agrees with the upregulated GO terms and KEGG pathways, where the CC terms were related to respiration and KEGG pathway related to oxidative phosphorylation. This is because increased cell production requires increased energy levels.

Interestingly, the downregulated MF terms of the APCs were “chemokine activity”, “cytokine activity” and “chemokine receptor binding”. These GO terms were also identified as MF terms unique to the APCs as per the UpSet plot. Chemokines and cytokines regulate immune cell communication, modulate immune responses by directing relevant cells to the site of infection and subsequently results in inflammation (Kaiser and Stäheli, 2014). Downregulation of these functions is in contrast to the upregulated DEGs found in the APCs that would naturally result in a pro-inflammatory response. This may be due to a regulatory process that reduced inflammation or controlled excessive immune responses as shown in the T cell group above, in order to protect the host.

Downregulation of the BP term related to the “immune system process” and KEGG pathways related to “NOD-like receptor signaling pathway” and “toll-like receptor signaling pathway” was also noted. NOD-like receptors, which are a class of pattern recognition receptors (PRRs), initiate molecular signaling activities and are involved in the detection of pathogens and the regulation of immune responses. The NOD-like receptors play an important role in detecting infections, cellular stress, and tissue injury as well as trigger the adaptive immune and inflammatory responses (Kattner, 2024). Therefore, downregulation of the NOD-like receptor signaling pathway results in a decrease in the activation of NOD-like receptors, which may lead to a reduced immune response and lower inflammation. Regulation of this pathway controls the balance of an effective immune defense while preventing excessive inflammation or tissue damage (Kattner, 2024).

GO terms of combined upregulated and downregulated DEGs

Go analysis on the combined upregulated and downregulated DEGs, revealed that the main MF terms, present in all the cell types, were related to protein binding and catalytic activity. These biochemical activities, refer to protein-protein interactions and proteins that facilitate in chemical reactions, by increasing the cellular energy required (Balakrishnan et al., 2013). The dominant BP terms seen across all the cell types, are in line with what was expected of immune cells. This was indicated by terms related to the immune system, biological regulation, response to stimulus, response to stress and cell differentiation. These terms showed that the cells were actively involved in responses towards a foreign threat as well as establishing relevant immune reactions. A study conducted by Qu et al., 2022, showing immunological responses of ALV-J infected chickens, found similar GO terms at 21 days post infection. They noted the upregulation of CD8+ T cells (Qu et al., 2022). The current study noted a lack of CD8+ T cells, a dominance of macrophages and CD4+ T cells and low numbers of B cells. Both studies found reduced levels of T cells and B cells. For these reasons, Qu et al., 2022, suggested that the immune response was at an early stage of infection. This is in accordance with what was found in the current study, where the innate immune system was active and adaptive immune response was initiated. Samples collected further on in the experiment may have better established how the immune responses would have developed and the effect that PCV-2 VLPs would have had on the quails. Wu et al., 2022, found that pigs and mice injected with PCV-2 VLPs elicited a high humoral and cellular response. They found that PCV-2 VLPs induced immune cell proliferation, such as CD4+ T cells, Th1-like T cells and B cells. This is in agreement with what was found in the current study.

Summary

From the proportion and distribution of cell types found in the study (dominance of macrophages and CD4+ T cells and low cell numbers of B cells), upregulation of specific MF terms (such as “structural molecule activity” and “structural constituent of ribosome”), CC terms (related to respiration and energy creation) and KEGG pathways (such as “oxidative phosphorylation”), it can be suggested that the quail immune system was actively degrading foreign threats (by phagocytosis), regulating cellular processes (by means of antigen presentation and inflammation) and initiating humoral and cell-mediated responses (by the production of antibodies, T cells and low presence of B cells). An innate immune response

and early adaptive immune response was therefore most likely active. It can, therefore, be noted that, 16 days post exposure to a booster PCV-2 VLP, the antigens will create a phagocytic response with early adaptive immunity with regulated inflammation.

This conclusion would be more sound, if more biological replicates were included (to enhance statistical power), more cell types were identified (by increasing sequencing depth), collecting samples at different points throughout the immune response and using better curated marker gene databases. Increasing the biological replicates would decrease biases and confounding variables, thereby increasing result reliability. The inability to identify some cell subtypes (specifically of T cells) may be related to limited resolution (Maxwell et al., 2024). Maxwell et al., 2024, found that reduced sequencing depth and numbers of cells analysed, limited the types of leukocyte (T cells and B cells) subtypes identified in chickens. Therefore, adequate sequencing depth is necessary and may be improved in future studies. Another reason may be that a specific T cell response was not achieved, at high levels, as PCV-2 naturally infects pigs and not birds. Therefore, little cross-reactivity between species was present, impacting the T cell response (Jing et al., 2016).

Finally, greater inferences on the quails' immune response could have been made if samples were collected periodically, throughout the experiment, for a longer duration. This would have allowed for development and progression of the immune response to be better understood and for identification of potential biomarkers and treatment options. Deeper correlations between gene signatures observed and potential protein-level verification could have been done using tests such as an immunoassay for suspected cytokines. Additionally, a kinetic study or challenge model may add greater detail to the potential tolerance mechanisms shown in the quail PBMC responses.

5. Chapter 5: General discussion and conclusions

5.1 General discussion

Understanding the complexities of the immune system of potential beneficial animal models is useful when studying relationships such as host-virus interactions. This in turn may allow for the development of efficacious vaccines and therapeutics, preventative strategies and disease biology understanding. Immune imbalances or dysregulation, caused by viral infection, remains a major problem and understanding these imbalances and host susceptibility is important (Seo et al., 2014). Analysing the transcriptome of immunological samples can provide detail into the state of an immune response, which can be enhanced using cutting-edge technology, like scRNA-seq. Such technology provides detailed, high-resolution transcriptional information from individual cells (Zhang et al., 2020). Animal models play a pivotal role in studying molecular characteristics of host responses to infection. It is, therefore, imperative to know how they handle adverse conditions when exposed to foreign invaders, such as viruses.

The main aim of this study was to produce full-length PCV-2 VLPs in an *E.coli* expression system that would then be injected into Japanese quails, to stimulate an immune response to study the immune response. Expression of recombinant PCV-2 CP was successfully conducted in *E.coli* using the pProEX-HT vector, that contained the full-length PCV-2 CP gene, for expression. Following expression, an improved purification technique was established that allowed for better product purity and concentration to be achieved, compared to previous work done on this protein (Gunter et al., 2019). This technique included the completion of two rounds of the BugBuster protocol followed by ultrafiltration. Transmission electron microscopy confirmed the correct formation of the VLPs by identifying spherical structures of approximately 11 to 17 nm in diameter.

To elicit a cellular immune response and produce PCV-2 specific antibodies, Japanese quails were injected with the *E.coli* produced PCV-2 VLPs. The quails appeared to be well for the duration of the experiment, having experienced minimal stress. Following immunization, sera and egg samples were collected and total IgY isolated from the eggs. Western blots revealed the presence of anti-PCV-2 antibodies, from egg and serum samples, from quails

injected with the PCV-2 VLPs. This verified that a PCV-2 specific immune response was achieved by injecting the quails with 2 doses of PCV-2 VLPs. Antibodies were easily studied and isolated from both blood and egg yolk and anti-PCV-2 antibody easily detected from these samples. ELISA results also showed that all the quails injected with PCV-2 VLPs elicited an immune response specific to PCV-2. Higher levels of anti-PCV-2 antibody was noted in the egg yolk samples compared to the sera samples. This was expected as greater levels of antibodies are transferred to the egg yolk from the blood stream during passive immunity from parent to offspring (Esmailnejad et al., 2019). To our knowledge, no previous research is available on Japanese quails injected with PCV-2 and having produced PCV-2 specific antibodies.

PBMCs were then isolated, from whole blood samples, using density gradient centrifugation. By ensuring rapid isolation of PBMCs from fresh blood samples and performing the isolation at room temperature, cell viability of more than 90% was achieved for both samples. This was important as the PBMC samples gave a greater representation of cell diversity that was analysed using scRNA-seq.

Finally, the immune response of the quails was studied by conducting an in-depth analysis of cell composition, differential gene expression and biological pathways by performing scRNA-seq. Using the 10X Genomics platform, 8325 cells were analysed for the PCV-2 sample and 4312 cells for the control sample. To ensure that the data was of an acceptable quality and that the pipeline worked well, the entire pipeline was first run using the pooled dataset. Thereafter the pooled dataset was demultiplexed using scSplit. The same pipeline was then repeated on the demultiplexed data, to annotate the data and conduct downstream differential expression analysis, followed by GO analysis. The pooled samples for the PCV-2 and control conditions were demultiplexed into the original 16 samples representing eight quails per condition. PBMCs from all 16 quails were isolated and sequenced with no less than 217 cells and a maximum of 931 cells obtained from a single quail. Four major cell types were present in the sample, namely macrophages and APCs that made up the innate immune response and B cells and T cells (further subclustered into Tregs, Th1-like T cells and Th2-like T cells) that formed the adaptive immune system. Macrophages were the dominant cell type in the PCV-2 group and based on the DEGs and

GO terms upregulated, it was most likely that the cells were in the phagocytic stage. Both the innate and adaptive immune systems were regulating cellular processes, while also initiating humoral and cell-mediated responses by means of antibody production. Following 2 injections and testing samples approximately 2 weeks after the second injection, it can be noted that the quails were most likely experiencing an innate immune response as well as early adaptive immune response.

5.2 Conclusions

This study aimed to express PCV-2 VLPs in *E. coli* and purify a large enough concentration for antibody production and immunological analysis. It further aimed to understand the immune response biology of PCV-2 by evaluating the evolution of the innate and adaptive immune system of Japanese quail, using scRNA-seq. More specifically, the aim was to use bioinformatic tools to analyse the cell type-specific gene expression profiles, molecular functions and biological pathways, related to the immune response of quails injected with PCV-2 VLPs versus naive birds.

Adequate concentrations of PCV-2 VLPs were successfully expressed in E.*coli* and purified using an improved purification protocol established in this study. This was confirmed using immunoassays and TEM analysis. Verified PCV-2 VLPs were injected into Japanese quails and animal studies successfully conducted with no experiment-related injury or harm to any of the animals. The quails were able to elicit a specific immune response to PCV-2 after injection of the two doses of PCV-2 VLPs. Antibodies were easily studied and isolated from both blood and egg yolk and anti-PCV-2 antibody easily detected from these samples. Additionally, viable PBMCs were successfully isolated in high concentrations from quail whole blood. Using scRNA-seq, cells of both the innate and adaptive immune system were identified. DEGs, specific to each sample and experimental condition was successfully obtained and studied as well as the biological pathways involved. Six cell types belonging to the innate and adaptive immune system were present. From analysis of the samples taken 16 days post booster injection, it can be presumed that quails can adequately handle exposure to viral components with no major harm and may therefore be a suitable animal model.

5.3 Future research

As this was a preliminary study on quail immunological responses, a small cohort was used for the experiments. To reduce costs, limit animal usage and establish working protocols, only one control group and one experimental group of 8 quails each were used. This may have limited the statistical power of the samples and created biases and confounding variables (a small number of subjects may have been influenced by variables that could not be evenly distributed). Future studies should employ a bigger cohort with more experimental groups. Additionally, blood samples of each individual animal were pooled per group. Errors during experimentation or external factors introduced erroneously would have affected all the blood samples. Here too, having a bigger cohort could allow for less pooling of samples.

Working with a species that was not well studied may have negatively affected the depth at which inferences could be made. Annotating clusters manually was a limitation. The cell annotations could have been more specific with a well annotated transcriptome and better curated marker gene databases. Such databases and an appropriate quail reference atlas is not yet available and could, therefore, not be used in this study. However, improvement in this area could be an avenue for future research.

Future research may include the use of VLPs from a virus known to infect avian species, or specifically quails, that may then be injected into birds. This will result in immunological responses specific to birds, providing greater detail into how the immune system recognizes and responds to the virus. It will also allow better understanding of the humoral and cellular immune responses elicited which can be beneficial in developing effective vaccines.

The anti-PCV-2 IgYs that were generated in this study, could be beneficial for swine health management. The PCV-2 specific antibodies could be used in serological detection in diagnosing infections and assessing herd immunity. Using techniques like enzyme-linked immunosorbent assay or indirect immunofluorescence assay, one may monitor vaccination efficacy and identify infections (Li et al., 2023). The anti-PCV-2 IgYs may also be used as a passive immunization option for susceptible piglets that do not receive maternal antibodies

(Esmailnejad et al., 2019). A study conducted by Li et al., 2015, showed that IgY antibodies can effectively neutralize viral and bacterial pathogens in swine. Therefore, the generated IgYs could be an alternative protection mechanism in piglets infected with viral pathogens, such as PCV-2.

Lastly, Using the pseudobulk approach of DESeq2 may have led to inaccurate estimates of variation. This method aggregates gene counts across clusters, possibly overlooking variability within clusters resulting in underpowered analyses and false negative observations. Future research should aim to increase the number of biological replicates to enhance statistical power. Alternatively, exploring single-cell differential expression methods could be beneficial, as these approaches treat each cell as an individual sample in the analysis.

6. References

Abu Nasar, Aminoor Rahman, Hoque, N., Talukder, A.K., Das, Z.C., 2016. A survey of Japanese quail (Coturnix coturnix japonica) farming in selected areas of Bangladesh. Vet World 9, 940–947. https://doi.org/10.14202/vetworld.2016.940-947

Agrati, C., Bartolini, B., Bordoni, V., Locatelli, F., Capobianchi, M.R., Di Caro, A., Castilletti, C., Ippolito, G., 2023. Emerging viral infections in immunocompromised patients: A great challenge to better define the role of immune response. Front. Immunol. 14, 1147871. https://doi.org/10.3389/fimmu.2023.1147871

Alberts, B., Johnson, A, Lewis, J, Raff, M, Roberts, K, Walter, P, 2002. B Cells and Antibodies. New York: Garland Science 4, 401–405. https://doi.org/10: 0-8153-3218-1

Arts, R.J.W., Huang, P.-K., Yang, D., Joosten, L.A.B., Van Der Meer, J.W.M., Oppenheim, J.J., Netea, M.G., Cheng, S.-C., 2018. High-Mobility Group Nucleosome-Binding Protein 1 as Endogenous Ligand Induces Innate Immune Tolerance in a TLR4-Sirtuin-1 Dependent Manner in Human Blood Peripheral Mononuclear Cells. Front. Immunol. 9, 526. https://doi.org/10.3389/fimmu.2018.00526

Baer, J., Lansford, R., Cheng, K., 2015. Japanese Quail as a Laboratory Animal Model, in: Laboratory Animal Medicine. Elsevier, pp. 1087–1108. https://doi.org/10.1016/B978-0-12-409527-4.00022-5

Balakrishnan, R., Harris, M.A., Huntley, R., Van Auken, K., Cherry, J.M., 2013. A guide to best practices for Gene Ontology (GO) manual annotation. Database 2013, bat054–bat054. https://doi.org/10.1093/database/bat054

Ball, G.F., Balthazart, J., 2010. Japanese Quail as a Model System for Studying the Neuroendocrine Control of Reproductive and Social Behaviors. ILAR Journal 51, 310–325. https://doi.org/10.1093/ilar.51.4.310

Baumgartner, J., 1994. Japanese quail production, breeding and genetics. World's Poultry Science Journal 50, 227–235.

Berthelot, U., Piché, S.R., Brisson, G., Doyen, A., 2024. Exploring the use of ultrafiltration-diafiltration for the concentration and purification of mealworm proteins. Future Foods 9, 100382. https://doi.org/10.1016/j.fufo.2024.100382

Bhatwa, A., Wang, W., Hassan, Y.I., Abraham, N., Li, X.-Z., Zhou, T., 2021. Challenges Associated With the Formation of Recombinant Protein Inclusion Bodies in Escherichia coli and Strategies to Address Them for Industrial Applications. Front. Bioeng. Biotechnol. 9, 630551. https://doi.org/10.3389/fbioe.2021.630551

Bhuin, T., Roy, J.K., 2014. Rab proteins: The key regulators of intracellular vesicle transport. Experimental Cell Research 328, 1–19. https://doi.org/10.1016/j.yexcr.2014.07.027

Birhan, M., 2019. Systematic review on avian immune systems. jwpr 9, 144–150. https://doi.org/10.36380/scil.2019.jlsb23

Blunt, R., McOrist, S., McKillen, J., McNair, I., Jiang, T., Mellits, K., 2011. House fly vector for porcine circovirus 2b on commercial pig farms. Veterinary Microbiology 149, 452–455. https://doi.org/10.1016/j.vetmic.2010.11.019

Bredell, H., Smith, J.J., Prins, W.A., Görgens, J.F., Van Zyl, W.H., 2016. Expression of rotavirus VP6 protein: a comparison amongst *Escherichia coli, Pichia pastoris* and *Hansenula polymorpha*. FEMS Yeast Research 16, fow001. https://doi.org/10.1093/femsyr/fow001

Buchanan, J., Taylor, E., 2020. Mitochondrial Pyruvate Carrier Function in Health and Disease across the Lifespan. Biomolecules 10, 1162. https://doi.org/10.3390/biom10081162

Bull, M., Lee, D., Stucky, J., Chiu, Y.-L., Rubin, A., Horton, H., McElrath, M.J., 2007. Defining blood processing parameters for optimal detection of cryopreserved antigen-specific responses for HIV vaccine trials. Journal of Immunological Methods 322, 57–69. https://doi.org/10.1016/j.jim.2007.02.003

Caetano-Anolles, K., Seo, M., Rodriguez-Zas, S., Oh, J.-D., Han, J.Y., Lee, K., Park, T.S., Shin, S., Jiao Jiao, Z., Ghosh, M., Jeong, D.K., Cho, S., Kim, H., Song, K.-D., Lee, H.-K., 2015. Comprehensive Identification of Sexual Dimorphism-Associated Differentially Expressed Genes in Two-Way Factorial Designed RNA-Seq Data on Japanese Quail (Coturnix coturnix japonica). PLoS ONE 10, e0139324. https://doi.org/10.1371/journal.pone.0139324

Cao, L., Lv, W., Feng, X., Chen, L., Yang, L., Guo, J., 2024. Complete genome sequence of a porcine circovirus type 2 strain, PCV2/CN/GD/2018/10, obtained in Guangdong, China, in 2018. Microbiol Resour Announc 13, e01003-23. https://doi.org/10.1128/mra.01003-23

Cao, M., Wei, Y., Shi, W., Feng, L., Huang, L., 2024. Investigation of porcine circovirus type 2 and porcine circovirus type 3 infections based on dual TaqMan fluorescent quantitative PCR method and genetic evolutionary analysis of these two viruses. Front. Microbiol. 15, 1385137. https://doi.org/10.3389/fmicb.2024.1385137

Caudai, C., Galizia, A., Geraci, F., Le Pera, L., Morea, V., Salerno, E., Via, A., Colombo, T., 2021. AI applications in functional genomics. Computational and Structural Biotechnology Journal 19, 5762–5790. https://doi.org/10.1016/j.csbj.2021.10.009

Chaplin, D.D., 2010. Overview of the immune response. Journal of Allergy and Clinical Immunology 125, S3–S23. https://doi.org/10.1016/j.jaci.2009.12.980

Chen, L., Deng, H., Cui, H., Fang, J., Zuo, Z., Deng, J., Li, Y., Wang, X., Zhao, L., 2018. Inflammatory responses and inflammation-associated diseases in organs. Oncotarget 9, 7204–7218. https://doi.org/10.18632/oncotarget.23208

Chen, S., Zhou, Z., Li, Y., Du, Y., Chen, G., 2023. Application of single-cell sequencing to the research of tumor microenvironment. Front. Immunol. 14, 1285540. https://doi.org/10.3389/fimmu.2023.1285540

Chivukula, M., Dabbs, D.J., 2011. Chapter 21 - Immunocytology, in: Dabbs, D.J. (Ed.), Diagnostic Immunohistochemistry (Third Edition). W.B. Saunders, Philadelphia, pp. 890–918. https://doi.org/10.1016/B978-1-4160-5766-6.00025-X

Choi, Y., Nam, M.-W., Lee, H.K., Choi, K.-C., 2023. Use of cutting-edge RNA-sequencing technology to identify biomarkers and potential therapeutic targets in canine and feline cancers and other diseases. J Vet Sci 24, e71. https://doi.org/10.4142/jvs.23036

Crisci, E., Bárcena, J., Montoya, M., 2013. Virus-like particle-based vaccines for animal viral infections. Inmunología 32, 102–116. https://doi.org/10.1016/j.inmuno.2012.08.002

Dai, M., Feng, M., Li, Z., Chen, W., Liao, M., 2021a. Chicken peripheral blood lymphocyte response to ALV-J infection assessed by single-cell RNA sequencing. https://doi.org/10.1101/2021.01.12.426350

Dai, M., Zhao, L., Li, Z., Li, X., You, B., Zhu, S., Liao, M., 2021b. The Transcriptional Differences of Avian CD4+CD8+ Double-Positive T Cells and CD8+ T Cells From Peripheral Blood of ALV-J Infected Chickens Revealed by Smart-Seq2. Front. Cell. Infect. Microbiol. 11, 747094. https://doi.org/10.3389/fcimb.2021.747094

Dai, M., Zhu, S., An, Z., You, B., Li, Z., Yao, Y., Nair, V., Liao, M., 2023. Dissection of key factors correlating with H5N1 avian influenza virus driven inflammatory lung injury of chicken identified by single-cell analysis. PLoS Pathog 19, e1011685. https://doi.org/10.1371/journal.ppat.1011685

Danecek, P., Bonfield, J.K., Liddle, J., Marshall, J., Ohan, V., Pollard, M.O., Whitwham, A., Keane, T., McCarthy, S.A., Davies, R.M., Li, H., 2021. Twelve years of SAMtools and BCFtools. GigaScience 10, giab008. https://doi.org/10.1093/gigascience/giab008

Dei Giudici, S., Mura, L., Bonelli, P., Hawko, S., Angioi, P.P., Sechi, A.M., Denti, S., Sulas, A., Burrai, G.P., Madrau, M.P., Antuofermo, E., Oggiano, A., 2023. Evidence of Porcine Circovirus Type 2 (PCV2) Genetic Shift from PCV2b to PCV2d Genotype in Sardinia, Italy. Viruses 15, 2157. https://doi.org/10.3390/v15112157

Derbois, C., Palomares, M.-A., Deleuze, J.-F., Cabannes, E., Bonnet, E., 2023. Single cell transcriptome sequencing of stimulated and frozen human peripheral blood mononuclear cells. Sci Data 10, 433. https://doi.org/10.1038/s41597-023-02348-z

Désert, C., Merlot, E., Zerjal, T., Bed'hom, B., Härtle, S., Le Cam, A., Roux, P.-F., Baeza, E., Gondret, F., Duclos, M.J., Lagarrigue, S., 2016. Transcriptomes of whole blood and PBMC in chickens. Comparative Biochemistry and Physiology Part D: Genomics and Proteomics 20, 1–9. https://doi.org/10.1016/j.cbd.2016.06.008

Diptesh, A., Deshmukh, S., Sodhi, S., Banga, H.S., 2020. Differential susceptibility and immune response in chicken and Japanese quail towards *Avibacterium paragallinarum*. Journal of Applied Animal Research 48, 575–586. https://doi.org/10.1080/09712119.2020.1848844

Domínguez-Oliva, A., Hernández-Ávalos, I., Martínez-Burnes, J., Olmos-Hernández, A., Verduzco-Mendoza, A., Mota-Rojas, D., 2023. The Importance of Animal Models in Biomedical Research: Current Insights and Applications. Animals 13, 1223. https://doi.org/10.3390/ani13071223

Du, Q., Wu, X., Wang, T., Yang, X., Wang, Z., Niu, Y., Zhao, X., Liu, S.-L., Tong, D., Huang, Y., 2018. Porcine Circovirus Type 2 Suppresses IL-12p40 Induction via Capsid/gC1qR-Mediated MicroRNAs and Signalings. The Journal of Immunology 201, 533–547. https://doi.org/10.4049/jimmunol.1800250

Dustin, M.L., Cooper, J.A., 2000. The immunological synapse and the actin cytoskeleton: molecular hardware for T cell signaling. Nat Immunol 1, 23–29. https://doi.org/10.1038/76877

El Helaly Goher, M.N., Moghaieb, R.E., El- Menawey, M.A.-R., Ramzy Stino, F.K., 2024. Differential Gene Expression Profiling during Avian Immune Organ Development: Insights from Thymus and Bursa of Fabricius Transcriptome Analysis. jwpr 1. https://doi.org/10.36380/jwpr.2024.4

El-Husseiny, M.H., Hagag, N.M., Pushko, P., Tretyakova, I., Naguib, M.M., Arafa, A.S., 2021. Evaluation of Protective Efficacy of Influenza Virus Like Particles Prepared from H5N1 Virus of Clade 2.2.1.2 in Chickens. Vaccines 9, 715. https://doi.org/10.3390/vaccines9070715

Erf, G.F., 2004. Cell-mediated immunity in poultry. Poultry Science 83, 580–590. https://doi.org/10.1093/ps/83.4.580

Eschke, M., Moore, P.F., Chang, H., Alber, G., Keller, S.M., 2023. Canine peripheral blood TCRαβ T cell atlas: Identification of diverse subsets including CD8A+ MAIT-like cells by combined single-cell transcriptome and V(D)J repertoire analysis. Front. Immunol. 14, 1123366. https://doi.org/10.3389/fimmu.2023.1123366

Esmailnejad, A., Abdi-Hachesoo, B., Hosseini Nasab, E., Shakoori, M., 2019. Production, purification, and evaluation of quail immunoglobulin Y against Salmonella typhimurium and Salmonella enteritidis. Molecular Immunology 107, 79–83. https://doi.org/10.1016/j.molimm.2019.01.012

Esteban-Amo, M.J., Jiménez-Cuadrado, P., Serrano-Lorenzo, P., De La Fuente, M.Á., Simarro, M., 2024. Succinate Dehydrogenase and Human Disease: Novel Insights into a Well-Known Enzyme. Biomedicines 12, 2050. https://doi.org/10.3390/biomedicines12092050

Fan, M., Bian, L., Tian, X., Hu, Z., Wu, W., Sun, L., Yuan, G., Li, S., Yue, L., Wang, Ying, Wu, L., Wang, Yongquan, Yan, Z., Ren, J., Li, X., 2023. Infection characteristics of porcine circovirus type 2 in different herds from intensive farms in China, 2022. Front. Vet. Sci. 10, 1187753. https://doi.org/10.3389/fvets.2023.1187753

Fehér, E., Jakab, F., Bányai, K., 2023. Mechanisms of circovirus immunosuppression and pathogenesis with a focus on porcine circovirus 2: a review. Veterinary Quarterly 43, 1–18. https://doi.org/10.1080/01652176.2023.2234430

Flores-Santin, J., Burggren, W.W., 2021. Beyond the Chicken: Alternative Avian Models for Developmental Physiological Research. Front. Physiol. 12. https://doi.org/10.3389/fphys.2021.712633

Fort, M., Sibila, M., Pérez-Martín, E., Nofrarías, M., Mateu, E., Segalés, J., 2009. One dose of a porcine circovirus 2 (PCV2) sub-unit vaccine administered to 3-week-old conventional piglets elicits cell-mediated immunity and significantly reduces PCV2 viremia in an experimental model. Vaccine 27, 4031–4037. https://doi.org/10.1016/j.vaccine.2009.04.028

Franzén, O., Gan, L.-M., Björkegren, J.L.M., 2019. PanglaoDB: a web server for exploration of mouse and human single-cell RNA sequencing data. Database 2019, baz046. https://doi.org/10.1093/database/baz046

Franzo, G., Ruiz, A., Grassi, L., Sibila, M., Drigo, M., Segalés, J., 2020. Lack of Porcine circovirus 4 Genome Detection in Pig Samples from Italy and Spain. Pathogens 9, 433. https://doi.org/10.3390/pathogens9060433

Gao, L., Chen, S., Hong, M., Zhou, W., Wang, B., Qiu, J., Xia, J., Zhao, P., Fu, L., Wang, J., Dai, Y., Xie, N., Yang, Q., Huang, H.-D., Gao, X., Zou, C., 2021. Kinectin 1 promotes the growth of triple-negative breast cancer via directly co-activating NF-kappaB/p65 and enhancing its transcriptional activity. Sig Transduct Target Ther 6, 250. https://doi.org/10.1038/s41392-021-00652-x

Gao, Q., Yang, C., Ren, C., Zhang, S., Gao, X., Jin, M., Chen, H., Ma, W., Zhou, H., 2020. Eukaryotic Translation Elongation Factor 1 Delta Inhibits the Nuclear Import of the Nucleoprotein and PA-PB1 Heterodimer of Influenza A Virus. J Virol 95, e01391-20. https://doi.org/10.1128/JVI.01391-20

Gao, Y., Wang, H., Wang, S., Sun, M., Fang, Z., Liu, X., Cai, X., Tu, Y., 2022. Self-Assembly of Porcine Parvovirus Virus-like Particles and Their Application in Serological Assay. Viruses 14, 1828. https://doi.org/10.3390/v14081828

Garrison, E., Marth, G., 2012. Haplotype-based variant detection from short-read sequencing.

Gautron, J., Stapane, L., Le Roy, N., Nys, Y., Rodriguez-Navarro, A.B., Hincke, M.T., 2021. Avian eggshell biomineralization: an update on its structure, mineralogy and protein tool kit. BMC Mol and Cell Biol 22. https://doi.org/10.1186/s12860-021-00350-0

Gill, S.E., Gharib, S.A., Bench, E.M., Sussman, S.W., Wang, R.T., Rims, C., Birkland, T.P., Wang, Y., Manicone, A.M., McGuire, J.K., Parks, W.C., 2013. Tissue Inhibitor of Metalloproteinases–3 Moderates the Proinflammatory Status of Macrophages. Am J Respir Cell Mol Biol 49, 768–777. https://doi.org/10.1165/rcmb.2012-0377OC

Gottesman, S., 1996. PROTEASES AND THEIR TARGETS IN ESCHERICHIA COLI1. Annual Review of Genetics. https://doi.org/10.1146/annurev.genet.30.1.465

Grabski, A., Mccormick, M., Mierendorf, R., 1999. BugBuster™ and Benzonase®: The clear solutions to simple efficient extraction of E. coli proteins. Innovations 10, 17–19.

Guerra, J., Pinto, C., Pinto, P., Pinheiro, M., Santos, C., Peixoto, A., Escudeiro, C., Barbosa, A., Porto, M., Francisco, I., Lopes, P., Isidoro, A.R., Cunha, A.L., Albuquerque, C., Claro, I., Oliveira, C., Silva, J., Teixeira, M.R., 2023. Frequency of CDH1, CTNNA1 and CTNND1 Germline Variants in Families with Diffuse and Mixed Gastric Cancer. Cancers 15, 4313. https://doi.org/10.3390/cancers15174313

Gunter, C.J., Regnard, G.L., Rybicki, E.P., Hitzeroth, I.I., 2019. Immunogenicity of plant-produced porcine circovirus-like particles in mice. Plant Biotechnology Journal 17, 1751–1759. https://doi.org/10.1111/pbi.13097

Guo, J., Hou, L., Zhou, J., Wang, D., Cui, Y., Feng, X., Liu, J., 2022. Porcine Circovirus Type 2 Vaccines: Commercial Application and Research Advances. Viruses 14, 2005. https://doi.org/10.3390/v14092005

Holgado-Martín, R., Arnal, J.L., Sibila, M., Franzo, G., Martín-Jurado, D., Risco, D., Segalés, J., Gómez, L., 2023. First detection of porcine circovirus 4 (PCV-4) in Europe. Virol J. 20(1):230. Published 2023 Oct 10. https://doi.org/10.1186/s12985-023-02181-1

Hanamsagar, R., Reizis, T., Chamberlain, M., Marcus, R., Nestle, F.O., De Rinaldis, E., Savova, V., 2020. An optimized workflow for single-cell transcriptomics and repertoire profiling of purified lymphocytes from clinical samples. Sci Rep 10. https://doi.org/10.1038/s41598-020-58939-y

Harrison, P.W., Amode, M.R., Austine-Orimoloye, O., Azov, A.G., Barba, M., Barnes, I., Becker, A., Bennett, R., Berry, A., Bhai, J., Bhurji, S.K., Boddu, S., Branco Lins, P.R., Brooks, L., Ramaraju, S.B., Campbell, L.I., Martinez, M.C., Charkhchi, M., Chougule, K., Cockburn, A., Davidson, C., De Silva, N.H., Dodiya, K., Donaldson, S., El Houdaigui, B., Naboulsi, T.E., Fatima, R., Giron, C.G., Genez, T., Grigoriadis, D., Ghattaoraya, G.S., Martinez, J.G., Gurbich, T.A., Hardy, M., Hollis, Z., Hourlier, T., Hunt, T., Kay, M., Kaykala, V., Le, T., Lemos, D., Lodha, D., Marques-Coelho, D., Maslen, G., Merino, G.A., Mirabueno, L.P., Mushtaq, A., Hossain, S.N., Ogeh, D.N., Sakthivel, M.P., Parker, A., Perry, M., Piližota, I., Poppleton, D., Prosovetskaia, I., Raj, S., Pérez-Silva, J.G., Salam, A.I.A., Saraf, S., Saraiva-Agostinho, N., Sheppard, D., Sinha, S., Sipos, B., Sitnik, V., Stark, W., Steed, E., Suner, M.-M., Surapaneni, L., Sutinen, K., Tricomi, F.F., Urbina-Gómez, D., Veidenberg, A., Walsh, T.A., Ware, D., Wass, E., Willhoft, N.L., Allen, J., Alvarez-Jarreta, J., Chakiachvili, M., Flint, B.,

Giorgetti, S., Haggerty, L., Ilsley, G.R., Keatley, J., Loveland, J.E., Moore, B., Mudge, J.M., Naamati, G., Tate, J., Trevanion, S.J., Winterbottom, A., Frankish, A., Hunt, S.E., Cunningham, F., Dyer, S., Finn, R.D., Martin, F.J., Yates, A.D., 2024. Ensembl 2024. Nucleic Acids Research 52, D891–D899. https://doi.org/10.1093/nar/gkad1049

He, Z., Wu, M., Tian, H., Wang, L., Hu, Y., Han, F., Zhou, J., Wang, Y., Zhou, L., 2024. Euglena's atypical respiratory chain adapts to the discoidal cristae and flexible metabolism. Nat Commun 15, 1628. https://doi.org/10.1038/s41467-024-46018-z

Hedlund, L., Jensen, P., 2022. Effects of stress during commercial hatching on growth, egg production and feather pecking in laying hens. PLoS ONE 17, e0262307. https://doi.org/10.1371/journal.pone.0262307

Hodek, P., Trefil, P., Simunek, J., Hudecek, J., Stiborova, M., 2013. Optimized Protocol of Chicken Antibody (IgY) Purification Providing Electrophoretically Homogenous Preparations. International Journal of Electrochemical Science 8, 113–124. https://doi.org/10.1016/S1452-3981(23)14006-5

Homma, K., Jinno, M., Sato, K., Ando, A., 1968. Studies on perfect and imperfect albinism in the Japanese quail (Coturnix coturnix japonica). Nihon Chikusan Gakkaiho 39, 348–352.

Hong, N.A., Kabra, N.H., Hsieh, S.N., Cado, D., Winoto, A., 1999. In Vivo Overexpression of Dad1, the Defender Against Apoptotic Death-1, Enhances T Cell Proliferation But Does Not Protect Against Apoptosis. The Journal of Immunology 163, 1888–1893. https://doi.org/10.4049/jimmunol.163.4.1888

Hu, C., Li, T., Xu, Y., Zhang, X., Li, F., Bai, J., Chen, J., Jiang, W., Yang, K., Ou, Q., Li, X., Wang, P., Zhang, Y., 2023. CellMarker 2.0: an updated database of manually curated cell markers in human/mouse and web tools based on scRNA-seq data. Nucleic Acids Research 51, D870–D876. https://doi.org/10.1093/nar/gkac947

Huang, M., Lu, L., Lin, C., Zheng, Y., Pan, X., Wang, S., Chen, S., Zhang, Y., Liu, C., Ge, G., Zeng, Y.A., Chen, J., 2023. LRP12 is an endogenous transmembrane inactivator of α4 integrins. Cell Reports 42, 112667. https://doi.org/10.1016/j.celrep.2023.112667

Huang, Y., McCarthy, D.J., Stegle, O., 2019. Vireo: Bayesian demultiplexing of pooled single-cell RNA-seq data without genotype reference. Genome Biol 20, 273. https://doi.org/10.1186/s13059-019-1865-2

Huss, D., Poynter, G., Lansford, R., 2008. Japanese quail (Coturnix japonica) as a laboratory animal model. Lab Anim 37, 513–519. https://doi.org/10.1038/laban1108-513

Hwang, B., Lee, J.H., Bang, D., 2018. Single-cell RNA sequencing technologies and bioinformatics pipelines. Exp Mol Med 50, 1–14. https://doi.org/10.1038/s12276-018-0071-8

Jerram, A., Guy, T.V., Beutler, L., Gunasegaran, B., Sluyter, R., Fazekas De St Groth, B., McGuire, H.M., 2021. Effects of storage time and temperature on highly multiparametric flow analysis of peripheral blood samples; implications for clinical trial samples. Bioscience Reports 41. https://doi.org/10.1042/bsr20203827

Jiao, Q., Yang, L., Liu, X., Wen, Y., Tian, L., Qian, P., Chen, H., Li, X., 2023. Isolation and pathogenicity of porcine circovirus type 2 in mice from Guangxi province, China. Virol J 20, 195. https://doi.org/10.1186/s12985-023-02161-5

Jin, X., Zhang, X., Li, J., Yu, W., Chen, F., 2018. Activation of chicken macrophages during in vitro stimulation and expression of immune genes. ajvr 79, 1306–1312. https://doi.org/10.2460/ajvr.79.12.1306

Jing, L., Laing, K.J., Dong, L., Russell, R.M., Barlow, R.S., Haas, J.G., Ramchandani, M.S., Johnston, C., Buus, S., Redwood, A.J., White, K.D., Mallal, S.A., Phillips, E.J., Posavad, C.M., Wald, A., Koelle, D.M., 2016. Extensive CD4 and CD8 T Cell Cross-Reactivity between Alphaherpesviruses. J Immunol. 1;196(5):2205-2218.

Jota Baptista, C.V., Faustino-Rocha, A.I., Oliveira, P.A., 2021. Animal Models in Pharmacology: A Brief History Awarding the Nobel Prizes for Physiology or Medicine. Pharmacology 106, 356–368. https://doi.org/10.1159/000516240

Jovic, D., Liang, X., Zeng, H., Lin, L., Xu, F., Luo, Y., 2022. Single-cell RNA sequencing technologies and applications: A brief overview. Clinical & Translational Med 12, e694. https://doi.org/10.1002/ctm2.694

Kaiser, P., Stäheli, P., 2014. Chapter 10 - Avian Cytokines and Chemokines, in: Schat, K.A., Kaspers, B., Kaiser, P. (Eds.), Avian Immunology (Second Edition). Academic Press, Boston, pp. 189–204. https://doi.org/10.1016/B978-0-12-396965-1.00010-8

Kattner, A.A., 2024. Evolutionary edge: NOD-like receptors in immunity. Biomedical Journal 47, 100702. https://doi.org/10.1016/j.bj.2024.100702

Kawasaki, Takumi, Kawai, T., 2014. Toll-like receptor signaling pathways. Frontiers in Immunology 5.

Kim, K., Choi, K., Shin, M., Hahn, T.-W., 2024. A porcine circovirus type 2d-based virus-like particle vaccine induces humoral and cellular immune responses and effectively protects pigs against PCV2d challenge. Front. Microbiol. 14, 1334968. https://doi.org/10.3389/fmicb.2023.1334968

Kim, K., Hahn, T.-W., 2021. Evaluation of novel recombinant porcine circovirus type 2d (PCV2d) vaccine in pigs naturally infected with PCV2d. Vaccine 39, 529–535. https://doi.org/10.1016/j.vaccine.2020.12.013

Kirrella, A.A.K., El-Kassas, S., Mostfa, S.M., Younes, H.H., Helal, M., Ragab, M., 2023. The comparison of two different plumage-color lines of Japanese quail (Coturnix japonica) disclosed a significant effect in increasing abdominal fat contents with increasing age. Trop Anim Health Prod 55, 180. https://doi.org/10.1007/s11250-023-03601-8

Kolberg, L., Raudvere, U., Kuzmin, I., Adler, P., Vilo, J., Peterson, H., 2023. g:Profiler—interoperable web service for functional enrichment analysis and gene identifier mapping (2023 update). Nucleic Acids Research 51, W207–W212. https://doi.org/10.1093/nar/gkad347

Kovacs-Nolan, J., Mine, Y., 2004. Passive Immunization Through Avian Egg Antibodies. Food Biotechnology 18, 39–62. https://doi.org/10.1081/FBT-120030384

Kroeger, M., Vargas-Bermudez, D.S., Jaime, J.,Parada, J., Groeltz,J., Gauger, P., Piñeyro, P., 2024. First detection of PCV4 in swine in the United States: codetection with PCV2 and PCV3 and direct detection within tissues. *Sci Rep* **14**, 15535. https://doi.org/10.1038/s41598-024-66328-

Kwesi-Maliepaard, E.M., Aslam, M.A., Alemdehy, M.F., Van Den Brand, T., McLean, C., Vlaming, H., Van Welsem, T., Korthout, T., Lancini, C., Hendriks, S., Ahrends, T., Van Dinther, D., Den Haan, J.M.M., Borst, J., De Wit, E., Van Leeuwen, F., Jacobs, H., 2020. The histone methyltransferase DOT1L prevents antigen-independent

differentiation and safeguards epigenetic identity of CD8$^+$ T cells. Proc. Natl. Acad. Sci. U.S.A. 117, 20706–20716. https://doi.org/10.1073/pnas.1920372117

Lagumdzic, E., Pernold, C.P.S., Ertl, R., Palmieri, N., Stadler, M., Sawyer, S., Stas, M.R., Kreutzmann, H., Rümenapf, T., Ladinig, A., Saalmüller, A., 2023. Gene expression of peripheral blood mononuclear cells and CD8+ T cells from gilts after PRRSV infection. Front. Immunol. 14, 1159970. https://doi.org/10.3389/fimmu.2023.1159970

Lavoie, E.T., Sorrell, E.M., Perez, D.R., Ann Ottinger, M., 2007. Immunosenescence and age-related susceptibility to influenza virus in Japanese quail. Developmental & Comparative Immunology 31, 407–414. https://doi.org/10.1016/j.dci.2006.07.009

Lawlor, N., Nehar-Belaid, D., Grassmann, J.D.S., Stoeckius, M., Smibert, P., Stitzel, M.L., Pascual, V., Banchereau, J., Williams, A., Ucar, D., 2021. Single Cell Analysis of Blood Mononuclear Cells Stimulated Through Either LPS or Anti-CD3 and Anti-CD28. Front. Immunol. 12, 636720. https://doi.org/10.3389/fimmu.2021.636720

Lee, W., Syed Atif, A., Tan, S.C., Leow, C.H., 2017. Insights into the chicken IgY with emphasis on the generation and applications of chicken recombinant monoclonal antibodies. Journal of Immunological Methods 447, 71–85. https://doi.org/10.1016/j.jim.2017.05.001

Li, D., Du, Q., Wu, B., Li, J., Chang, L., Zhao, X., Huang, Y., Tong, D., 2017. Immunogenicity of adenovirus vaccines expressing the PCV2 capsid protein in pigs. Vaccine 35, 4722–4729. https://doi.org/10.1016/j.vaccine.2017.07.031

Li, G., He, W., Zhu, H., Bi, Y., Wang, R., Xing, G., Zhang, C., Zhou, J., Yuen, K., Gao, G.F., Su, S., 2018. Origin, Genetic Diversity, and Evolutionary Dynamics of Novel Porcine Circovirus 3. Advanced Science 5, 1800275. https://doi.org/10.1002/advs.201800275

Li, X., Wang, C.-Y., 2021. From bulk, single-cell to spatial RNA sequencing. Int J Oral Sci 13, 36. https://doi.org/10.1038/s41368-021-00146-0

Li, X., Wang, L., Zhen, Y., Li, S., Xu, Y., 2015. Chicken egg yolk antibodies (IgY) as non-antibiotic production enhancers for use in swine production: a review. *J Animal Sci Biotechnol* **6**, 40. https://doi.org/10.1186/s40104-015-0038-8

Li, Y., Yu, P., Bao, Y., Ren, Y., Zhao, S., Zhang, X., 2023. Production of virus-like particles of porcine circovirus 2 in baculovirus expression system and its application for antibody detection. BMC Vet Res 19, 87. https://doi.org/10.1186/s12917-023-03648-7

Liu, K., Kong, L., Graham, D.B., Carey, K.L., Xavier, R.J., 2021. SAC1 regulates autophagosomal phosphatidylinositol-4-phosphate for xenophagy-directed bacterial clearance. Cell Reports 36, 109434. https://doi.org/10.1016/j.celrep.2021.109434

Liu, Q., Tikoo, S.K., Babiuk, L.A., 2001. Nuclear Localization of the ORF2 Protein Encoded by Porcine Circovirus Type 2. Virology 285, 91–99. https://doi.org/10.1006/viro.2001.0922

Macosko, E.Z., Basu, A., Satija, R., Nemesh, J., Shekhar, K., Goldman, M., Tirosh, I., Bialas, A.R., Kamitaki, N., Martersteck, E.M., Trombetta, J.J., Weitz, D.A., Sanes, J.R., Shalek, A.K., Regev, A., McCarroll, S.A., 2015. Highly Parallel Genome-wide Expression Profiling of Individual Cells Using Nanoliter Droplets. Cell 161, 1202–1214. https://doi.org/10.1016/j.cell.2015.05.002

Maity, H., Samanta, K., Deb, R., Gupta, V., 2023. Revisiting Porcine Circovirus Infection: Recent Insights and Its Significance in the Piggery Sector. Vaccines 11, 1308. https://doi.org/10.3390/vaccines11081308

Mankertz, A., Çaliskan, R., Hattermann, K., Hillenbrand, B., Kurzendoerfer, P., Mueller, B., Schmitt, C., Steinfeldt, T., Finsterbusch, T., 2004. Molecular biology of Porcine circovirus: analyses of gene expression and viral replication. Veterinary Microbiology 98, 81–88. https://doi.org/10.1016/j.vetmic.2003.10.014

Mao, Y., Shi, D., Li, G., Jiang, P., 2022. Citrulline depletion by ASS1 is required for proinflammatory macrophage activation and immune responses. Molecular Cell 82, 527-541.e7. https://doi.org/10.1016/j.molcel.2021.12.006

Marshall, J.S., Warrington, R., Watson, W., Kim, H.L., 2018. An introduction to immunology and immunopathology. Allergy Asthma Clin Immunol 14, 49. https://doi.org/10.1186/s13223-018-0278-1

Mashaly, M.M., Hendricks, G.L., Kalama, M.A., Gehad, A.E., Abbas, A.O., Patterson, P.H., 2004. Effect of Heat Stress on Production Parameters and Immune Responses of Commercial Laying Hens. Poultry Science 83, 889–894. https://doi.org/10.1093/ps/83.6.889

Maxwell, M., Söderlund, R., Härtle, S., Wattrang, E., 2024. Single-cell RNA-seq mapping of chicken peripheral blood leukocytes. BMC Genomics 25, 124. https://doi.org/10.1186/s12864-024-10044-4

Mehrzad, J., Shojaei, S., Keivan, F., Forouzanpour, D., Sepahvand, H., Kordi, A., Hooshmand, P., 2024. Avian Innate and Adaptive Immune Components: A Comprehensive Review. J Poult Sci Avian Dis 2, 73–96. https://doi.org/10.61838/kman.jpsad.2.3.7

Mills, A.D., Crawford, L.L., Domjan, M., Faure, J.M., 1997. The behavior of the japanese or domestic quail Coturnix japonica. Neuroscience & Biobehavioral Reviews 21, 261–281. https://doi.org/10.1016/S0149-7634(96)00028-0

Misinzo, G., Delputte, P.L., Meerts, P., Lefebvre, D.J., Nauwynck, H.J., 2006. Porcine Circovirus 2 Uses Heparan Sulfate and Chondroitin Sulfate B Glycosaminoglycans as Receptors for Its Attachment to Host Cells. J Virol 80, 3487–3494. https://doi.org/10.1128/JVI.80.7.3487-3494.2006

Mo, X., Li, X., Yin, B., Deng, J., Tian, K., Yuan, A., 2019. Structural roles of PCV2 capsid protein N-terminus in PCV2 particle assembly and identification of PCV2 type-specific neutralizing epitope. PLoS Pathog 15, e1007562. https://doi.org/10.1371/journal.ppat.1007562

Moreno-Lanceta, A., Medrano-Bosch, M., Fundora, Y., Perramón, M., Aspas, J., Parra-Robert, M., Baena, S., Fondevila, C., Edelman, E.R., Jiménez, W., Melgar-Lesmes, P., 2023. RNF41 orchestrates macrophage-driven fibrosis resolution and hepatic regeneration. Sci. Transl. Med. 15, eabq6225. https://doi.org/10.1126/scitranslmed.abq6225

Moro-García, M.A., Mayo, J.C., Sainz, R.M., Alonso-Arias, R., 2018. Influence of Inflammation in the Process of T Lymphocyte Differentiation: Proliferative, Metabolic, and Oxidative Changes. Front. Immunol. 9, 339. https://doi.org/10.3389/fimmu.2018.00339

Morris, K.M., Hindle, M.M., Boitard, S., Burt, D.W., Danner, A.F., Eory, L., Forrest, H.L., Gourichon, D., Gros, J., Hillier, L.W., Jaffredo, T., Khoury, H., Lansford, R., Leterrier, C., Loudon, A., Mason, A.S., Meddle, S.L., Minvielle, F., Minx, P., Pitel, F., Seiler,

J.P., Shimmura, T., Tomlinson, C., Vignal, A., Webster, R.G., Yoshimura, T., Warren, W.C., Smith, J., 2020. The quail genome: insights into social behaviour, seasonal biology and infectious disease response. BMC Biol 18. https://doi.org/10.1186/s12915-020-0743-4

Mylvaganam, S., Freeman, S.A., Grinstein, S., 2021. The cytoskeleton in phagocytosis and macropinocytosis. Current Biology 31, R619–R632. https://doi.org/10.1016/j.cub.2021.01.036

Najdi, S, Nikbakht Brujeni, G, Sheikhi, N, Chakhkar, S, 2016. Development of anti-Helicobacter pylori immunoglobulins Y (IgYs) in quail. Iranian Journal of Veterinary Research 17.

Nassiri, I., Kwok, A.J., Bhandari, A., Bull, K.R., Garner, L.C., Klenerman, P., Webber, C., Parkkinen, L., Lee, A.W., Wu, Y., Fairfax, B., Knight, J.C., Buck, D., Piazza, P., 2024. Demultiplexing of single-cell RNA-sequencing data using interindividual variation in gene expression. Bioinformatics Advances 4, vbae085. https://doi.org/10.1093/bioadv/vbae085

Navas, A., Giraldo-Parra, L., Prieto, M.D., Cabrera, J., Gómez, M.A., 2019. Phenotypic and functional stability of leukocytes from human peripheral blood samples: considerations for the design of immunological studies. BMC Immunol 20. https://doi.org/10.1186/s12865-019-0286-z

Neavin, D., Senabouth, A., Arora, H., Lee, J.T.H., Ripoll-Cladellas, A., sc-eQTLGen Consortium, Franke, L., Prabhakar, S., Ye, C.J., McCarthy, D.J., Melé, M., Hemberg, M., Powell, J.E., 2024. Demuxafy: improvement in droplet assignment by integrating multiple single-cell demultiplexing and doublet detection methods. Genome Biol 25, 94. https://doi.org/10.1186/s13059-024-03224-8

Nebor, D., Gillinder, K.R., Robledo, R.F., Graber, J.H., Philip, V., Ilsley, M., Bieker, J.J., Perkins, A., Peters, L.L., 2016. Identifying Novel Modifiers of Embryonic Globin Expression By Combining Chipseq, Rnaseq and eQTL Mapping in the Adult Nan Mouse Model. Blood 128, 398–398. https://doi.org/10.1182/blood.V128.22.398.398

Oh, H., Kwon, O., Kong, M.J., Park, K.M., Baek, J.-H., 2023. Macrophages promote Fibrinogenesis during kidney injury. Front. Med. 10, 1206362. https://doi.org/10.3389/fmed.2023.1206362

Olson, W.C., Smolkin, M.E., Farris, E.M., Fink, R.J., Czarkowski, A.R., Fink, J.H., Chianese-Bullock, K.A., Slingluff, C.L., 2011. Shipping blood to a central laboratory in multicenter clinical trials: effect of ambient temperature on specimen temperature, and effects of temperature on mononuclear cell yield, viability and immunologic function. J Transl Med 9. https://doi.org/10.1186/1479-5876-9-26

Opriessnig, T., Karuppannan, A.K., Castro, A.M.M.G., Xiao, C.-T., 2020. Porcine circoviruses: current status, knowledge gaps and challenges. Virus Research 286, 198044. https://doi.org/10.1016/j.virusres.2020.198044

Ouyang, T., Niu, G., Liu, X., Zhang, X., Zhang, Y., Ren, L., 2019. Recent progress on porcine circovirus type 3. Infection, Genetics and Evolution 73, 227–233. https://doi.org/10.1016/j.meegid.2019.05.009

Park, Y., Min, K., Kim, N.H., Kim, J., Park, M., Kang, H., Sohn, E.-J., Lee, S., 2021. Porcine circovirus 2 capsid protein produced in N. benthamiana forms virus-like particles that elicit production of virus-neutralizing antibodies in guinea pigs. New Biotechnology 63, 29–36. https://doi.org/10.1016/j.nbt.2021.02.005

Pasquini, G., Rojo Arias, J.E., Schäfer, P., Busskamp, V., 2021. Automated methods for cell type annotation on scRNA-seq data. Computational and Structural Biotechnology Journal 19, 961–969. https://doi.org/10.1016/j.csbj.2021.01.015

Pereira, J.P., Kelly, L.M., Cyster, J.G., 2010. Finding the right niche: B-cell migration in the early phases of T-dependent antibody responses. International Immunology 22, 413–419. https://doi.org/10.1093/intimm/dxq047

Picelli, S., Faridani, O.R., Björklund, Å.K., Winberg, G., Sagasser, S., Sandberg, R., 2014. Full-length RNA-seq from single cells using Smart-seq2. Nat Protoc 9, 171–181. https://doi.org/10.1038/nprot.2014.006

Qu, X., Li, X., Li, Z., Liao, M., Dai, M., 2022a. Chicken Peripheral Blood Mononuclear Cells Response to Avian Leukosis Virus Subgroup J Infection Assessed by Single-Cell RNA Sequencing. Front. Microbiol. 13, 800618. https://doi.org/10.3389/fmicb.2022.800618

Qu, X., Li, X., Li, Z., Liao, M., Dai, M., 2022b. Chicken Peripheral Blood Mononuclear Cells Response to Avian Leukosis Virus Subgroup J Infection Assessed by Single-Cell RNA Sequencing. Front. Microbiol. 13, 800618. https://doi.org/10.3389/fmicb.2022.800618

Quan, F., Liang, X., Cheng, M., Yang, H., Liu, K., He, S., Sun, S., Deng, M., He, Y., Liu, W., Wang, S., Zhao, S., Deng, L., Hou, X., Zhang, X., Xiao, Y., 2023. Annotation of cell types (ACT): a convenient web server for cell type annotation. Genome Med 15, 91. https://doi.org/10.1186/s13073-023-01249-5

Qureshi, M., 2003. Avian macrophage and immune response: an overview. Poultry Science 82, 691–698. https://doi.org/10.1093/ps/82.5.691

Rahman, S., Van Nguyen, S., Icatlo Jr., F.C., Umeda, K., Kodama, Y., 2013. Oral passive IgY-based immunotherapeutics: A novel solution for prevention and treatment of alimentary tract diseases. Human Vaccines & Immunotherapeutics 9, 1039–1048. https://doi.org/10.4161/hv.23383

Rai, V., Upmanyu, V., Mohd, G., Kumar, R., Koppad, S., Ansari, A., Bora, D.P., Pandey, A.B., Dhar, P., Tiwari, A.K., 2020. Comparing the efficiency of different Escherichia coli strains in producing recombinant capsid protein of porcine circovirus type 2. Molecular and Cellular Probes 52, 101556. https://doi.org/10.1016/j.mcp.2020.101556

Rajeswari, S, Antonysamy, M., Choraria, A., Zhang, Xiao-Ying, 2018. Applications of Chicken Egg Yolk Antibodies (Igy) in Healthcare: A Review. BJSTR 2. https://doi.org/10.26717/BJSTR.2017.01.000649

Ramstead, A.G., Wallace, J.A., Lee, S.-H., Bauer, K.M., Tang, W.W., Ekiz, H.A., Lane, T.E., Cluntun, A.A., Bettini, M.L., Round, J.L., Rutter, J., O'Connell, R.M., 2020. Mitochondrial Pyruvate Carrier 1 Promotes Peripheral T Cell Homeostasis through Metabolic Regulation of Thymic Development. Cell Reports 30, 2889-2899.e6. https://doi.org/10.1016/j.celrep.2020.02.042

Reyes, R., Cardeñes, B., Machado-Pineda, Y., Cabañas, C., 2018. Tetraspanin CD9: A Key Regulator of Cell Adhesion in the Immune System. Front. Immunol. 9, 863. https://doi.org/10.3389/fimmu.2018.00863

Rong, N., Liu, J., 2023. Development of animal models for emerging infectious diseases by breaking the barrier of species susceptibility to human pathogens. Emerging Microbes & Infections 12, 2178242. https://doi.org/10.1080/22221751.2023.2178242

Rosano, G.L., Ceccarelli, E.A., 2014. Recombinant protein expression in Escherichia coli: advances and challenges. Front. Microbiol. 5. https://doi.org/10.3389/fmicb.2014.00172

Sagrera, M., Garza-Moreno, L., Sibila, M., Oliver-Ferrando, S., Cárceles, S., Casanovas, C., Prieto, P., García-Flores, A., Espigares, D., Segalés, J., 2024. Frequency of PCV-2 viremia in nursery piglets from a Spanish swine integration system in 2020 and 2022 considering PRRSV infection status. Porc Health Manag 10, 4. https://doi.org/10.1186/s40813-024-00354-0

Salter, D., Balander, R., Crittenden, L., 1999. Evaluation of Japanese quail as a model system for avian transgenesis using avian leukosis viruses. Poultry Science 78, 230–234. https://doi.org/10.1093/ps/78.2.230

Sandell, M.I., Tobler, M., Hasselquist, D., 2009. Yolk androgens and the development of avian immunity: an experiment in jackdaws (*Corvus monedula*). Journal of Experimental Biology 212, 815–822. https://doi.org/10.1242/jeb.022111

Satija, R., Farrell, J.A., Gennert, D., Schier, A.F., Regev, A., 2015. Spatial reconstruction of single-cell gene expression data. Nat Biotechnol 33, 495–502. https://doi.org/10.1038/nbt.3192

Schädler, J., Sigrist, B., Meier, S.M., Albini, S., Wolfrum, N., 2019. Virus-like particles in a new vaccination approach against infectious laryngotracheitis. Journal of General Virology 100, 1013–1026. https://doi.org/10.1099/jgv.0.001272

Scholtz, N.D., Halle, I., Dänicke, S., Hartmann, G., Zur, B., Sauerwein, H., 2010. Effects of an active immunization on the immune response of laying Japanese quail (Coturnix coturnix japonica) fed with or without genetically modified Bacillus thuringiensis-maize. Poultry Science 89, 1122–1128. https://doi.org/10.3382/ps.2010-00678

See, Peter, Lum, Josephine, Chen, J., Ginhoux, F., 2018. A Single-Cell Sequencing Guide for Immunologists. Frontiers in Immunology 9.

Segalés, J., Kekarainen, T., Cortey, M., 2013. The natural history of porcine circovirus type 2: From an inoffensive virus to a devastating swine disease? Veterinary Microbiology 165, 13–20. https://doi.org/10.1016/j.vetmic.2012.12.033

Seo, H.W., Han, K., Park, C., Chae, C., 2014. Clinical, virological, immunological and pathological evaluation of four porcine circovirus type 2 vaccines. The Veterinary Journal 200, 65–70. https://doi.org/10.1016/j.tvjl.2014.02.002

Seta, Y., Kawakatsu, K., Degawa, S., Goto, T., Nishikata, T., 2023. Morphological Evidence for Novel Roles of Microtubules in Macrophage Phagocytosis. IJMS 24, 1373. https://doi.org/10.3390/ijms24021373

Shen, H., Xue, C., Lv, L., Wang, W., Liu, Q., Liu, K., Chen, X., Zheng, J., Li, X., Cao, Y., 2013. Assembly and immunological properties of a bivalent virus-like particle (VLP) for avian influenza and Newcastle disease. Virus Research 178, 430–436. https://doi.org/10.1016/j.virusres.2013.09.009

Somasundaram, R., Choraria, A., Antonysamy, M., 2020. An approach towards development of monoclonal IgY antibodies against SARS CoV-2 spike protein (S) using phage display method: A review. International Immunopharmacology 85, 106654. https://doi.org/10.1016/j.intimp.2020.106654

Sun, J., Huang, M., Xiao, F., Xi, Z., 2015. Echinoderm microtubule-associated protein -like protein 5 in anterior temporal neocortex of patients with intractable epilepsy.

Iranian Journal of Basic Medical Sciences 18, 1008–1013. https://doi.org/10.22038/ijbms.2015.5465
Sun, J., Zhong, X., Fu, X., Miller, H., Lee, P., Yu, B., Liu, C., 2022. The Actin Regulators Involved in the Function and Related Diseases of Lymphocytes. Front. Immunol. 13, 799309. https://doi.org/10.3389/fimmu.2022.799309
Sun, L., Su, Y., Jiao, A., Wang, X., Zhang, B., 2023. T cells in health and disease. Sig Transduct Target Ther 8, 235. https://doi.org/10.1038/s41392-023-01471-y
Sun, W., Shen, J., Liu, J., Han, K., Liang, L., Gao, Y., 2022. Gene Signature and Prognostic Value of Ubiquitin-Specific Proteases Members in Hepatocellular Carcinoma and Explored the Immunological Role of USP36. Front. Biosci. (Landmark Ed) 27, 190. https://doi.org/10.31083/j.fbl2706190
Swaminath, S., Russell, A.B., 2024. The use of single-cell RNA-seq to study heterogeneity at varying levels of virus–host interactions. PLoS Pathog 20, e1011898. https://doi.org/10.1371/journal.ppat.1011898
Swiatczak, B., Cohen, I.R., 2015. Gut feelings of safety: tolerance to the microbiota mediated by innate immune receptors. Microbiology and Immunology 59, 573–585. https://doi.org/10.1111/1348-0421.12318
Taghizadeh, M.S., Niazi, A., Afsharifar, A., 2024. Virus-like particles (VLPs): A promising platform for combating against Newcastle disease virus. Vaccine: X 16, 100440. https://doi.org/10.1016/j.jvacx.2024.100440
Tan, Y.S., Lei, Y.L., 2019. Isolation of Tumor-Infiltrating Lymphocytes by Ficoll-Paque Density Gradient Centrifugation, in: Allen, I.C. (Ed.), Mouse Models of Innate Immunity, Methods in Molecular Biology. Springer New York, New York, NY, pp. 93–99. https://doi.org/10.1007/978-1-4939-9167-9_8
Tang, F., Barbacioru, C., Wang, Y., Nordman, E., Lee, C., Xu, N., Wang, X., Bodeau, J., Tuch, B.B., Siddiqui, A., Lao, K., Surani, M.A., 2009. mRNA-Seq whole-transcriptome analysis of a single cell. Nature Methods 6, 377–382. https://doi.org/10.1038/nmeth.1315
Trundova, M., Celer, V., 2007. Expression of porcine circovirus 2 ORF2 gene requires codon optimized E. coli cells. Virus Genes 34, 199–204. https://doi.org/10.1007/s11262-006-0043-2
Turvey, S.E., Broide, D.H., 2010. Innate immunity. Journal of Allergy and Clinical Immunology 125, S24–S32. https://doi.org/10.1016/j.jaci.2009.07.016
Vahey, M.T., Nau, M.E., Jagodzinski, L.L., Yalley-Ogunro, J., Taubman, M., Michael, N.L., Lewis, M.G., 2002. Impact of Viral Infection on the Gene Expression Profiles of Proliferating Normal Human Peripheral Blood Mononuclear Cells Infected with HIV Type 1 RF. AIDS Research and Human Retroviruses 18, 179–192. https://doi.org/10.1089/08892220252781239
Verreault, D., Létourneau, V., Gendron, L., Massé, D., Gagnon, C.A., Duchaine, C., 2010. Airborne porcine circovirus in Canadian swine confinement buildings. Veterinary Microbiology 141, 224–230. https://doi.org/10.1016/j.vetmic.2009.09.013
Waligora-Dupriet, A.J., Dugay, A., Auzeil, N., Nicolis, I., Rabot, S., Huerre, M.R., Butel, M.J., 2009. Short-chain fatty acids and polyamines in the pathogenesis of necrotizing enterocolitis: Kinetics aspects in gnotobiotic quails. Anaerobe 15, 138–144. https://doi.org/10.1016/j.anaerobe.2009.02.001
Wang, R., Lan, C., Benlagha, K., Camara, N.O.S., Miller, H., Kubo, M., Heegaard, S., Lee, P., Yang, L., Forsman, H., Li, X., Zhai, Z., Liu, C., 2024. The interaction of innate

immune and adaptive immune system. MedComm 5, e714. https://doi.org/10.1002/mco2.714

Wang, Y.W., Sunwoo, H., Cherian, G., Sim, J.S., 2004. Maternal dietary ratio of linoleic acid to alpha-linolenic acid affects the passive immunity of hatching chicks. Poultry Science 83, 2039–2043. https://doi.org/10.1093/ps/83.12.2039

Wang, Z., Xie, L., Ding, G., Song, S., Chen, L., Li, G., Xia, M., Han, D., Zheng, Y., Liu, J., Xiao, T., Zhang, H., Huang, Y., Li, Y., Huang, M., 2021. Single-cell RNA sequencing of peripheral blood mononuclear cells from acute Kawasaki disease patients. Nat Commun 12, 5444. https://doi.org/10.1038/s41467-021-25771-5

Warren, W.C., Rice, E.S., Meyer, A., Hearn, C.J., Steep, A., Hunt, H.D., Monson, M.S., Lamont, S.J., Cheng, H.H., 2023. The immune cell landscape and response of Marek's disease resistant and susceptible chickens infected with Marek's disease virus. Sci Rep 13, 5355. https://doi.org/10.1038/s41598-023-32308-x

Wilk, A.J., Rustagi, A., Zhao, N.Q., Roque, J., Martínez-Colón, G.J., McKechnie, J.L., Ivison, G.T., Ranganath, T., Vergara, R., Hollis, T., Simpson, L.J., Grant, P., Subramanian, A., Rogers, A.J., Blish, C.A., 2020. A single-cell atlas of the peripheral immune response in patients with severe COVID-19. Nat Med 26, 1070–1076. https://doi.org/10.1038/s41591-020-0944-y

Wu, K., Hu, W., Zhou, B., Li, B., Li, X., Yan, Q., Chen, W., Li, Y., Ding, H., Zhao, M., Fan, S., Yi, L., Chen, J., 2022. Immunogenicity and Immunoprotection of PCV2 Virus-like Particles Incorporating Dominant T and B Cell Antigenic Epitopes Paired with CD154 Molecules in Piglets and Mice. IJMS 23, 14126. https://doi.org/10.3390/ijms232214126

Wu, P.-C., Chen, T.-Y., Chi, J.-N., Chien, M.-S., Huang, C., 2016. Efficient expression and purification of porcine circovirus type 2 virus-like particles in Escherichia coli. Journal of Biotechnology 220, 78–85. https://doi.org/10.1016/j.jbiotec.2016.01.017

Wu, X., Zhai, X., Lai, Y., Zuo, L., Zhang, Y., Mei, X., Xiang, R., Kang, Z., Zhou, L., Wang, H., 2019. Construction and Immunogenicity of Novel Chimeric Virus-Like Particles Bearing Antigens of Infectious Bronchitis Virus and Newcastle Disease Virus. Viruses 11, 254. https://doi.org/10.3390/v11030254

Wu, Z., Kaiser, P., 2011. Antigen presenting cells in a non-mammalian model system, the chicken. Immunobiology 216, 1177–1183. https://doi.org/10.1016/j.imbio.2011.05.012

Xu, J., Falconer, C., Nguyen, Q., Crawford, J., McKinnon, B.D., Mortlock, S., Senabouth, A., Andersen, S., Chiu, H.S., Jiang, L., Palpant, N.J., Yang, J., Mueller, M.D., Hewitt, A.W., Pébay, A., Montgomery, G.W., Powell, J.E., Coin, L.J.M., 2019. Genotype-free demultiplexing of pooled single-cell RNA-seq. Genome Biol 20, 290. https://doi.org/10.1186/s13059-019-1852-7

Xu, X., Qian, J., Qin, L., Li, J., Xue, C., Ding, J., Wang, W., Ding, W., Yin, R., Jin, N., Ding, Z., 2020. Chimeric Newcastle Disease Virus-like Particles Containing DC-Binding Peptide-Fused Haemagglutinin Protect Chickens from Virulent Newcastle Disease Virus and H9N2 Avian Influenza Virus Challenge. Virol. Sin. 35, 455–467. https://doi.org/10.1007/s12250-020-00199-1

Yamawaki, T.M., Lu, D.R., Ellwanger, D.C., Bhatt, D., Manzanillo, P., Arias, V., Zhou, H., Yoon, O.K., Homann, O., Wang, S., Li, C.-M., 2021. Systematic comparison of high-

throughput single-cell RNA-seq methods for immune cell profiling. BMC Genomics 22, 66. https://doi.org/10.1186/s12864-020-07358-4

Yang, J., Zhang, L., Zhang, C., Lu, Y., 2021. Exploration on the expression and assembly of virus-like particles. Biotechnology Notes 2, 51–58. https://doi.org/10.1016/j.biotno.2021.08.003

Yi, P.-C., Zhuo, L., Lin, J., Chang, C., Goddard, A., Yoon, O.K., 2023. Impact of delayed PBMC processing on functional and genomic assays. Journal of Immunological Methods 519, 113514. https://doi.org/10.1016/j.jim.2023.113514

Zhai, S.-L., Chen, S.-N., Wei, Z.-Z., Zhang, J.-W., Huang, L., Lin, T., Yue, C., Ran, D.-L., Yuan, S.-S., Wei, W.-K., Long, J.-X., 2011. Co-existence of multiple strains of porcine circovirus type 2 in the same pig from China. Virol J 8, 517. https://doi.org/10.1186/1743-422X-8-517

Zhai, S.-L., Lu, S.-S., Wei, W.-K., Lv, D.-H., Wen, X.-H., Zhai, Q., Chen, Q.-L., Sun, Y.-W., Xi, Y., 2019. Reservoirs of Porcine Circoviruses: A Mini Review. Front. Vet. Sci. 6, 319. https://doi.org/10.3389/fvets.2019.00319

Zhang, J.-Y., Wang, X.-M., Xing, X., Xu, Z., Zhang, C., Song, J.-W., Fan, X., Xia, P., Fu, J.-L., Wang, S.-Y., Xu, R.-N., Dai, X.-P., Shi, L., Huang, L., Jiang, T.-J., Shi, M., Zhang, Y., Zumla, A., Maeurer, M., Bai, F., Wang, F.-S., 2020. Single-cell landscape of immunological responses in patients with COVID-19. Nat Immunol 21, 1107–1118. https://doi.org/10.1038/s41590-020-0762-x

Zhu, A., Ibrahim, J.G., Love, M.I., 2019. Heavy-tailed prior distributions for sequence count data: removing the noise and preserving large differences. Bioinformatics 35, 2084–2092. https://doi.org/10.1093/bioinformatics/bty895

Zhu, Q., Conrad, D.N., Gartner, Z.J., 2024. deMULTIplex2: robust sample demultiplexing for scRNA-seq. Genome Biol 25, 37. https://doi.org/10.1186/s13059-024-03177-y